BSC

Design Calculation or Analysis Cover Sheet

Complete only applicable items.

1. QA: QA

2. Page 1

3. System	4. Document Identifier
Waste Handling System	000-00C-MGR0-03400-000-00A

5. Title

Release Fractions for Spent Nuclear Fuel and High-Level Waste

6. Group

Preclosure Safety Analysis

7. Document Status Designation

☐ Preliminary   ☒ Committed   ☐ Confirmed   ☐ Cancelled/Superseded

8. Notes/Comments

This document supersedes the *Commercial SNF Accident Release Fractions* (000-00C-MGR0-01700-000-000). The change of the document identifier and title reflects the change of the scope of work and document status designation.

Both originators worked on the entire document.

Attachments	Total Number of Pages
Attachment A	4
Attachment B	4
Attachment C	4
Attachment D	2
Attachment E	2+CD

RECORD OF REVISIONS

9. No.	10. Reason For Revision	11. Total # of Pgs.	12. Last Pg. #	13. Originator (Print/Sign/Date)	14. Checker (Print/Sign/Date)	15. EGS (Print/Sign/Date)	16. Approved/Accepted (Print/Sign/Date)
00A	Initial issue.	126	126 of 126	D. Wesley Wu / Richard I. Smith	Jorge Schulz	Sen-Sung Tsai	Mark K. Wisenburg

DISCLAIMER

The calculations contained in this document were developed by Bechtel SAIC Company, LLC (BSC) and are intended solely for the use of BSC in its work for the Yucca Mountain Project.

CONTENTS

INTENTIONALLY LEFT BLANK

TABLES

Page

INTENTIONALLY LEFT BLANK

FIGURES

Page

INTENTIONALLY LEFT BLANK

ACRONYMS

AED	aerodynamic equivalent diameter
ANL	Argonne National Laboratory
ANSI	American National Standards Institute
ARF	airborne release fraction
ATM	Approved Testing Material
BWR	boiling water reactor
CRCF	Canister Receipt and Closure Facilities
CSF	crud spallation fraction
DOE	U.S. Department of Energy
DPC	dual-purpose canister
DR	damage ratio
EPA	U.S. Environmental Protection Agency
EPF	energy partition factor
EPRI	Electric Power Research Institute
GSD	geometric standard deviation
HEPA	High Efficiency Particulate Air
HLW	high-level radioactive waste
ICRP	International Commission on Radiological Protection
IHF	Initial Handling Facility
INEL	Idaho National Engineering Laboratory
ISFSI	independent spent fuel storage installation
LPF	leak path factor
MAR	material at risk
MGD	mean geometric diameter
MGSD	mass geometric standard deviation
MMD	mass median diameter
NRC	U.S. Nuclear Regulatory Commission
PNNL	Pacific Northwest National Laboratory
PULF	pulverization fraction
PWR	pressurized water reactor
RCF	respirable correction factor
RED	canister reduction factor
RF	respirable fraction

SAR   safety analysis report
SNF   spent nuclear fuel
SSCs   structures, systems, and components

TAD   transport, aging, and disposal

WHF   Wet Handling Facility

ELEMENTAL SYMBOLS AND RELEVANT UNITS

°C	degrees Celsius (unit of temperature)
Ci	Curie (unit of activity)
cm^2	square centimeters (unit of area)
cm/s^2	centimeters per square second (unit of gravitational acceleration)
Co	Cobalt
Cs	Cesium
CsI	Cesium iodide
CsO_2	Cesium oxide
CsOH	Cesium hydroxide
Fe	Iron
g/cm^3	grams per cubic centimeter (unit of density)
GWd/MTU	Gigawatt - days per metric tons of uranium (unit of fuel burnup)
^3H	Tritium
I	Iodine
in^2	square inches (unit of area)
IO_2	Iodine dioxide
I_2O_4	Iodine tetraoxide
J/cm^3	Joules per cubic centimeter (unit of energy density)
K	degrees Kelvin (unit of temperature)
Kr	Krypton
MPa	Mega-Pascal (unit of pressure)
MWd/MTU	Megawatt - days per metric tons of uranium (unit of fuel burnup)
Pa	Pascal (unit of pressure)
psig	pounds per square inch, gauge (unit of pressure)
Ru	Ruthenium
RuO_2	Ruthenium dioxide
RuO_4	Ruthenium tetroxide
s	second
Sr	Strontium
SrI_2	Strontium iodide
SrO	Strontium oxide
SrO_2	Strontium peroxide
UO_2	Uranium dioxide
U_3O_8	Triuranium octaoxide
μCi	micro-Curies (unit of activity)

μm   micro-meters, micron (unit of length/diameter)

1. PURPOSE

1.1 SCOPE

An accident at the Yucca Mountain repository in a dry environment involving commercial spent nuclear fuel (SNF), or defense high-level radioactive waste (HLW) could result in a release of radioactive material. The purpose of this analysis is to determine two important accident parameters associated with commercial SNF and HLW that are used to calculate the radiation dose consequences of such an accident and thereby support the licensing basis of the repository. These parameters are the airborne release fraction (ARF) and the respirable fraction (RF), both of which are defined in Section 4.3.1.

ARFs and RFs depend on type of waste form. For the commercial SNF, radionuclides could be released from the inside of breached fuel rods (or pins), and from the detachment of radioactive material (crud – material deposited on spent-fuel assembly surfaces) from the outside surfaces of fuel rods and other components of fuel assemblies. For the HLW, the vitrified glass in a sealed canister could fail during an accident, releasing a fraction of its inventory into air. Releases occur only during an accident.

In addition, commercial SNF is further divided into two categories based on the integrity of fuel assembly, i.e. intact fuel and failed fuel. Commercial SNF is also divided into two categories in terms of fuel burnup, i.e. low burnup fuel and high burnup fuel. Furthermore, when commercial SNF is exposed to air after an accident, it oxidizes into U_3O_8 powder, which can be released if air flow is available to pick up the powder.

Therefore, this document determines the following ARFs and RFs for use in various radiation dose consequence analyses:

1. ARF and RF for a burst rupture release involving intact and failed low burnup commercial SNF (Sections 6.1 to 6.3),

2. ARF and RF for a fuel oxidation release involving low burnup commercial SNF (Section 6.4),

3. ARF and RF for a burst rupture release involving intact and failed high burnup commercial SNF (Section 6.5),

4. ARF and RF for a fuel oxidation release involving high burnup commercial SNF (Section 6.6), and

5. ARF and RF for a HLW canister release (Section 6.7).

Discussions of categorization and methodologies used to determine ARFs and RFs are provided in Section 4.3.

1.2   BACKGROUND

Based on the current transport, aging, and disposal (TAD) canister-based repository design concept (Reference 2.2.12 [DIRS 182131], Section 1.2.2), most of the commercial SNF will be shipped to the repository in TAD canisters. These canisters are handled – but not opened – and inserted into waste packages within the Canister Receipt and Closure Facilities (CRCF). A small fraction of the commercial SNF waste stream is expected to be shipped as uncanistered fuel or in dual-purpose canisters (DPCs) requiring repackaging into TAD canisters. These waste streams are processed in the Wet Handling Facility (WHF). The commercial SNF received in TAD canisters that cannot be processed immediately in the CRCF, and the DPCs that cannot be processed immediately in the WHF can be received in the Receipt Facility and transferred into aging overpacks and sent to the Aging Facility. The repository is designed to receive at least 90% commercial SNF in TAD canisters and no more than 10% as uncanistered (bare, intact) assemblies in rail or truck transportation casks (Reference 2.2.12 [DIRS 182131], Section 2.2.1.3).

Among the commercial SNF assemblies received at the repository, some could be damaged at the reactor sites. This type of fuel is placed in failed fuel canisters with a mesh screen at each end (Reference 2.2.20 [DIRS 145022], p.C-1) and then placed in TAD canisters, DPCs, or directly into shipping casks. This canistered failed commercial SNF includes four categories: (1) mechanically and cladding-penetration damaged commercial SNF, (2) consolidated and reconstituted assemblies, (3) fuel rods, pieces, and debris, and (4) nonfuel components, which are considered as failed commercial SNF in this document.

Accidents may involve two types of commercial SNF waste forms characterized as (1) intact (i.e., bare unconfined) fuel assemblies, and (2) canistered (i.e., confined) failed commercial SNF. The received TAD canisters contain both intact fuel assemblies and canistered failed assemblies that are not opened at the repository. The bare unconfined and canistered failed assemblies may be received in transportation casks or DPCs that would have to be opened at the repository. In contrast to bare unconfined intact fuel assemblies, the container that confines the canistered fuel assemblies provides an additional barrier that reduces the radioactive material release should the fuel rod cladding breach during an accident. Because this analysis determines only release fractions associated with the fuel assemblies, it does not take credit for the additional barrier.

Defense HLW canisters are received and processed within the CRCF (Reference 2.2.12 [DIRS 182131], Section 4.1.1), but the Initial Handling Facility (IHF) shall also be capable of receiving and processing defense HLW canisters (Reference 2.2.12 [DIRS 182131], Section 1.2.2).

1.3   LIMITATIONS

This analysis determines release fractions from SNF directly, not SNF in transportation casks, waste packages, or TAD canisters. Airborne release fractions and respirable fractions for crush/impact events determined in this report, in general, are applicable to events with impact energy of 1.2 J/cm^3 or less (Reference 2.2.24 [DIRS 103756], p.4-52).

2. REFERENCES

2.1 PROCEDURES/DIRECTIVES

2.1.1 EG-DSK-3003, Rev. 07. *Desktop Information For Format Of Calculations And Analyses And Treatment Of Inputs And Assumptions.* Las Vegas, Nevada: Bechtel SAIC Company. ACC: ENG. 20070709.0006.

2.1.2 EG-DSK-3013, Rev. 02. *Desktop Information for Using Calctrac.* Las Vegas, Nevada: Bechtel SAIC Company. ACC: ENG. 20070516.0024.

2.1.3 EG-PRO-3DP-G04B-00037, Rev. 09. *Calculations and Analyses.* Las Vegas, Nevada: Bechtel SAIC Company. ACC: ENG. 20070717.0004.

2.1.4 IT-PRO-0011, Rev. 07. *Software Management.* Las Vegas, Nevada: Bechtel SAIC Company. ACC: DOC. 20070905.0007.

2.1.5 LS-PRO-0201, Rev. 05. *Preclosure Safety Analyses Process.* Las Vegas, Nevada: Bechtel SAIC Company. ACC: ENG.20071010.0021.

2.1.6 PA-PRO-0301, Rev. 03. *Managing Technical Product Inputs.* Las Vegas, Nevada: Bechtel SAIC Company. ACC: DOC. 20070615.0003.

2.1.7 QA-DIR-10, Rev. 01. *Quality Management Directive.* Las Vegas, Nevada: Bechtel SAIC Company. ACC: DOC.20070330.0001.

2.2 DESIGN INPUTS

2.2.1 10 CFR 71. 2006. Energy: Packaging and Transportation of Radioactive Material. Internet Accessible. **176575**

2.2.2 10 CFR 72. 2006. Energy: Licensing Requirements for the Independent Storage of Spent Nuclear Fuel, High-Level Radioactive Waste, and Reactor-Related Greater than Class C Waste. Internet Accessible. **176577**

2.2.3 Ahn, T.M. 1996. *Dry Oxidation and Fracture of LWR Spent Fuels.* NUREG-1565. Washington, D.C.: U.S. Nuclear Regulatory Commission. TIC: 231667. **101547**

2.2.4 Anderson, B.L.; Carlson, R.W.; and Fischer, L.E. 1996. *Containment Analysis for Type B Packages Used to Transport Various Contents.* NUREG/CR-6487. Washington, D.C.: U.S. Nuclear Regulatory Commission. TIC: 237945. **145345**

2.2.5 ANSI N13.1-1969. *Guide to Sampling Airborne Radioactive Materials in Nuclear Facilities.* New York, New York: American National Standards Institute. TIC: 204994. **106261**

2.2.6 ANSI/ANS-5.10-1998. *Airborne Release Fractions at Non-Reactor Nuclear Facilities.* La Grange Park, Illinois: American Nuclear Society. TIC: 235073. **103755**

2.2.7   B&W Fuel Company 1991. *Final Design Package Babcock & Wilcox BR-100 100 Ton Rail/Barge Spent Fuel Shipping Cask.* Volume 2. 51-1203400-01. DBABE0000-00272-1000-00014 REV 00. Lynchburg, Virginia: B&W Fuel Company. ACC: MOV.19960802.0083. **104439**

2.2.8   Baker, D.A.; Bailey, W.J., Beyer, C.E.; Bold, F.C.; and Tawil, J.J. 1988. *Assessment of the Use of Extended Burnup Fuel in Light Water Power Reactors*. NUREG/CR-5009. Washington, D.C.: U.S. Nuclear Regulatory Commission. TIC: 234496. **158889**

2.2.9   Bernard, L.C.; Jacoud, J.L.; and Vesco, P. 2002. "An Efficient Model for the Analysis of Fission Gas Release." *Journal of Nuclear Materials, 302,* 125-134. [New York, New York]: Elsevier. TIC: 259051. **178772**

2.2.10 Boase, D.G. and Vandergraaf, T.T. 1977. "The Canadian Spent Fuel Storage Canister: Some Materials Aspects." *Nuclear Technology, 32,* 60-71. La Grange Park, Illinois: American Nuclear Society. TIC: 237173. **117977**

2.2.11 BSC (Bechtel SAIC Company) 2005. *Commercial Spent Nuclear Fuel Handling in Air Study.* 000-30R-MGR0-00700-000-000. Las Vegas, Nevada: Bechtel SAIC Company. ACC: ENG.20050325.0012. **173261**

2.2.12 BSC (Bechtel SAIC Company) 2007. *Basis of Design for the TAD Canister-Based Repository Design Concept.* 000-3DR-MGR0-00300-000-001. Las Vegas, Nevada: Bechtel SAIC Company. ACC: ENG.20071002.0042. **182131**

2.2.13 BSC (Bechtel SAIC Company) 2007. *Characteristics for the Representative Commercial Spent Fuel Assembly for Preclosure Normal Operations.* 000-PSA-MGR0-00700-000-00A. Las Vegas, Nevada: Bechtel SAIC Company. ACC: ENG.20070521.0008. **180185**

2.2.14 BSC (Bechtel SAIC Company) 2007. *GROA Airborne Release Dispersion Factor Calculation.* 000-PSA-MGR0-00600-000-00A. Las Vegas, Nevada: Bechtel SAIC Company. ACC: ENG.20070601.0022. **180308**

2.2.15 BSC (Bechtel SAIC Company) 2007. *Initial Handling Facility: Lift-Height Calculation.* 51A-MJC-IH00-00100-000-00A. Las Vegas, Nevada: Bechtel SAIC Company. ACC: ENG.20070713.0010. **182031**

2.2.16 Chun, R.; Witte, M.; and Schwartz, M. 1987. *Dynamic Impact Effects on Spent Fuel Assemblies*. UCID-21246. Livermore, California: Lawrence Livermore National Laboratory. ACC: HQX.19881020.0031. **144357**

2.2.17 Colle, J.Y; Hiernaut, J.-P; Papaioannou, D.; Ronchi, C.; and Sasahara, A. 2006. "Fission Product release in High-burn-up UO_2 oxidized to U_3O_8" *Journal of Nuclear Materials, 348,* 229-242. [New York, New York]: Elsevier. TIC: to be submitted. **179470**

2.2.18 Cooper, C.D. and Alley, F.C. 1994. *Air Pollution Control, A Design Approach.* 2nd Edition. Prospect Heights, Illinois: Waveland Press. TIC: 241199. **158659**

2.2.19 Crane Company 1988. *Flow of Fluids Through Valves, Fittings, and Pipe.* Technical Paper No. 410. Joliet, Illinois: Crane Company. TIC: 237812. **149707**

2.2.20 CRWMS M&O 1999. *1999 Design Basis Waste Input Report for Commercial Spent Nuclear Fuel.* B00000000-01717-5700-00041 REV 01. Washington, D.C.: CRWMS M&O. ACC: MOV.19991217.0001. **145022**

2.2.21 Davis, P.R.; Strenge, D.L.; and Mishima, J. 1998. *Accident Analysis for Continued Storage.* Las Vegas, Nevada: Jason Technologies. ACC: MOL.20001010.0214. **103711**

2.2.22 Dennis, R., ed. 1976. *Handbook on Aerosols.* TID-26608. Oak Ridge, Tennessee: Energy Research and Development Administration, Technical Information Center. TIC: 242478. **158805**

2.2.23 DOE (U.S. Department of Energy) 1992. *Characteristics of Potential Repository Wastes.* DOE/RW-0184-R1. Volume 1. Washington, D.C.: U.S. Department of Energy, Office of Civilian Radioactive Waste Management. ACC: HQO.19920827.0001. **102812**

2.2.24 DOE (U.S. Department of Energy) 1994. *Analysis of Experimental Data.* Volume 1 of *Airborne Release Fractions/Rates and Respirable Fractions for Nonreactor Nuclear Facilities.* DOE-HDBK-3010-94. Washington, D.C.: U.S. Department of Energy. TIC: 233366. **103756**

2.2.25 Einziger, R.E. and Strain, R.V. 1984. "Effect of Cladding Defect Size on the Oxidation of Irradiated Spent LWR Fuel Below 360ºC." *Proceedings of International Workshop on Irradiated Fuel Storage: Operating Experience and Development Programs, October 17 and 18, 1984, Toronto, Ontario, Canada.* Naqvi, S.J. and Frost, C.R., eds. Pages 599-625. Toronto, Ontario, Canada: Ontario Hydro. TIC: 220186. **172756**

2.2.26 Einziger, R.E. and Cook, J.A. 1985. "Behavior of Breached Light Water Reactor Spent Fuel Rods in Air and Inert Atmospheres at +229 degrees Celsius." *Nuclear Technology, 69,* 55-71. La Grange Park, Illinois: American Nuclear Society. TIC: 242380. **126202**

2.2.27 Einziger, R.E. 1991. "Effects of an Oxidizing Atmosphere in a Spent Fuel Packaging Facility." *Proceedings of the Topical Meeting on Nuclear Waste Packaging, FOCUS '91, September 29–October 2, 1991, Las Vegas, Nevada.* Pages 88-99. La Grange Park, Illinois: American Nuclear Society. TIC: 231173. **166177**

2.2.28 EPRI (Electric Power Research Institute) 1986. *Oxidation of Spent Fuel Between 250 and 360°C.* EPRI NP-4524. Palo Alto, California: Electric Power Research Institute. TIC: 228313. **127313**

2.2.29 Graves, H.W., Jr. 1979. *Nuclear Fuel Management.* New York, New York: John Wiley & Sons. TIC: 242479. **158816**

2.2.30 Goode, J.H.; Stacy, R.G.; Vaughen, V.C.A. 1980. *Head-End Reprocessing Studies of H.B. Robinson-2 Fuel: II. Parametric Voloxidation Studies.* ORNL/TM-6888. Oak Ridge, TN: Oak Ridge National Laboratory. ACC: MOL.20070430.0140. **180520.**

2.2.31 Goode, J.H.; Stacy, R.G.; Vaughen, V.C.A. 1980. *Comparison Studies of Head-End Reprocessing using Three LWR Fuels.* ORNL/TM-7103. Oak Ridge, TN: Oak Ridge National Laboratory. ACC: MOL.20070430.0138. **180519**

2.2.32 Guenther, R.J.; Blahnik, D.E.; Campbell, T.K.; Jenquin, U.P.; Mendel, J.E.; and Thornhill, C.K. 1988. *Characterization of Spent Fuel Approved Testing Material--ATM-106.* PNL-5109-106. Richland, Washington: Pacific Northwest Laboratory. ACC: NNA.19911017.0105. **109206**

2.2.33 Guenther, R.J.; Blahnik, D.E.; Campbell, T.K.; Jenquin, U.P.; Mendel, J.E.; Thomas, L.E.; and Thornhill, C.K. 1988. *Characterization of Spent Fuel Approved Testing Material ATM--103.* PNL-5109-103. Richland, Washington: Pacific Northwest Laboratory. ACC: NNA.19911017.0104. **109205**

2.2.34 Hanson, B.D. 1998. *The Burnup Dependence of Light Water Reactor Spent Fuel Oxidation.* PNNL-11929. Richland, Washington: Pacific Northwest National Laboratory. TIC: 238459. **101672**

2.2.35 Holtec International 1995. *10 CFR 72 Topical Safety Analysis Report for the Holtec International Storage, Transport and Repository Cask System (HI-STAR 100 Cask System).* HI-941184, Rev. 3. [Marlton, New Jersey]: Holtec International. TIC: 249856. **131475**

2.2.36 ICRP (International Commission on Radiological Protection) 1994. *Human Respiratory Tract Model for Radiological Protection.* Volume 24, Nos. 1-3 of *Annals of the ICRP.* Smith, H., ed. ICRP Publication 66. [New York, New York]: Pergamon. TIC: 249223. **153705**

2.2.37 INEL (Idaho National Engineering Laboratory) 1996. *Safety Analysis Report for the INEL TMI-2 Independent Spent Fuel Storage Installation, Revision 0.* Docket 72-20. Idaho Falls, Idaho: U.S. Department of Energy, Idaho Operations Office. TIC: 233637. **103308**

2.2.38 INEL 1998. *Fort St. Vrain Independent Spent Fuel Storage Installation Safety Analysis Report, Revision 2.* Docket No. 72-09. Idaho Falls, Idaho: U.S. Department of Energy, Idaho Operations Office. ACC: MOL.20010721.0047. **155101**

2.2.39 Iwasaki, M.; Sakurai, T.; Ishikawa, N.; and Kobayashi, Y. 1968. "Oxidation of UO2 Pellets in Air: Effect of Heat-Treatment of Pellet on Particle Size Distribution of Powders Produced." *Journal of Nuclear Science and Technology, 5,* (12), 652-653. [Tokyo, Japan: Atomic Energy Society of Japan]. TIC: 255938. **172518**

2.2.40 Jain, V.; Cragnolino, G.; and Howard, L. 2004. *A Review Report on High Burnup Spent Nuclear Fuel — Disposal Issues.* CNWRA 2004-08. San Antonio, Texas: Center for Nuclear Waste Regulatory Analyses. ACC: MOL.20070220.0298. **178808**

2.2.41 Jardine, L.J.; Mecham, W.J.; Reedy, G.T.; and Steindler, M.J. 1982. *Final Report of Experimental Laboratory-Scale Brittle Fracture Studies of Glasses and Ceramics.* ANL-82-39. Argonne, Illinois: Argonne National Laboratory. TIC: 225736. **116838**

2.2.42 Jernkvist, L.O. and Massih, A.R. 2004. *Assessment of Core Failure Limits for Light Water Reactor Fuel Under Reactivity Initiated Accidents.* SKI Report 2005:16. Stockholm, Sweden: Swedish Nuclear Power Inspectorate. TIC: 259069. **178782**

2.2.43 Johnson, L.; Ferry, C.; Poinssot, C.; and Lovera, P. 2005. "Spent Fuel Radionuclide Source-Term Model for Assessing Spent Fuel Performance in Geological Disposal. Part I: Assessment of the Instant Release Fraction." *Journal of Nuclear Materials, 346,* 56-65. [New York, New York]: Elsevier. TIC: 259052. **178773**

2.2.44 Kohli, R.; Stahl, D.; Pasupathi, V.; Johnson, A.B.; and Gilbert, E.R. 1985. "The Behavior of Breached Boiling Water Reactor Fuel Rods on Long-Term Exposure to Air and Argon at 598 K." *Nuclear Technology, 69,* 186-197. La Grange Park, Illinois: American Nuclear Society. TIC: 245332. **126191**

2.2.45 Koo, Y-H.; Lee, B-H.; Cheon, J-S.; and Sohn, D-S. 2001. "Pore Pressure and Swelling in the Rim Region of LWR High Burnup UO{subcript 2} Fuel." *Journal of Nuclear Materials, 295,* 213-220. [New York, New York]: Elsevier. TIC: 257267. **178774**

2.2.46 Koo, Y-H.; Oh, J-Y.; Lee, B-H.; and Sohn, D-S. 2003. "Three-Dimensional Simulation of Threshold Porosity for Fission Gas Release in the Rim Region of LWR UO_2 Fuel." *Journal of Nuclear Materials, 321,* 249-255. [New York, New York]: Elsevier. TIC: 259053. **178775**

2.2.47 Lassmann, K.; Walker, C.T.; van der Laar, J.; and Lindstrom, F. 1995. "Modelling the High Burnup UO2 Structure in LWR Fuel." *Journal of Nuclear Materials, 226,* ([1-2]), 1-8. [Amsterdam, The Netherlands]: Elsevier. TIC: 247875. **119370**

2.2.48 Levy, I.S.; Chin, B.A.; Simonen, E.P.; Beyer, C.E.; Gilbert, E.R.; Johnson, A.B., Jr. 1987. *Recommended Temperature Limits for Dry Storage of Spent Light Water Reactor Zircaloy-Clad Fuel Rods in Inert Gas.* PNL-6189. Richland, Washington: Pacific Northwest Laboratory. TIC: 231836. **144349**

2.2.49 Liu, C.; Cox, D.S.; Barrand, R.D.; and Hunt, C.E.L. 1992. "Particle Size Distributions of U_3O_8 Produced by Oxidation in Air at 300-900ºC." *Proceeding of the 13th Annual Conference, Saint John, NB, June 7-10, 1992. 1,* 1-22. [Toronto, Ontario, Canada]: Canadian Nuclear Society. TIC: 256950. **172864**

2.2.50 Lorenz, R.A.; Collins, J.L.; and Malinauskas, A.P. 1979. "Fission Product Source Terms for the Light Water Reactor Loss-of-Coolant Accident." *Nuclear Technology, 46,* 404-410. [La Grange Park, Illinois: American Nuclear Society]. TIC: 242480. **158822**

2.2.51 Lorenz, R.A.; Collins, J.L.; Malinauskas, A.P.; Kirkland, O.L.; and Towns, R.L. 1980. *Fission Product Release From Highly Irradiated LWR Fuel.* NUREG/CR-0722. Washington, D.C.: U.S. Nuclear Regulatory Commission. TIC: 211434. **100990**

2.2.52 Luna, R.E.; Neuhauser, K.S.; and Vigil, M.G. 1999. *Projected Source Terms for Potential Sabotage Events Related to Spent Fuel Shipments.* SAND99-0963. Albuquerque, New Mexico: Sandia National Laboratories. ACC: MOL.19990609.0160. **104918**

2.2.53 MacDougall, H.R.; Scully, L.W.; and Tillerson, J.R., eds. 1987. *Nevada Nuclear Waste Storage Investigations Project, Site Characterization Plan Conceptual Design Report.* SAND84-2641. Volume 4, Appendices F-O. Albuquerque, New Mexico: Sandia National Laboratories. ACC: NN1.19880902.0017. **104779**

2.2.54 Manaktala, H.K. 1993. *Characteristics of Spent Nuclear Fuel and Cladding Relevant to High-Level Waste Source Term.* CNWRA 93-006. San Antonio, Texas: Center for Nuclear Waste Regulatory Analyses. TIC: 208034. **101719**

2.2.55 MathSoft. 2001. *Mathcad, User's Guide with Reference Manual, Mathcad 2001 Professional.* Cambridge, Massachusetts: MathSoft. TIC: 252786. **165446**

2.2.56 Matzke, H. and Spino, J. 1997. "Formation of the Rim Structure in High Burnup Fuel." *Journal of Nuclear Materials, 248,* 170-179. [New York, New York]: Elsevier. TIC: 259055. **178776**

2.2.57 McKinnon, M. A.; and Cunningham, M. E. 2003. *Dry Storage Demonstration for High-Burnup Spent Nuclear Fuel— Feasibility Study.* PNNL-14390. Richland, Washington: Pacific Northwest National Laboratory. ACC: submitted. **178809**

2.2.58 Mecham, W.J.; Jardine, L.J.; Pelto, R.H.; Reedy, G.T.; and Steindler, M.J. 1981. *Interim Report of Brittle-Fracture Impact Studies: Development of Methodology.* ANL-81-27. Argonne, Illinois: Argonne National Laboratory, Chemical Engineering Division. ACC: NNA.19890411.0034. **158827**

2.2.59 Mishima, J. and Olson, K.M. 1990. "Estimate of the Source Term for a Repository Surface Facility from the Routine Processing of Spent Fuel." *High Level Radioactive Waste Management, Proceedings of the International Topical Meeting, Las Vegas, Nevada, April 8-12, 1990. 2,* 1132-1137. La Grange Park, Illinois: American Nuclear Society. TIC: 202058. **160588**

2.2.60 NAC (Nuclear Assurance Corporation) 1995. *Safety Analysis Report for the NAC Legal Weight Truck Cask.* Revision 13. Docket Number 9225. T-88004. Norcross, Georgia: NAC International. TIC: 2449. **158874**

2.2.61 Novak, J.; Hastings, I.J.; Mizzan, E.; and Chenier, R.J. 1983. "Postirradiation Behavior of UO2 Fuel I: Elements at 220 to 250 Degrees C in Air." *Nuclear Technology, 63,* 254-263. La Grange Park, Illinois: American Nuclear Society. TIC: 217080. **125697**

2.2.62 NRC (U.S. Nuclear Regulatory Commission) 1975. *Reactor Safety Study: An Assessment of Accident Risks in U.S. Commercial Nuclear Power Plants.* WASH-1400. Washington, D.C.: U.S. Nuclear Regulatory Commission. TIC: 236923. **107799**

2.2.63 NRC 1997. *Standard Review Plan for Dry Cask Storage Systems*. NUREG-1536. Washington, D.C.: U.S. Nuclear Regulatory Commission. ACC: MOL.20010724.0307. **101903**

2.2.64 NRC 2000. *Standard Review Plan for Transportation Packages for Spent Nuclear Fuel*. NUREG-1617. Washington, D.C.: U.S. Nuclear Regulatory Commission. TIC: 249470. **154000**

2.2.65 NRC 2000. *Standard Review Plan for Spent Fuel Dry Storage Facilities*. NUREG-1567. Washington, D.C.: U.S. Nuclear Regulatory Commission. TIC: 247929. **149756**

2.2.66 NRC 2003. "Interim Staff Guidance - 5, Revision 1. Confinement Evaluation." ISG-5, Rev 1. Washington, D.C.: U.S. Nuclear Regulatory Commission. Accessed January 24, 2003. ACC: MOL.20030124.0247. http://www.ncr.gov/reading-rm/doc-collections/isg/spent-fuel.html. **160582**

2.2.67 PGE (Portland General Electric) n.d. *Trojan Independent Spent Fuel Storage Installation, Safety Analysis Report*. PGE-1069. Portland, Oregon: Portland General Electric. TIC: 243815. **103449**

2.2.68 Regulatory Guide 1.25, Rev. 0. 1972. Assumptions Used for Evaluating the Potential Radiological Consequences of a Fuel Handling Accident in the Fuel Handling and Storage Facility for Boiling and Pressurized Water Reactors. Washington, D.C.: U.S. Nuclear Regulatory Commission. ACC: MOL.20050329.0044. **107691**

2.2.69 Regulatory Guide 1.183. 2000. *Alternative Radiological Source Terms for Evaluating Design Basis Accidents at Nuclear Power Reactors*. Washington, D.C.: U.S. Nuclear Regulatory Commission. ACC: MOL.20050518.0242. **173584**

2.2.70 Regulatory Guide 1.195. 2003. *Methods and Assumptions for Evaluating Radiological Consequences of Design Basis Accidents at Light-Water Nuclear Power Reactors*. Washington, D.C.: U.S. Nuclear Regulatory Commission. ACC: MOL.20060105.0195. **166293**

2.2.71 SAIC (Science Applications International Corporation) 1998. *Nuclear Fuel Cycle Facility Accident Analysis Handbook*. NUREG/CR-6410. Washington, D.C.: U.S. Nuclear Regulatory Commission. ACC: MOL.20010726.0069. **103695**

2.2.72 Sanders, T.L.; Seager, K.D.; Rashid, Y.R.; Barrett, P.R.; Malinauskas, A.P.; Einziger, R.E.; Jordan, H.; Duffey, T.A.; Sutherland, S.H.; and Reardon, P.C. 1992. *A Method for Determining the Spent-Fuel Contribution to Transport Cask Containment Requirements*. SAND90-2406. Albuquerque, New Mexico: Sandia National Laboratories. ACC: MOV.19960802.0116. **102072**

2.2.73 Sandoval, R.P.; Einziger, R.E.; Jordan, H.; Malinauskas, A.P.; and Mings, W.J. 1991. *Estimate of CRUD Contribution to Shipping Cask Containment Requirements*. SAND88-1358. Albuquerque, New Mexico: Sandia National Laboratories. ACC: MOV.19960802.0114. **103696**

2.2.74   Shetler, J.R. 1993. "Docket No. 72-11, Rancho Seco Independent Spent Fuel Storage Installation, Revision 1 to the Rancho Seco Independent Spent Fuel Storage Installation License Application and Safety Analysis Report." Letter from J.R. Shetler (SMUD) to R.E. Cunningham (NRC), October 27, 1993, DAGM/NUC 91-135, with attachment. TIC: 226550. **157601**

2.2.75   SNC (Sierra Nuclear Corporation) 1996. *Safety Analysis Report for the TranStor™ Storage Cask System.* SNC-96-72SAR, Revision A. Scotts Valley, California: Sierra Nuclear Corporation. TIC: 248383. **150946**

2.2.76   SNC 1997. *Safety Analysis Report for the TranStor™ Shipping Cask System.* SNC-95-71SAR, Rev. 2. Scotts Valley, California: Sierra Nuclear Corporation. TIC: 243170. **141465**

2.2.77   Spino, J.; Stalios, A.D.; Santa Cruz, H.; and Baron, D. 2006. "Stereological Evolution of the Rim Structure in PWR-Fuels at Prolonged Irradiation: Dependencies with Burn-Up and Temperature." *Journal of Nuclear Materials, 354,* 66-84. [New York, New York]: Elsevier. TIC: 259066. **178778**

2.2.78   Spino, J.; Vennix, K.; and Coquerelle, M. 1996. "Detailed Characterisation of the Rim Microstructure in PWR Fuels in the Burn-Up Range 40-67 GWd/tM." *Journal of Nuclear Materials, 231,* 179-190. [New York, New York]: Elsevier. TIC: 257447. **174080**

2.2.79   Sprung, J.L.; Ammerman, D.J.; Breivik, N.L.; Dukart. R.J.; Kanipe, F.L.; Koski, J.A.; Mills, G.S.; Neuhauser, K.S.; Radloff, H.D.; Weiner, R.F.; and Yoshimura, H.R. 2000. *Reexamination of Spent Fuel Shipment Risk Estimates.* NUREG/CR-6672. Two volumes. Washington, D.C.: U.S. Nuclear Regulatory Commission. ACC: MOL.20001010.0217. **152476**

2.2.80   Stone, J.A.; Johnson, D.R. 1979. "Measurement of Radioactive Gaseous Effluents from Voloxidation and Dissolution of Spent Nuclear Fuel. "*Proceedings of the Fifteenth DOE Nuclear Air Cleaning Conference.* First, M.W. (ed.). *CONF-780819-P2,* pp.570-583. Washington, DC: U.S. DOE. TIC: 202122. **180521**

2.2.81   Transnuclear 1989. *TN-24 Dry Storage Cask Topical Report.* E-7107. Hawthorne, New York: Transnuclear. TIC: 232651. **158882**

2.2.82   Une, K.; Hirai, M.; Nogita, K.; Hosokawa, T.; Suzawa, Y.; Shimizu, S.; and Etoh, Y. 2000. "Rim Structure Formation and High Burnup Fuel Behavior of Large-Grained UO_2 Fuels." *Journal of Nuclear Materials, 278,* 54-63. [New York, New York]: Elsevier. TIC: 259068. **178780**

2.2.83   Van Wylen, G.J. and Sonntag, R.E. 1986. *Fundamentals of Classical Thermodynamics.* New York, New York: John Wiley & Sons. TIC: 245655. **108881**

2.2.84   Vectra Technologies 1995. *Safety Analysis Report for the Standardized NUHOMS® Horizontal Modular Storage System for Irradiated Nuclear Fuel.* NUH-0003, Rev. 3A.

Volume 1. Docket 72-1004. San Jose, California: Vectra Technologies. TIC: 104635. **157643**

2.2.85 Vectra Technologies 1996. *Safety Analysis Report for the NUHOMS®-MP187 Multi-Purpose Cask*. NUH-05-151, Rev. 2. Two volumes. Docket 71-9255. San Jose, California: Vectra Technologies. TIC: 233483. **105288**

2.2.86 Virginia Electric and Power Company 1995. *North Anna Power Station Independent Spent Fuel Storage Installation, License Application*. Docket No. 72-16. Richmond, Virginia: Virginia Electric and Power Company. TIC: 104549. **158884**

2.2.87 Walker, C.T.; Bagger, C.; and Mogensen, M. 1996. "Observations on the Release of Cesium from UO[sub]2 Fuel." *Journal of Nuclear Materials, 240,* (1), 32-42. Amsterdam, The Netherlands: Elsevier. TIC: 246925. **143273**

2.2.88 Weast, R.C. ed. 1972. *CRC Handbook of Chemistry and Physics*. 53rd Edition. Cleveland, Ohio: Chemical Rubber Company. TIC: 219220. **127163**

2.2.89 Westinghouse 1996. *Safety Analysis Report Large On-Site Transfer and On-Site Storage Segment, CLIN 0004PC*. MPC-CD-02-016, Rev. 1. Monroeville, Pennsylvania: Westinghouse Government and Environmental Services Company. ACC: MOV.19961028.0056. **130528**

2.2.90 Wilmot, E.L. 1981. *Transportation Accident Scenarios for Commercial Spent Fuel*. SAND80-2124. Albuquerque, New Mexico: Sandia National Laboratories. ACC: HQO.19871023.0215. **104724**

2.3 DESIGN CONSTRAINTS

None

2.4 DESIGN OUTPUTS

This analysis does not support any specific engineering drawing, specification, or design list. The results of this analysis are used as inputs for other preclosure safety analyses.

INTENTIONALLY LEFT BLANK

3. ASSUMPTIONS

3.1 ASSUMPTIONS REQUIRING VERIFICATION

The assumption listed in this section is based on preliminary results from the PNNL fuel in air tests. Final report of the tests is not available. Test data sent via E-mail are used in this document, as included in Attachment D. Information from the E-mail is treated as an assumption requiring verification, and the assumption is tracked using *Desktop Information for Using Calctrac* (Reference 2.1.2).

3.1.1 Particle Size Distribution of Fuel Oxidation Powder

Particle size distributions of fuel oxidation powder are similar between high burnup fuel and low burnup fuel in terms of particle volume (or mass).

Rationale: Release tests of fuel oxidation powder were performed at PNNL using powder oxidized from ATM-109A fuel (about 60 GWd/MTU) and ATM-105 fuel (about 30 GWd/MTU). Particle size distribution was measured by an optical particle counter in a range of 0.5 to 20 μm. Particle size distributons measured for oxidation powder from both types of fuel indicate that the volumetric size distributions are similar. The preliminary test data were sent through email and data processing are discussed in Attachment D.

Usage: This assumption is used to limit a condition of fuel oxidation in Section 6.6.4.

3.2 ASSUMPTIONS NOT REQUIRING VERIFICATION

3.2.1 Fuel Rod Damage

A guillotine break or a longitudinal split of a fuel rod is not considered credible in a repository accident.

Rationale: The mechanism of fuel failure in this analysis is consistent with the failure mechanisms considered in SAND80-2124 (Reference 2.2.90 [DIRS 104724], p.11), which defines an impact rupture as a rupture of the cladding produced by bending or other deformation of a fuel rod. No mention is made of a guillotine break or longitudinal split. Intact fuel is also considered rugged and capable of sustaining severe impact environments (Reference 2.2.90 [DIRS 104724], p.18). Chun et al. states that the weakest fuel assembly, the Westinghouse 17 × 17, can sustain a static load in bending equivalent to 63 g's at 380°C without exceeding the cladding yield strength (Reference 2.2.16 [DIRS 144357], Section 4.0).

Usage: This assumption is used to limit the severity of fuel rod damage to be considered in the analysis in Sections 6.1 and 6.5.4. This assumption does not apply to cladding split due to fuel oxidation after an accident.

3.2.2 Crud Respirable Fraction for PWR and BWR Fuel

The respirable fraction for crud from both PWR and BWR fuel is 1.

Rationale: This is a bounding assumption. Particle size distribution of crud from BWR fuel has been determined to have a mean geometric diameter (MGD) of 3.0 μm, and a geometric standard deviation (GSD) of 1.87 (Reference 2.2.73 [DIRS 103696], p.II-5). The respirable fraction is estimated using the BWR crud particle size distribution in Section 6.2.3. However, there is no data available for crud particle size from PWR fuel. It is expected that the PWR crud particles are smaller than those considered for the BWR fuel (Reference 2.2.73 [DIRS 103696], pp.23 to 26). Therefore, the respirable fraction is conservatively taken as 1.

Usage: This assumption is used for the respirable fraction for both PWR and BWR crud in Section 6.2.3.

3.2.3   Initial Particle Size for Fuel Fines

The mass median diameter (MMD) of material initially released into air from commercial SNF is 150 μm.

Rationale: This assumption is based on fuel fines collected from burst rupture tests in NUREG/CR-0722 (Reference 2.2.51 [DIRS 100990], p.105 and Appendix C). These tests provided release fractions from commercial SNF. The tests conducted by Lorenz et al. (Reference 2.2.51 [DIRS 100990]) are based on a spent fuel burnup of approximately 30 GWd/MTU, which may be lower than the burnup of some commercial SNF accepted at the repository. The discussion of high burnup fuel is provided in Section 6.5. The fuel fines were measured with a scanning electron microscope and determined to be "typically 150 μm" in diameter in the furnace tube near the point of the fuel pin rupture. This represents more than 97 percent of the total mass released from the burst rupture tests (Reference 2.2.51 [DIRS 100990], Table 42). Given that 97% of the release has a diameter of 150 μm, the MMD for the total release would not be significantly different when the other 3% of the mass is included.

A MMD of 150 μm may be considered conservative when applied to drop or impact events, because larger particulates are likely to be initially aerosolized in these events due to the brittle nature of the fuel (assuming reasonable drop heights). The impact tests on unclad, depleted, ceramic UO_2 pellets in ANL-81-27 (Reference 2.2.58 [DIRS 158827], p.26, pp.34 to 35) indicate that MMDs measured are in a range of 18 mm and 32 mm (not μm). These MMDs are significantly larger than the 150-μm MMD assumed in this analysis for the initially aerosolized commercial SNF. Because larger particles are essentially irrespirable and carry a large portion of the total mass, larger MMDs equate to smaller respirable fractions (RFs) with other parameters being equal (e.g., the standard deviation). Thus, the selection of 150-μm to represent the MMD of initially released material into air from commercial SNF due to a drop or impact event is a conservative assumption.

Another series of tests performed on single pellets of UO_2 by Alvarez is cited in SAND90-2406 (Reference 2.2.72 [DIRS 102072], Section IV-4). Alvarez performed a series of tests on pellets of clad UO_2 that were both depleted and irradiated. These tests involved the detonation of explosive charges near the fuel. This resulted in a significantly greater amount of energy imparted to the fuel than occurred in the burst rupture tests or a drop or impact event considered in this analysis. Hence, the measured MMDs from these tests, which ranged from approximately 30 to 100 μm, are not considered applicable to this analysis. The difference, however, between

the 100-µm MMD from Alvarez's explosive tests and the 150-µm diameter considered in this analysis are not significant.

The selection of MMD of 150 µm is based on the preceding technical bases, and on NUREG/CR-0722 (Reference 2.2.51 [DIRS 100990], p.105 and Appendix C), which provides the release fractions recommended in guidance documents that are applicable to NRC licensed facilities, such as NUREG-1536 (Reference 2.2.63 [DIRS 101903], Table 7.1) and NUREG/CR-6487 (Reference 2.2.4 [DIRS 145345], Table 6-2).

Usage: This assumption is used to determine the respirable fraction of fuel particles initially released during an accident event. More discussion and usage of this assumption is given in Section 6.2.2.1.

3.2.4   Mass Fraction of Fuel Particles

Three percent of the total mass of material initially released into air from commercial SNF fuel fines has a geometric diameter of less than 12 µm.

Rationale: This assumption is based on fuel fines collected from burst rupture tests described in NUREG/CR-0722 (Reference 2.2.51 [DIRS 100990], p.105). In these burst rupture tests, it was determined that only a small fraction, 0.8 to 2.9 percent, of the fuel mass ejected from the fuel was carried out of the furnace tube into the thermal gradient tube and filter pack (Reference 2.2.51 [DIRS 100990], Table 42). The fraction was determined using the mass in the thermal gradient tube and the filter packs divided by the total mass released, as shown in Reference 2.2.51 ([DIRS 100990], Table 42). Considering the deposition of the released fuel particles due to gravity, fuel particles of diameters greater than 12 to 15 µm are considered to have settled out before reaching the thermal gradient tube. The most conservative interpretation of these data with respect to the respirable fraction is to select the highest release fraction (i.e., 3 percent) and the smallest diameter (i.e., 12 µm). This results in the calculation of a conservative respirable fraction.

This assumption is based on the preceding technical arguments, the confirmatory analysis in Attachment A, and the fact that these data come from a source (Reference 2.2.51 [DIRS 100990], p.105) that is commonly cited for establishing release fractions for commercial SNF.

Usage: This assumption is used to determine respirable fraction of fuel particles initially released during an accident, which is used in Section 6.2.2.1.

3.2.5   Damage of Failed Fuel in Canister

Mechanically damaged commercial SNF and cladding-penetration damaged commercial SNF (both of which are received in canisters and both of which include some assembly-like structure) do not pulverize under a drop or impact event. Fuel rods, pieces, debris, and non-fuel components (which are also contained in canisters but without an assembly-like structure) can be pulverized up to 20% under a drop or impact event.

Rationale: All failed commercial SNF received at the repository will be contained in a canister (Reference 2.2.20 [DIRS 145022], p.C-1). For mechanically damaged commercial SNF and cladding-penetration damaged commercial SNF (both of which are received in canisters and both of which include some assembly-like structure), the canister structure, cladding, and grids/spacers provide sufficient structural support to prevent the fuel from undergoing any significant amount of pulverization. If a drop or impact event occurs, the assembly-like structure limits the release of fuel particles to only through the damaged structure. Since some of the fuel rods are already damaged, fission gases have already escaped and there is no high pressure inside the damaged fuel rods thus limiting the amount of radionuclides released. The undamaged rods in the assembly may burst due to the drop and impact, and the high pressure inside of these fuel rods pushes the radionuclides out of the rod, which is a process similar to the burst rupture tests.

The release from a canister containing fuel rods, debris, and pieces due to a drop or impact event is based on impact rupture tests. Because the event damages the canister and then fractures the fuel pellets, a fraction of fuel particles are released, which is a process similar to the impact rupture tests. The support provided by the canister for fuel rods, pieces, and debris minimizes the amount of fuel to be pulverized. The value of 20 percent is selected because the canister absorbs some impact energy; it is based on the similar conservative assumption made in SAND84-2641 (Reference 2.2.53 [DIRS 104779], pp. 5-15 to 5-26).

Usage: This assumption is used for justifying that ARFs for failed commercial SNF are bounded by the ARFs developed for intact commercial SNF in Section 6.3. It is also used for calculating ARFs for failed fuel rods, debris and pieces.

3.2.6   Availability of Oxygen During Fuel Oxidation

Sufficient oxygen is available for complete spent fuel oxidation from UO_2 to U_3O_8 to occur.

Rationale: The fuel rod defect size or breach size due to an accident has significant impact on the fuel oxidation process because the availability of oxygen may be limited. EPRI NP-4524 (Reference 2.2.28 [DIRS 127313], p. iii) determined that both the size and shape of the cladding defect appear to influence the time to cladding splitting. For high temperatures (above 283°C), the time to cladding splitting was longer for the sharp small defect than for the large circular defect. For example, the incubation time for a 27 μm defect at 360°C was found to be between 52 and 60 hours, while the incubation time for a 760 μm defect at the same temperature was 20 hours (Reference 2.2.28 [DIRS 127313], Table 3-3). From EPRI NP-4524, the larger the defect size, the shorter the incubation time. In addition, the larger the defect, the more oxygen that could become available, which could then cause more oxidation and reduce the incubation time still further. This effect may be valid only for defects small enough such that the size limits oxygen availability.

 Einziger and Strain (Reference 2.2.25 [DIRS 172756], p.605) also discuss the effects of cladding damage size on incubation time. The incubation time varied inversely with the size of the original defect implying that the defect size was inhibiting access of oxygen through the cladding to the fuel. This effect is shown in Einziger and Strain (Reference 2.2.25 [DIRS 172756], Figure 8).

Although the defect size and shape may have an impact on oxygen availability, during an event involving drop or collisions of SNF assemblies, it would be difficult to quantify the type, size, and shape of defects that may occur. Therefore, no credit is taken for the oxidation retardation effects of pinholes and hairline cracks.   In other words, under this assumption, sufficient oxygen is always available to support complete oxidation of commercial SNF, no matter how small the defect size.   This is a conservative assumption, particularly for a small defect where the availibity of oxygen may be limited, and one that results in the most conservative result for incubation time.

Usage: This assumption is used to estimate the maximum fuel oxidation after an accident in Section 6.4.

3.2.7   Fuel Oxidation Time after an Accident

For purposes of determining the fraction of fuel oxidized after an accident, it is assumed that recovery actions to limit oxidation release are taken within 30 days (720 hours) after the event.

Rationale: If a waste package or canister is breached during an accident, spent fuel can be exposed to air and, if the cladding has failed, begin to oxidize. Although measures can be taken to limit post-accident oxidation (e.g., cooling), it is conservative to assume that the oxidation continues unabated until the accident is terminated by recovering materials safely and/or placing the facility into a safe condition. Recovery actions to limit releases are not expected to exceed 30 days (Reference 2.2.66 [DIRS 160582], Table 7.1).

Usage: This assumption is used to estimate the fraction of fuel oxidation after an accident in Section 6.4.

INTENTIONALLY LEFT BLANK

4. METHODOLOGY

4.1 QUALITY ASSURANCE

This analysis is prepared in accordance with EG-PRO-3DP-G04B-00037, *Calculations and Analyses* (Reference 2.1.3). The release fraction values developed in this analysis are used to support radiological consequence calculations for the Yucca Mountain License Application. Therefore, this analysis is subject to the *Quality Management Directive* (Reference 2.1.7). The *Desktop Information for Format of Calculations and Analyses and Treatment of Inputs and Assumptions,* EG-DSK-3003 (Reference 2.1.1) is used as guidance. LS-PRO-0201, *Preclosure Safety Analyses Process* (Reference 2.1.5), is also followed in the preparation of the analysis. Input data are identified and tracked in accordance with PA-PRO-0301, *Managing Technical Product Inputs* (Reference 2.1.6) because all inputs in this document are currently located in the Document Input Reference System (DIRS). Per Section 3.3.2.F of EG-PRO-3DP-G04B-00037, input links are developed for those references located within Infoworks. Software used for the calculations is tracked in accordance with IT-PRO-0011, *Software Management* (Reference 2.1.4).

4.2 USE OF COMPUTER SOFTWARE

The variable input parameters used to calculate respirable fractions (i.e., mean geometric diameter, geometric standard deviation, particle density, dynamic shape factor, and maximum respirable or cut-off particle diameter) are described in Section 6.2. Mathcad 13 (Reference 2.2.55 [DIRS 165446]) is used to convert number particle size distribution to mass particle size distribution. Mathcad 13 is classified as Level 2 software usage per IT-PRO-0011, *Software Management*, that is not required to be qualified in accordance with IT-PRO-0011. The calculations were verified using known inputs in the Mathcad application to ensure correct results.

The Microsoft Excel 2000 spreadsheet program is used to perform simple calculations as documented in Section 6. User-defined formulas, input, and results are documented in sufficient detail in Section 6 to allow for independent duplication of various computations without recourse to the originator. Excel is classified as Level 2 software usage per IT-PRO-0011, *Software Management*, that is not required to be qualified in accordance with IT-PRO-0011. The calculations were verified with hand calculations.

4.3 METHODS

Commercial SNF assemblies or confinement systems (e.g., casks, canisters, or waste packages) that contain assemblies may become involved in an accident event sequence at the repository. Such accidents could potentially compromise the confinement boundaries that prevent or reduce the amount of radioactive material released from fuel assemblies during the event sequences. Confinement boundaries include fuel structure, fuel cladding, container confinement boundaries, and facility confinement boundaries. Radioactive material may be released in the form of gases, volatiles, or particulates.

In addition to the confinement boundaries, the physical properties of commercial SNF fuel fines and crud (surface deposits) affect the calculated radiation dose resulting from event sequences

involving commercial SNF assemblies. In particular, the distribution of particle sizes (diameters and masses) affects the fraction of material that is locally deposited as opposed to the fraction that remains airborne (as an aerosol) long enough to reach potential offsite or onsite receptors. Furthermore, only the respirable fraction of aerosolized fuel fines and crud that reach a receptor contributes significantly to inhalation doses.

4.3.1 Definitions of Release Fractions

As discussed in Section 1.1, the purpose of this analysis is to specify and document two important accident parameters: the airborne release fraction and the respirable fraction, which are defined as follows:

> Airborne Release Fraction (ARF): the coefficient used to estimate the amount of a radioactive material that can be suspended in air and made available for airborne transport under a specific set of induced physical stresses. It is applicable to events and situations that are completed during the course of the event.

> Respirable Fraction (RF): the fraction of airborne radionuclides as particles that can be transported through air and inhaled into the human respiratory system and is commonly assumed to include particles 10-μm Aerodynamic Equivalent Diameter (AED) and less.

The analysis first addresses the ARFs for commercial SNF following an event sequence at the repository that involves either a drop of or an impact to a shipping cask, canister, or waste package loaded with commercial SNF or an uncanistered, unconfined commercial SNF assembly, or canistered failed commercial SNF. In the analysis, the event occurs in a dry environment (i.e., not in a pool). After the ARFs have been determined for commercial SNF, the fraction of the airborne material that is respirable (RF) is determined.

The methodology applied in this analysis is consistent with those presented in NUREG/CR-6410 (Reference 2.2.71 [DIRS 103695], Section 3.2.5.2) and DOE-HDBK-3010-94 (Reference 2.2.24 [DIRS 103756], Section 1.2).

An ARF for each radionuclide, or appropriate grouping of radionuclides (e.g., fuel fines), released from commercial SNF is determined from experimental data, analyses, or previous precedents established in documents approved by the NRC or conservative estimates, or both. Attachment B includes a summary of some of the fractions used in licensing documents for other nuclear facilities. The definition of ARF and RF above is also applicable to HLW as dicussed in Section 4.3.7 and 6.7.

4.3.2 Airborne Release Fractions

The ARFs presented in literature shown in Section 6.1.1 are considered for intact commercial SNF. The original source of input data considered is from the burst rupture tests conducted by Lorenz et al. (Reference 2.2.51 [DIRS 100990]). Analyses are performed for each group of radionuclides: gases, volatiles, fuel fines and crud from the commercial SNF. ARFs are determined based on these analyses and an assessment of the various ARFs found in the published literature. Justifications of the applicability of the ARF values for use in Yucca

Mountain repository radiological dose calculations are provided. The analyses are documented in Section 6.1.

4.3.3   Respirable Fractions

The method to determine the RF for particulates from commercial SNF fuel fines and crud is presented in Section 6.2. In general, the RF is determined by comparing the mass fraction of released particles that are respirable to the total release from the burst rupture. These mass fractions can be obtained from a cumulative mass distribution if a particle size distribution is known. For intact commercial SNF, the RF of the aerosolized particulates measured in various burst rupture tests (Reference 2.2.51 [DIRS 100990]) is quantified. From the test results of particles released from a segment of fuel rod, a particle size distribution is interpreted and assumed (see Assumptions 3.2.3 and 3.2.4). Calculations are performed in Mathcad, and the corresponding files are attached to this document and listed in Attachment E.

4.3.4   Release from Impact Events

Experiments reported in ANL-81-27 (Reference 2.2.58 [DIRS 158827], p.26, pp.34 to 35, and Table 2) and ANL-82-39 (Reference 2.2.41 [DIRS 116838]) provide data that are applicable to a drop or impact event that involves material pulverization. The experiments involved unconfined (i.e., no cladding) glass and UO_2 ceramic specimens impacted by dropped weights.

The test data from the experiments may be used to generate a pulverization fraction (PULF), which is defined as the fraction of airborne material that is respirable and is numerically equal to the product of ARF and RF. It should be noted that these test data and their associated pulverization fractions may not be appropriate without modifications for application to dropped or impacted intact fuel assemblies because the surface area of the impacting component (i.e., the fuel assembly) is smaller than the surface impacted (i.e., the ground) (Reference 2.2.71 [DIRS 103695], p.3-87).

The relationship for determining the PULF provided in SAND84-2641 (Reference 2.2.53 [DIRS 104779], p.5-17) is based on the experimental data collected in ANL-81-27 (Reference 2.2.58 [DIRS 158827]). This relationship, as given in SAND84-2641 (Reference 2.2.53 [DIRS 104779], p.5-17), is as follows:

$$PULF = \frac{Impact\,Energy}{Specimen\,Volume} = (2 \times 10^{-4}) \times \frac{E}{V} \qquad\qquad \text{Equation 1}$$

The coefficient of 2×10^{-4} is from the fraction of respirable airborne particulates (i.e., sizes less than 10 μm physical diameter, as shown in Figure 3 and Figure 4) of the initial UO_2 specimen mass at an impact energy density of 1.2 J/cm^3. Because a respirable particle is commonly defined as 10 μm and less AED instead of 10 μm physical diameter, the PULF equation above is very conservative.

The impact energy term in Equation 1 can be determined as the potential energy imparted by a drop event (i.e., $E = m\,g\,h$). Substituting the material density (ρ) in place of the mass (m) over the volume (V), the expression may be restated as:

$$PULF = A \times \rho \times g \times h \qquad\qquad \text{Equation 2}$$

where

> A = an empirical correlation equal to 2×10^{-11} cm-s^2/g, which comes from the Equation 1 coefficient of 2×10^{-4} and other factors from unit conversions,
> ρ = particle density (g/cm^3),
> g = gravitational acceleration (980 cm/s^2),
> h = fall height (cm).

Equation 2 is presented in DOE-HDBK-3010-94 (Reference 2.2.24 [DIRS 103756], Section 4.3.3), based on SAND84-2641 (Reference 2.2.53 [DIRS 104779], p.5-17). For UO_2, the value of the empirical correlation is based on two experimental data points from single energy density (1.2 J/cm^3) impaction tests on three unconfined UO_2 pellets (Reference 2.2.58 [DIRS 158827], Table 2 and pp.30 to 35). The linearity of the correlation with respect to fall height is not based on data for UO_2, but is based on impaction tests for Pyrex and SRL 131 (Savannah River Site glass frit) over the range of energy densities of 1.2 to 10 J/cm^3 (Reference 2.2.41 [DIRS 116838], Figure 13 and pp.28 to 31). For Pyrex, the linearity is poor at low energy densities.

In an attempt to correct some of the conservatism associated with extrapolating small specimen impact test data to large masses of glass or ceramic materials, SAND84-2641 (Reference 2.2.53 [DIRS 104779], pp.5-15 to 5-26) modified the PULF correlation by including an energy partition factor (EPF) to account for the energy absorbed by components of a fuel assembly (e.g., cladding, spacer grids, nozzles) and the non-uniform energy density impact applied to a dropped fuel assembly. The value of the EPF is further discussed in Section 6.3.2.3.

In addition, the mass fraction as a function of particle size provided by impact rupture tests (Reference 2.2.58 [DIRS 158827], Figures 16 and 17) is used to calculate the RF directly from the airborne release fraction and respirable release fraction, which is discussed in 6.2.2.2.

The ARFs and RFs applicable to failed commercial SNF are discussed in Section 6.3.

4.3.5   Spent Fuel Oxidation

Hanson (Reference 2.2.34 [DIRS 101672], Section 2.1) describes the oxidation of spent fuel in air as a two-step process of the form $UO_2 \rightarrow UO_{2.4} \rightarrow U_3O_8$. The transition from $UO_2 \rightarrow UO_{2.4}$ does not result in appreciable fuel pellet density changes. However, the transition from $UO_{2.4} \rightarrow U_3O_8$ results in a volume expansion due to density reduction from 10.96 g/cm^3 to 8.35 g/cm^3 (Reference 2.2.34 [DIRS 101672], Table 2.1). The increase in volume as spent fuel oxidizes to U_3O_8 places stress on portions of unfailed cladding, which may cause cladding splitting and expose more spent fuel to air. Furthermore, the oxidized U_3O_8 is in a powder form whose particle size distribution depends on the temperature and spent fuel burnup. The U_3O_8 powder could

become airborne after an accident through ventilation flow or because of recovery actions that disturb the powder.

The split fractions of fuel rod cladding for PWR and BWR fuel rods are estimated based on the highest allowed cladding temperature, 400°C, and an average burnup. Based on the estimate (see the Excel file listed in Attachment E), almost entire length of a fuel rod is split and the UO_2 fuel is fully oxidized. Using this conservative estimate, the ARFs and RFs for gases and volatiles are selected based on the experimental data on fully oxidized high burnup fuel in a recently published paper (Reference 2.2.17 [DIRS 179470], pp.229-242), while the ARFs and RFs for particulates are selected using analog experimental data in DOE-HDBK-3010-94 (Reference 2.2.24 [DIRS 103756], Section 4.4.1.1). The radionuclide release from the oxidized spent fuel after an accident scenario is in addition to the initial burst release from the accident. The ARFs and RFs for fuel oxidation are discussed and recommendations are provided in Section 6.4.

4.3.6   Spent Nuclear Fuel Burnup

The assembly-average burnup level for commercial SNF was less than 40 GWd/MTU before the early 1990s, with the exception of lead test assemblies. Today, the majority of the spent fuel discharged has a burnup level in excess of 45 GWd/MTU (Reference 2.2.57 [DIRS 178809], Section 2.2). Spent nuclear fuel exceeding 45 GWd/MTU is classified as high burnup fuel (Reference 2.2.40 [DIRS 178808], p.1-1). The current reactor operating burnup limit is 62 GWd/MTU (peak rod), and the nuclear industry is pursuing an increase of peak rod burnup from 62 to 75 GWd/MTU. It is estimated that 30 percent of the spent nuclear fuel to be received at the Yucca Mountain repository could potentially be classified as high burnup fuel (Reference 2.2.40 [DIRS 178808], p.1-1).

The characteristics and radionuclide inventories of representative and bounding commercial PWR and BWR SNF have been developed (Reference 2.2.13 [DIRS 180185], Table 19 and Table II-1). Table 1 summarizes the four different combinations of initial enrichment, burnup, and decay time for the source term used in the preclosure consequence analysis. The representative PWR and BWR SNF assemblies have a burnup of 50 GWd/MTU, which are categorized as low burnup fuel for this document only. The Bounding BWR assembly has a burnup of 75 GWd/MTU and the bounding PWR assembly has a burnup of 80 GWd/MTU, which are categorized as high burnup fuel for this document only. The reason of this categorization is to set each type of fuel with an appropriate release fraction considered in this document.

Table 1. PWR and BWR Spent Fuel Assemblies

Spent Fuel Assembly	Initial Enrichment (Percent)	Burnup (GWd/MTU)	Decay Time (Years)	Category
Representative PWR	4.2	50	10	Low burnup fuel
Bounding PWR	5	80	5	High burnup fuel
Representative BWR	4.0	50	10	Low burnup fuel
Bounding BWR [b]	5	75	5	High burnup fuel

Source: Reference 2.2.13 [DIRS 180185], Table 19 and Table II-1

PWR = pressurized water reactor; BWR = boiling water reactor;
GWd = gigawatt days; MTU = metric tons uranium.

The characteristics of high burnup fuel that were not considered in the previous preclosure consequence analyses are included in Section 6.5. The release fractions associated with high burnup spent fuel based on the literature data are discussed in Section 6.5; the impacts on ARF and RF when high burnup fuel undergoes oxidation are addressed in Section 6.6.

4.3.7   High Level Radioactive Waste

As mentioned in Section 1.2, defense HLW canisters are received and processed within the CRCF, and may be also received and processed in the IHF. The release of radioactive material from HLW occurs only when a canister of HLW is breached during a drop or impact event. Therefore, the PULF equation provided in Section 4.3.4 is applicable to HLW canister. Section 6.7 of this document discusses release fractions for HLW canisters.

5. LIST OF ATTACHMENTS

INTENTIONALLY LEFT BLANK

6.   ANALYSES AND CALCULATIONS

This section contains the analyses and calculations of the airborne release fractions and respirable fractions for various radionuclides from different sources. The ARFs and RFs for intact commercial SNF are discussed in Section 6.1 and Section 6.2. The ARFs and RFs for failed or damaged commercial SNF (Section 6.3) are also analyzed and compared with intact commercial SNF. Release fractions for oxidation after spent fuel UO_2 is exposed to air due to an accident are considered and calculated in Section 6.4. Characteristics of high burnup fuel as well as release fractions from high burnup fuel with and without fuel oxidation are discussed in Sections 6.5 and 6.6. The ARF and RF for HLW are developed based on current repository facility design as documented in Section 6.7.

6.1   AIRBORNE RELEASE FRACTIONS FOR INTACT COMMERCIAL SNF

The ARFs from commercial SNF account for the fact that some of the commercial SNF radionuclides are retained in the fuel matrix or exist in a chemical or physical form that is not capable of being released under credible accident conditions. The documents containing release fractions reviewed in this analysis and their sources are provided in Section 6.1.1. Based on the data from these reviewed documents, the ARFs are determined for intact commercial SNF.

6.1.1   Literature Review and Input Data

Input parameters for ARF in this analysis are taken from published literature, principally from the NRC regulatory guidance and NUREG reports. Some references do not use the term ARF. They use instead fractions available for release, or release fractions. These release fractions may include large particles that are not suspended in air for a very long time. Treating these release fractions as equivalent to ARFs is a conservative approach because the airborne particles are only a fraction of all released particles.

Table 2 lists the twelve references that provide the ARFs (fractions available for release, or release fractions) for commercial SNF. All of them are considered reliable sources. Eight out of twelve documents are either NRC regulatory guidance or NUREG reports. The other four include an American National Standards Institute (ANSI) standard, a DOE handbook, and two testing reports from Argonne National Laboratory (ANL). These documents were used as the basis for various NRC license applications for the handling, transport, and storage of commercial SNF, and are applicable to the credible accident scenarios at the repository. Therefore, the recommended values from these reference sources are appropriate for use in accident consequence calculations for the Yucca Mountain repository.

Table 2. References for Release Fractions

Source Document	Data Available	Comments
ANL-81-27 (Reference 2.2.58 [DIRS 158827])	Experimental data on impact tests for fuel fines	Measured release fractions from the impact tests on bare unclad UO_2 pellets and simulated vitrified glass. It provides the release fractions as a function of particle size based on the tests, which can be used as inputs for respirable fractions based on impact events.
ANL-82-39 (Reference 2.2.41 [DIRS 116838])	Experimental data on impact tests for fuel fines	Measured release fractions for various materials in many impact tests. It provides the linearity of respirable release fraction as a function of energy density in a range of interest.
ANSI/ANS-5.10-1998 (Reference 2.2.6 [DIRS 103755], Table A1)	ARFs for gases, fuel fines, volatiles, crud	Generic ARFs for gases, fuel fines and crud are taken from several different sources based on crush/impact tests. It also recommends the release fraction for HLW.
DOE-HDBK-3010-94 (Reference 2.2.24 [DIRS 103756])	ARFs for gases, fuel fines	Generic ARFs and RFs are provided based on a compendium and analysis of experimental data for various scenarios. It provides inputs for ARFs and RFs that can be used for commercial SNF and HLW for impact events
ISG-5 (Reference 2.2.66 [DIRS 160582], Table 7.1)	ARFs for gases, fuel fines, volatiles, crud	Fractions available for release are considered the same as ARFs, and their values are cited from NUREG/CR-6487 (Reference 2.2.4 [DIRS 145345]), as shown in Table 3
NUREG-1536 (Reference 2.2.63 [DIRS 101903], Table 7.1)	ARFs for gases, fuel fines, volatiles, crud	Fractions available for release are considered the same as ARFs, and their values are cited from Regulatory Guide 1.25 (Reference 2.2.68 [DIRS 107691]) and SAND80-2124 (Reference 2.2.90 [DIRS 104724]), as shown in Table 3
NUREG-1567 (Reference 2.2.65 [DIRS 149756], Table 9.2)	ARFs for gases, fuel fines, volatiles, crud	Fractions available for release are considered the same as ARFs, and their values are cited from NUREG/CR-6487 (Reference 2.2.4 [DIRS 145345]), as shown in Table 3
NUREG-1617 (Reference 2.2.64 [DIRS 154000], Table 4-1)	ARFs for gases, fuel fines, volatiles, crud	Release fractions are considered the same as ARFs, their values are cited from NUREG/CR-6487 (Reference 2.2.4 [DIRS 145345]), as shown in Table 3
NUREG/CR-0722 (Reference 2.2.51 [DIRS 100990])	Experimental data based on burst rupture tests for Cs, I, Ru, and fuel fines	Measured release fractions are from several burst rupture tests on 1-foot fuel segments. It provides the key experimental data for release fractions that are widely cited in many regulatory guidance documents.
NUREG/CR-6410 (Reference 2.2.71 [DIRS 103695], p.3-9)	ARFs for noble gases, iodine, tritium, fuel fines	ARFs for fuel fines are cited from NUREG/CR-0722 (Reference 2.2.51 [DIRS 100990]), other ARFs are from other impact tests, as shown in Table 3
NUREG/CR-6487 (Reference 2.2.4 [DIRS 145345], Table 6-2)	ARFs for gases, fuel fines, volatiles, crud	Release fractions are considered the same as ARFs, and their values are based on limited experimental data. It appears that ARF for gases is taken from Regulatory Guide 1.25 (Reference 2.2.68 [DIRS 107691]), ARF for fuel fines is taken from SAND90-2406 (Reference 2.2.72 [DIRS 102072], p.84)
Regulatory Guide 1.25 (Reference 2.2.68 [DIRS 107691], P.25.2)	ARFs for ^{85}Kr, ^{129}I	Gas released from the fuel rod gap in fuel handling accidents is based on the Regulatory Position assumptions as shown in Table 3

Notes: ARF = airborne release fraction; and RF = respirable fraction

Release fractions are generally addressed in five categories based on their unique characteristics: fission product gases such as ^{85}Kr; iodines such as ^{129}I; volatiles such as ^{137}Cs; particulates such as fuel fines; and crud on the surface of cladding such as ^{60}Co. Iodine is also classified as a gas in this analysis as discussed in Section 6.1.1.3. Therefore, only four categories of ARFs are addressed in this calculation. The applicable release fractions for gases, volatiles, fuel fines and crud, and the ARFs for the four categories are examined, justified, and documented in Sections 6.1.2, 6.1.3, 6.1.4, and 6.1.5, respectively.

6.1.1.1 ARFs from Literature

The values of ARFs provided from seven references listed in Table 2 are summarized in Table 3. The other five references do not provide the ARFs for commercial SNF directly, but they include the test results that support the development of the ARFs. All seven references, which are either NRC regulatory guidance or NUREG reports, cover NRC regulatory positions for dry cask storage systems, spent fuel dry storage facilities, transportation packages for spent nuclear fuel, and nuclear fuel cycle facility. Some discussion of the listed values are provided in the notes of Table 3. In general, the ARF values from these references are the same or nearly the same, because most of them used the same original source of burst rupture tests (Reference 2.2.51 [DIRS 100990]), which is discussed further in Sections 6.1.2 to 6.1.5.

It should be noted that the ARFs for crud listed in Table 3 are the crud spallation fraction (CSF). The effective ARF for crud is the CSF multiplied by the fraction of the crud that becomes airborne during the fuel handling process. This is discussed in Section 6.1.5.

In Table 3, the recommended values for ARFs are given to one decimal place except for crud CSF, which is given to two decimal places. This is due to the high uncertainty associated with these fractions. To be consistent with the literature, the output of this analysis recommends release fractions with a similar precision, as more precise values are not warranted or needed.

6.1.1.2 Experimental Data from Literature

A review of the documents in Table 2 reveals two primary groups of experimental data that produced the majority of the cited release fractions for commercial SNF:

- Burst rupture tests on irradiated commercial SNF rod segments in a flowing steam environment. These experiments quantified and characterized fission product release under conditions postulated for a spent-fuel transportation accident (Reference 2.2.51 [DIRS 100990]).

- Impact rupture tests on three unconfined UO_2 pellets and simulated vitrified glass. These tests characterized the size distribution for the particles and fragments generated (Reference 2.2.58 [DIRS 158827]; Reference 2.2.41 [DIRS 116838]).

Table 3. Airborne Release Fractions From Fuel Retention

Radio-nuclide	ISG-5 [a]	NUREG-1536 [b]	NUREG-1567 [c]	NUREG-1617 [d]	NUREG/CR-6410 [e]	NUREG/CR-6487 [f]	Regulatory Guide 1.25 [g]
^{3}H	0.3	0.3	0.3	0.3	1×10^{-2}	0.3	- [i]
^{85}Kr	0.3	0.3	0.3	0.3	7×10^{-2}	0.3	0.3
^{129}I	0.3	0.1	0.3	0.3	2×10^{-3}	0.3	0.3
^{134}Cs & ^{137}Cs	2×10^{-4}	2.3×10^{-5}	2×10^{-4}	2×10^{-4}	-	2×10^{-4}	-
^{90}Sr	2×10^{-4}	2.3×10^{-5}	2×10^{-4}	2×10^{-4}	-	2×10^{-4}	-
^{106}Ru	2×10^{-4}	1.5×10^{-5}	2×10^{-4}	2×10^{-4}	-	2×10^{-4}	-
Fuel Fines	3×10^{-5}	-	3×10^{-5}	3×10^{-5}	2×10^{-4}	3×10^{-5}	-
Crud [h]	0.15/1	0.15	0.15/1	0.15/1	1×10^{-3}	0.15/1	-

Notes:
[a] ISG-5 (Reference 2.2.66 [DIRS 160582], Table 7.1) provides the fractions available for release to confinement evaluation of dry cask storage system. It classifies ^{3}H, ^{85}Kr, and ^{129}I as gases, and ^{134}Cs, ^{137}Cs, ^{90}Sr, and ^{106}Ru as volatile species.
[b] NUREG-1536 (Reference 2.2.63 [DIRS 101903], Table 7.1) provides the fractions available for release for radionuclides to be included in analyses of potential accidental release from dry cask storage systems. It does not provide a value for fuel fines. ISG-5 (Reference 2.2.66 [DIRS 160582]) indicates that NUREG-1536 will be revised to be consistent with NUREG/CR-6487 (Reference 2.2.4 [DIRS 145345])
[c] NUREG-1567 (Reference 2.2.65 [DIRS 149756], Table 9.2) provides the fractions available for release for radionuclides to be included in confinement analyses for spent fuel dry storage facilities. It classifies ^{3}H, ^{85}Kr, and ^{129}I as gases, and ^{134}Cs, ^{137}Cs, ^{90}Sr, and ^{106}Ru as volatile species.
[d] NUREG-1617 (Reference 2.2.64 [DIRS 154000], Table 4-1) provides release fractions for radionuclides to be included in analyses of packages designed to transport irradiated fuel rods. The release fraction for gases is used for ^{3}H, ^{85}Kr, and ^{129}I. The fraction for volatiles is used for ^{134}Cs, ^{137}Cs, ^{90}Sr, and ^{106}Ru.
[e] NUREG/CR-6410 (Reference 2.2.71 [DIRS 103695], Table 3-1, items 3.3.4.10d and 3.3.4.12a) provides bounding ARFs for spent nuclear fuel. The crud value represents the ARF for loose surface contamination.
[f] NUREG/CR-6487 (Reference 2.2.4 [DIRS 145345], Table 6-2) provides the release fractions for radionuclides to be included in analyses of packages designed to transport irradiated fuel rods. The release fraction for gases is used for ^{3}H, ^{85}Kr, and ^{129}I. The fraction for volatiles is used for ^{134}Cs, ^{137}Cs, ^{90}Sr, and ^{106}Ru.
[g] Regulatory Guide 1.25 (Reference 2.2.68 [DIRS 107691], p.25.2) presents ARFs for gas releases from fuel handling accidents.
[h] The value 0.15/1.0 means 0.15 for normal and off-normal conditions, and 1.0 for accident conditions. It is the fraction of crud that spalls off cladding, or crud spallation fraction (CSF), not the ARF as described in 6.1.5.
[i] " - " means not available or provided.

Burst Rupture Tests

In the burst rupture tests described in NUREG/CR-0722 (Reference 2.2.51 [DIRS 100990]), a pre-drilled fuel rod segment was heated to a temperature of about 900°C where rupture occurred. At this time, the pressure in the rod dropped, and fuel dust (fuel fines) was ejected from the fuel rod segment during the rupture. Release at the time of rupture proved to be more significant than the diffusion release that followed. This rupture process simulates the sudden release of radionuclides from a pressurized fuel rod when the fuel rod cladding breaches for any reason, including a drop event.

Most input data listed in Table 3 are based on the burst rupture data and that data was used in the same manner to produce the cited ARFs. Thus, although a burst rupture event is not necessarily equivalent to a drop event, these documents provide strong NRC precedents supporting use of the burst rupture data as a basis for analysis of a wide range of accidents involving commercial SNF.

Impact Rupture Tests

Under the impact rupture tests described in ANL-81-27 (Reference 2.2.58 [DIRS 158827]), three fuel pellets were dropped with energy density of 1.2 J/cm^3. Then all debris were collected, and the sizes of the debris were measured. The results indicated that the size of small particles (less than 1 mm) follows a lognormal distribution. The ARFs from these tests do not directly apply to a drop event for spent fuel with cladding, because only limited fuel particles can be released through breached cladding.

Airborne release fractions based on crash-impact forces on small pieces of unclad SNF pellets are provided in NUREG/CR-6410 (Reference 2.2.71 [DIRS 103695], Section 3.3.4.10). In this reference, the ARF for gases is relatively low (7%) and the ARF for fuel fines is relatively high (2×10^{-3}) compared with other reviewed reference sources. The same data set is also used in ANSI/ANS-5.10-1998 (Reference 2.2.6 [DIRS 103755], p.15). It should be noted that there is an apparent inconsistency in NUREG/CR-6410: Section 3.3.4.10 gives an ARF for fuel fines of 2×10^{-3} cited from crush impact data (Reference 2.2.69 [DIRS 103695], Section 3.3.4.10) while Table 3-1 (item 3.3.4.10d) – which purports to summarize what is in Section 3.3.4.10 – shows an ARF for fuel fines of 2×10^{-4} cited from Lorenz et al. (Reference 2.2.51 [DIRS 100990]). Although NUREG/CR-6410 (Reference 2.2.69 [DIRS 103695]) is generally applicable to repository operations, the applicability of release fractions derived from impact tests involving unconfined test specimens to accidents involving commercial SNF requires further consideration of the potential for large scale gross cladding damage (e.g., guillotine breaks or longitudinal splits).

Burst Rupture ARFs Applied to Impact Accidents

The release fractions from burst rupture tests are expected to produce conservative results when applied to repository accidents which are of an impact nature. In SAND80-2124 (Reference 2.2.90 [DIRS 104724], p.33), it is stated that an impact rupture is expected to produce more particles (through pulverization and grinding between pellets) than were present in the spent fuel before a burst rupture. There is less pressure, however, to exhaust these particles after an impact rupture. It is also expected that an impact rupture would have a more restricted release pathway because of cladding deformation (Reference 2.2.90 [DIRS 104724], p.33). Indeed, as reported in SAND80-2124 (Reference 2.2.90 [DIRS 104724], p.33), burst rupture release fractions were arbitrarily reduced by a factor of 10 to account for this physical expectation. It is apparent, however, that in more recent NRC guidance, such as NUREG-1536 (Reference 2.2.63 [DIRS 101903], Table 7.1), release fractions associated with burst ruptures (corrected for fuel rod length) should not be reduced if applied to impact accidents.

In addition to the assumption for severe clad damage (Assumption 3.2.1), application of test data in the determination of ARF and RF for large masses of commercial SNF (e.g., bare unconfined fuel assemblies) dropped from substantial heights (i.e., those that have an impact energy density greater than 1.2 J/cm^3) may be considered excessively conservative (Reference 2.2.24 [DIRS 103756], p.4-52). This is supported, albeit for a different brittle material, by a simple test showing that a 160-g glass cylinder bounces off a steel plate in a 10-m drop, rather than fracturing as would have been predicted by a similar correlation (Reference 2.2.41 [DIRS 116838], Section 8 of Appendix D). This reveals the largest deficiency potentially associated

with the use of these test data in the determination of ARF and RF for large masses of commercial SNF: whether the physical phenomena associated with damage produced by dropping a weight on an unclad fuel pellet can be equated to the damage produced by dropping a fuel assembly onto a potentially unyielding surface.

Based on the applicability of the data and previous licensing precedent, the burst rupture ARFs are considered applicable to accidents involving commercial SNF. ARFs derived from burst rupture experimental data referenced in technical guidance documents are summarized in Table 3. As can be seen in Table 3, however, the burst rupture ARFs may be interpreted or corrected in different manners to produce a range of ARFs for specific radionuclides released from commercial SNF, which can depend on the range of conditions such as temperature.

As stated in Assumption 3.2.5, the release fraction from a fuel assembly or assembly-like structure due to a drop or impact event is based on burst rupture tests, because the event damages the assembly first, and then fails the fuel rod. A high pressure inside a fuel rod would be expected to push the radionuclides out of the rod, which is a process similar to the burst rupture tests. In this analysis, the release fractions for intact commercial SNF, mechanically damaged commercial SNF and cladding-penetration damaged commercial SNF are considered to be contained in an assembly-like structure, and the developed ARFs and RFs are based on the burst rupture testing data. The release fractions for a fuel rod, debris, and pieces subject to a drop or impact event are based on impact rupture tests because the event could fracture the fuel pellets directly with a fraction of them released into air, which is a process similar to the impact rupture tests. In this analysis, the developed ARFs and RFs for a fuel rod, debris and pieces are therefore based on the impact rupture testing data.

6.1.1.3 Categorization of Radionuclides

Based on the TAD canister-based repository design concept (Reference 2.2.12 [DIRS 182131], Section 4.2.1.9.8), the CRCF is designed to prevent the cladding temperature for commercial SNF in disposable multi-element canisters, while within the CRCF, from exceeding: (1) 350°C for zircalloy clad assemblies; and (2) 400°C for stainless steel clad assemblies. In addition, the TAD canister is designed to maintain the cladding temperature for commercial SNF below 400ºC during normal operations and 570ºC during off-normal and accident conditions (Reference 2.2.12 [DIRS 182131], Sections 33.2.2.27 and 33.2.2.28). In addition, other literature (Reference 2.2.48 [DIRS 144349], p. 1.1) suggests that cladding surface temperatures be limited to approximately 400°C for fuel discharged at least 5 years from a reactor under normal conditions in shipping casks.

These design requirements are used to determine the radionuclide category for released radioactive material. The melting and boiling points for specific elements potentially released from breached fuel pins in this analysis are listed in Table 4. Melting and boiling points are also provided for some compounds that may be expected to form with these elements through common reactions (e.g., oxidation) as they are released from the fuel. These temperatures are used to establish whether radionuclides released from commercial SNF are to be treated as gases, volatiles, or particulates (e.g., fuel fines). The temperature characteristics of elements and compounds are taken from Reference 2.2.88 [DIRS 127163]), and are considered appropriate to be used in determining whether the elements or compounds are to be categorized as gases,

volatiles, or fuel fines. Commercial SNF cladding surface temperatures under accidents considered in this analysis are less than 570°C as discussed above.

Table 4. Temperature Characteristics of Various Elements/Compounds in Commercial SNF

Element/ Compound	Melting Temperature (°C)	Boiling Temperature (°C)	State Considered in this Analysis [a]	Page # In Weast[b]
Cesium	28.4	678	Volatile	B-10
CsI	621	1280		B-82
Cs_2O	400	-		B-82
CsOH [c]	272.3	-		B-82
Iodine	113	184	Gas	B-17
IO_2 or I_2O_4	130	-		B-96
Ruthenium	2310	3900	Volatile	B-28
RuO_2	Decomposes	-		B-131
RuO_4	25.5	Decomposes, 108		B-131
Strontium	769	1384	Fuel Fine	B-31
SrI_2	515	Decomposes		B-143
SrO	2430	3000		B-143
SrO_2	Decomposes	-		B-143

NOTES: [a] The states (e.g., gas, volatile, particulate) of the elements and compounds in this table are established based on the cladding temperature during an accident.

[b] This column refers to the page number in Weast (Reference 2.2.88 [DIRS 127163]) where the melting and boiling temperatures are located.

[c] Present only in a steam environment.

Based on the literature cited in Table 3, four groups of radionuclides of interest are categorized in this analysis. The gases category includes radionuclides such as ^{3}H, [85]Kr, and [129]I; the volatiles category includes radionuclides such as [134]Cs, ^{137}Cs and [106]Ru; the fuel fines category includes ^{90}Sr and all other heavy metal radionuclides; and crud includes radionuclides such as ^{60}Co and [55]Fe. Justification for this categorization is provided below and is based on the cladding temperature limits and thermal properties. This categorization is generally consistent with the literature in Table 3.

Krypton is an inert gas, and tritium (^{3}H) exists as a vapor. Therefore it is reasonable to classify both as gaseous radionuclides. Iodine and its oxides (if present) are conservatively treated as gases, because the boiling temperature of elemental iodine as shown in Table 4 is clearly below the cladding surface temperatures (400°C). No boiling temperatures were found for iodine oxides; the melting temperatures of these compounds, however, are comparable to that of elemental iodine. Hence, these iodine oxides are considered to also be in a gaseous state. It is consistent with regulatory precedent that [129]I be categorized as gas as shown in the notes of Table 3. In the commercial SNF burst rupture tests performed in NUREG/CR-0722 (Reference 2.2.51 [DIRS 100990], pp. 117 to 119, Tests HBU-7 to HBU-10), it was determined that iodine was released from breached fuel in either elemental form or as CsI. Although CsI is unlikely to be in

a gaseous form when released from the fuel matrix because of its relatively high boiling point, the treatment of the iodine in this compound as a gas is as conservative as the treatment of the Cs in this compound as a volatile (see following paragraph). This is based on the preceding technical argument, which is based on the melting and boiling temperatures of Cs and I.

Cesium and its compounds are treated as volatiles because the melting temperature of elemental cesium as shown in Table 4 is below the cladding temperature limit of 570ºC. It is probable that cesium released from commercial SNF would exist in the vapor phase because of the higher temperatures within a fuel pin with this surface temperature. This is confirmed by each of the burst rupture and diffusion tests performed in NUREG/CR-0722 (Reference 2.2.51 [DIRS 100990]). In each test, the cesium purged from a breached fuel rod was in the form of either condensed CsI or Cs_2UO_4 (fuel fine) or gaseous elemental cesium, CsI, Cs_2O, or CsOH (the latter, only in the presence of a flowing steam environment). When released to the cooler environment outside of the fuel, however, the elemental cesium and gaseous cesium compounds were either (1) quickly condensed and were removed by fuel fines, (2) condensed in a thermal gradient tube, (3) reacted with some nearby quartz to form a cesium silicate (particle), or (4) found deposited on the HEPA filters as particulates.

Ruthenium and its compounds are also treated as volatiles in this analysis because the melting and boiling temperatures of ruthenium compounds RuO_2 and RuO_4 as shown in Table 4 are below the cladding temperature limit of 570ºC (although the melting and boiling temperatures of elemental ruthenium are above the assumed temperature during an accident). The burst rupture tests performed in NUREG/CR-0722 (Reference 2.2.51 [DIRS 100990], pp. 117 to 119, Tests HBU-7 to HBU-10) determined that the vaporized ruthenium, in the form of RuO_2 and RuO_4, was negligible compared to the ruthenium captured in the fuel fines. The ruthenium in the fuel fines is considered to be in an elemental form and in a condensed state because of the existing temperatures. The formation and vaporization of RuO_2 and RuO_4 begins at approximately 500°C and 600°C respectively (Reference 2.2.51 [DIRS 100990], pp.116 to 117). These temperatures are in the range of the cladding temperature limit of 570ºC. RuO_4 is volatile. After these compounds have been purged from the fuel rod, they cool to temperatures where the RuO_4 reverts to RuO_2 and the RuO_2 decomposes to its elemental components. The elemental ruthenium resulting from this decomposition is in a solid/particulate form because of its high melting and boiling temperatures. Because of the presence of RuO_4, ruthenium and its compounds are conservatively treated as volatiles.

Strontium and its oxides (if present) are treated as particulates (e.g., fuel fine) because of their high melting and boiling temperatures. The melting and boiling temperatures of strontium and SrO as shown in Table 4 are clearly above the cladding temperature of 570ºC during an accident. Any formation of SrO_2 decomposes back to SrO (Reference 2.2.88 [DIRS 127163], p. B-143); thus, the state of this compound is not considered. SrI_2, whose melting point is below the assumed accident temperature, is not a compound released from spent nuclear fuel. The burst rupture tests for commercial SNF reported in NUREG/CR-0722 (Reference 2.2.51 [DIRS 100990], pp.117 to 119, Tests HBU-7 to HBU-10) indicated that iodine was released from breached fuel in either an elemental form or as CsI; no SrI_2 was mentioned. Thus, there is no consideration of the volatility of this compound, based on the preceding technical argument, which is based on melting and boiling temperatures.

Other radionuclides that are not classified as being in the gas and volatile categories are considered as fuel fines for commercial SNF.

Crud releases originate from the external surface of commercial SNF assemblies. In contrast to fuel fines, gases, and volatiles released from a fuel rod, the crud release fraction is not based on the fraction of fuel rods that are breached. Two radionuclides, ^{60}Co and ^{55}Fe, are considered in this category as discussed in Sections 6.1.5.

6.1.2   ARF for Gases from Commercial SNF

As fuel is irradiated in a nuclear power reactor, fission product atoms, of which approximately 15 percent are inert gases, are produced and buildup internal to the cladding of the fuel rods. Release of these fission gases from the fuel matrix to the plenum and the gap region between the fuel and the cladding is directly related to fuel pellet swelling, which is a strong function of linear power density.

Among these fission gases, three radionuclides important to potential repository accident exposures are considered in this analysis: ^{3}H, ^{85}Kr, and ^{129}I. This consideration does not exclude other related fission gas isotopes, such as ^{81}Kr, ^{127}Xe and ^{136}Xe being considered as fission gases if they are radionuclides of interest. Tritium (^{3}H) exists likely in the form of vapor (HTO), and is commonly treated as gas for licensing analyses as shown in the notes of Table 3. The isotopes of krypton and xenon are the most common fission gases in spent nuclear fuel. Iodine is considered as gas based on the discussion in Section 6.1.1.3.

In accordance with Regulatory Guide 1.25 (Reference 2.2.68 [DIRS 107691], p.25.2), all of the gap activity in the damaged rods is assumed to be released during an accident and consists of 30 percent ^{85}Kr, 10 percent of total noble gases other than ^{85}Kr, and 10 percent of the total radioactive iodine in the rods. These values are cited by NUREG-1536 (Reference 2.2.63 [DIRS 101903], Table 7.1) and NUREG-1567 (Reference 2.2.65 [DIRS 149756], Table 9.2) for use in analysis of potential accident releases, as listed in Table 3. Regulatory Guide 1.25 (Reference 2.2.68 [DIRS 107691], p.25.2) also states that 30 percent of the ^{127}I and ^{129}I inventory should be assumed to be released for the purpose of sizing filters.

The release fractions from Regulatory Guide 1.25 (Reference 2.2.68 [DIRS 107691], p.25.2) are used for oxide fuels and in cases where the following conditions are not exceeded:

- Peak linear power density of 20.5 kW/ft (67.25 kW/m) for highest power assembly discharged

- Maximum center-line operating fuel temperature less than 4,500°F (2,482°C) for this assembly

- Average burnup for the peak assembly of 25,000 MWd/MTU or less (which corresponds to a peak local burnup of about 45,000 MWd/MTU).

Both the more recently issued Regulatory Guides 1.183 (Reference 2.2.69 [DIRS 173584], Table 3) and 1.195 (Reference 2.2.70 [DIRS 166293], Table 2) provide the non-LOCA fraction of fission product fuel rod gap inventory available for release. These fractions are 0.08 for I-131,

0.10 for Kr-85, 0.05 for other noble gases and iodines. These fractions are significantly lower than the value of 0.3 in Regulatory Guide 1.25. The release fractions recommended in Regulatory Guides 1.183 and 1.195 have been found to be acceptable by the NRC for use with currently approved LWR fuel with a peak burnup up to 62,000 MWD/MTU (Reference 2.2.69 [DIRS 173584], footnote 11 and Reference 2.2.70 [DIRS 166293], footnote 7). Therefore, the release fractions for gases based on Regulatory Guide 1.25 provide bounding values for an accident event in the repository. Although some of these conditions for commercial SNF handled at the repository may be exceeded (such as for high burnup fuel, which is discussed in Section 6.5), the conservatism in these release fractions allows them to be applied to accidents involving commercial SNF handled at the repository. For example, according to Graves (Reference 2.2.29 [DIRS 158816], p.177 and Figure 8-9), peak power density rods of light water reactors typically release 5 to 10 percent of the fission gases to the gap, significantly less than the 30 percent recommended in Regulatory Guide 1.25 (Reference 2.2.68 [DIRS 107691], p.25.2). Furthermore, the suggested design release fraction for the linear power density equivalent to the peak power density of 20.5 kW/ft (i.e., 53.5 W/cm) is approximately 5 percent less than the value recommended by Regulatory Guide 1.25 (Reference 2.2.68 [DIRS 107691], p.25.2) according to Figure 8-9 in Graves (Reference 2.2.29 [DIRS 158816]).

Most of the reports summarized in Table 3 suggest a value of 0.3 for the ARFs for ^{3}H, ^{85}Kr, and ^{129}I – the value recommended in Regulatory Guide 1.25 (Reference 2.2.68 [DIRS 107691], p.25.2). Although not specifically addressed in Regulatory Guide 1.25 (Reference 2.2.68 [DIRS 107691]), the ARF for ^{3}H is conservatively taken to be equal to the ARF for a gas as ^{3}H is released in a gaseous form.

It is clear that an ARF value of 0.3 for all gases is conservative. The measured results provided in NUREG/CR-0722 (Reference 2.2.51 [DIRS 100990], Tables 4 and 5) indicate less than 1 percent of xenon and krypton is released to the plenum of fuel rods. An eight percent gas release fraction is recommended in WASH-1400 (Reference 2.2.62 [DIRS 107799], p.VII-13 and Table VII-1-1). Similarly, the value suggested in SAND80-2124 (Reference 2.2.90 [DIRS 104724], Table XVIII) for burst ruptures shows a lower release fraction for ^{85}Kr (22 percent). A release fraction for ^{131}I, though not a radionuclide of concern in the repository because of its short (8 day) half-life, is shown to increase with burnup, and for a fuel rod with a burnup of 60,000 MWd/MTU the release fraction is only 0.12 (Reference 2.2.8 [DIRS 158889], Table 3.6). The ARF for ^{129}I is conservatively assumed to be equal to 0.3, as noted in Regulatory Guide 1.25 (Reference 2.2.68 [DIRS 107691], p.25.2), and discussed in NUREG/CR-6487 (Reference 2.2.4 [DIRS 145345], p. 30). Much lower values of ARF for gases are recommended in NUREG/CR-6410 (Reference 2.2.69 [DIRS 103695], Table 3-1, items 3.3.4.10), as shown in Table 3. As a conservative approach, these lower values are not used in developing the ARF for gases released from commercial SNF.

Based on the above discussions and the input data in Table 3, a single ARF value of 0.3 for the gaseous radionuclides ^{85}Kr, ^{3}H, and ^{129}I is recommended in this document, as summarized in Table 5. This value is considered conservative based on values from Regulatory Guide 1.25 (Reference 2.2.68 [DIRS 107691], p.25.2) and NUREG/CR-6487 (Reference 2.2.4 [DIRS 145345], p.30). It is also consistent with the values used to evaluate transportation packages containing spent nuclear fuel as stated in NUREG-1617 (Reference 2.2.64 [DIRS 154000], Table 4-1). In addition, with the exception of the ARF for ^{129}I, this value is also consistent with the

ARFs used to evaluate dry storage cask systems in NUREG-1536 (Reference 2.2.63 [DIRS 101903], Table 7.1) and spent fuel dry storage facilities in NUREG-1567 (Reference 2.2.65 [DIRS 149756], Table 9.2).

6.1.3 ARF for Volatile Radionuclides from Commercial SNF

Some fission products are volatile. Among them, three radionuclides important to potential repository accident exposures are considered in this analysis: ^{134}Cs, ^{137}Cs, and ^{106}Ru. The rationale for classification of these radionuclides as volatiles is addressed in Section 6.1.1.3. Some input sources suggest that ^{90}Sr may also be a volatile radionuclide; however, ^{90}Sr at the repository is classified as fuel fines as discussed in Section 6.1.1.3. The ARF for fuel fines is addressed in Section 6.1.4.

The literature data on ARFs for volatiles are summarized in Table 3. Most reports consistently suggest that a value of 2×10^{-4} be used as the ARF for volatiles.

NUREG/CR-6487 (Reference 2.2.4 [DIRS 145345], p.30) suggests that 2×10^{-4} be used as a conservative bounding value for the fraction of the volatiles released from a fuel rod as a result of a cladding breach, based on limited experimental data. Although there is no specific reference given for the experimental data, it is likely that the data come from the burst rupture test data for cesium from NUREG/CR-0722 (Reference 2.2.51 [DIRS 100990], Table 40)[1] uncorrected for fuel rod length. Because cesium is considered a volatile in these NUREG reports (see Table 3), it is treated similarly to the fission and fill gases found in the fuel rod. These gases are fully purged from the gap and plenum regions during an event that breaches the cladding. Thus, no correction for fuel rod length to the measured release fraction is made for the potentially volatile Cs radioisotopes. Because this burst rupture value is uncorrected for fuel rod length or for impact rupture, the recommended value of 2×10^{-4} is considered conservative for the release of cesium during accidents at the repository.

In comparison, an ARF value of 2.3×10^{-5} is recommended for volatiles in NUREG-1536 (see Table 3). Although the source reference of SAND80-2124 (Reference 2.2.90 [DIRS 104724]) is given in NUREG-1536, the value of 2.3×10^{-5} is not clearly stated in SAND80-2124. It could be derived from the burst rupture data for cesium presented in NUREG/CR-0722 (Reference 2.2.51 [DIRS 100990], Table 40), and corrected for fuel rod length (i.e., divided by a factor of 10) according to SAND80-2124 (Reference 2.2.90 [DIRS 104724], p.33). The burst rupture release fraction of 2×10^{-5} was cited from NUREG/CR-0722 (Reference 2.2.51 [DIRS 100990]) in SAND80-2124 (Reference 2.2.90 [DIRS 104724], Table XII). However, this fraction was not directly used; rather it is used to determine the release fractions for an impact rupture from a spent fuel assembly to a cask cavity.[2]

---

[1] An average of the cesium released in these burst rupture tests (Reference 2.2.51 [DIRS 100990], Table 40) is determined to be 0.0306 percent, which is higher than the 0.02 percent used in NUREG/CR-6487 (Reference 2.2.4 [DIRS 145345], Table 6-2, pp. 30 and 31).

[2] The release fractions for impact rupture are the release fractions from burst rupture reduced by 90 percent to 10 percent of the burst rupture release fractions. SAND80-2124 (Reference 2.2.90 [DIRS 104724], Table XII) provides burst rupture experiments from NUREG/CR-0722 (Reference 2.2.51 [DIRS 100990], Table 40).

The burst release fractions of cesium and iodine from the cask cavity to the environment are calculated in SAND80-2124 (Reference 2.2.90 [DIRS 104724], Table XVIII, and Appendix A). The calculation method is based on Lorenz et al 1979 (Reference 2.2.50 [DIRS 158822], p.406, Equation 1), with the results of 4×10^{-3} for cesium and 7×10^{-3} for iodine. These values are significantly higher than other reference sources shown in Table 3. However, it appears that some input parameter ranges used in the calculations are out of the test parameter ranges. For example, the tested volume of plenum gas vented, V_B, ranged from 0 to 348 cm^3 (Reference 2.2.50 [DIRS 158822], p.406), while the calculated input used was 1100 cm^3 (Reference 2.2.90 [DIRS 104724], p.A-2). In addition, the gap inventory for cesium was 2.79% (Reference 2.2.50 [DIRS 158822], Table V), while this fraction was assumed to be 20% (Reference 2.2.90 [DIRS 104724], p.A-2), which results in the areal inventory of fission products in the gap space (M_0/A) being out of test range (1163 μg/cm^2 vs. 0.5 to 127 μg/cm^2 (Reference 2.2.90 [DIRS 104724], p.A-2 and Reference 2.2.50 [DIRS 158822], p.406)). Therefore, the burst release fractions of cesium and iodine from the cask cavity to the environment in SAND80-2124 (Reference 2.2.90 [DIRS 104724], Table XVIII) are higher and may not be applicable to those expected at the repository.

Although ruthenium was detected in some burst rupture tests reported in NUREG/CR-0722 (Reference 2.2.51 [DIRS 100990], pp.116 to 119), the amount of volatile ruthenium was negligible compared to the ruthenium contained in the fuel fines (Reference 2.2.51 [DIRS 100990], p.119). It is conservative to consider ^{106}Ru as a volatile radionuclide based on the results from these tests and discussions in Section 6.1.1.3. This selection is consistent with the regulatory precedents as shown in the notes of Table 3.

Based on the above discussions and input data in Table 3, a single ARF value of 2×10^{-4} for the volatile radionuclides (^{134}Cs, ^{137}Cs, and ^{106}Ru) is recommended for calculating the dose consequences of an accident at the repository. This value is considered conservative, as suggested in NUREG/CR-6487 (Reference 2.2.4 [DIRS 145345], p.30). The ARFs for volatiles from intact commercial SNF are summarized in Table 5.

6.1.4 ARF for Fuel Fines from Commercial SNF

Any fission product radionuclides that are not classified as either gases or volatiles are considered to be particulates or fuel fines in this analysis. The high melting and boiling temperatures of elemental strontium and of its compounds associated with release from the commercial SNF allow ^{90}Sr to be treated as fuel fines (see Section 6.1.1.3).

A fuel pellet is easy to break as reported in ANL-81-27 (Reference 2.2.58 [DIRS 158827]), and particulates are generated when a fuel assembly is involved in a drop event. Fuel fines could also be liberated/created from fuel pellets because of the shaking of the rod and the grinding action between fuel pellets that occurs during handling and transport of the fuel. Fuel fines also exist as residual material from the fuel manufacturing process and are produced during irradiation from pellet cracking. Pellet cracking is associated with thermal distortion caused while the fuel was at high temperatures. The higher temperature at the center of a fuel pellet produces circumferential tensile stresses that result in radial cracks.

The input data for ARFs for fuel fines from commercial SNF are summarized in Table 3. Most reports suggest a value of 3×10^{-5} be used as the ARF for fuel fines, except for NUREG/CR-6410 (Reference 2.2.69 [DIRS 103695], Table 3-1, items 3.3.4.10d) where a higher value of 2×10^{-4} was suggested based on NUREG/CR-0722 (Reference 2.2.51 [DIRS 100990]). However, most reports suggest ^{90}Sr is a volatile with a higher value, and only NUREG-1536 (Reference 2.2.63 [DIRS 101903], Table 7.1) recommends a value consistent with the ARF for fuel fines.

For fuel fines, an average of the release fractions from the four burst rupture tests performed in NUREG/CR-0722 (Reference 2.2.51 [DIRS 100990], Table 40)[3] is equal to 2.42×10^{-4}. This value is based on release measurements from the bursting of 1-ft segments of fuel rods. Assuming that the same amount of mass is released from a full-length fuel rod as was released from the test segment, SAND80-2124 (Reference 2.2.90 [DIRS 104724], pp.34 and 35) divided the average release fraction by a factor of 10, because a typical spent fuel rod would have roughly ten times the mass of fission products as would the 1-foot test section. Identical adjustments to the burst rupture data are made in NUREG/CR-6487 (Reference 2.2.4 [DIRS 145345], Table 6-2), which is the source for NUREG-1617 (Reference 2.2.64 [DIRS 154000], Table 4-1) and NUREG-1567 (Reference 2.2.65 [DIRS 149756], Table 9.2).

The validity of this correction may be considered unjustified based on the following arguments:

- The released internal pressure of the full-length fuel rod is expected to entrain particles from regions other than those directly near the burst point and carry them out of the fuel rod. Hence, the release fractions for these particles from the full-length fuel rod could be larger than the fractions from the 1-ft test segment if all particles were to escape.

- The larger volume of a full-length fuel rod is expected to result in a gas exhaust that is sustained over a longer period of time, albeit a very short time, than the exhaust of the 1-foot fuel rod segment. Although the pressure in a full-length fuel rod is less than the fuel rod pressure that causes a burst rupture, the larger volume of the full-length fuel rod would likely sustain a gas exhaust over a longer period of time, which may allow for more particles to be transported through the fuel pellet-clad gap and released out the break.

- A guillotine break or a longitudinal split of a fuel rod would produce a significant increase in the breach of the confinement compared to the breach caused in a burst rupture. This has the potential to significantly increase the amount of fuel fines that may escape a fuel rod.

The first two preceding arguments may be countered based on the trends of particle deposition in turbulent flow through vertical tubes from ANSI N13.1-1969 (Reference 2.2.5 [DIRS 106261], Table B3), and the characteristics of the flow paths these particles must travel through. The following arguments were considered to validate this interpretation (Reference 2.2.90 [DIRS 104724], pp.34 to 35) of the rod burst data and to ensure that it is conservative:

---

[3]   Burst rupture data were accumulated from tests performed at temperatures between 900°C and 1200°C and the internal pressure of the helium inserted into the fuel pin at the time of rupture was approximately 2.0 MPa.

- The fraction of particle deposition (independent of particle size) increases as tube diameter decreases (Reference 2.2.5 [DIRS 106261], Table B). For a fuel rod, the flow paths for exhausted gases consist of an annular gap (formed by the fuel pellet on the inside and the cladding on the outside) and any penetrating cracks and/or crevices through the fuel. The equivalent diameter of these flow paths is expected to be very small (e.g., less than approximately 0.03 cm for typical commercial SNF). Thus, the fraction of deposition is expected to be high for both the full-length fuel rod and the 1-ft fuel rod segment with only particles local to the breach being released. This suggests that there is no difference in the mass released from the full-length and 1-ft fuel rod segments.

- The fraction of particle deposition (independent of particle size) increases with the length of the tube (Reference 2.2.5 [DIRS 106261], Table B). Thus, the further a particle is from a cladding breach the greater its probability for being deposited along the tube before it can be released. For a full-length fuel rod, this trend reduces the amount of mass (theorized to be released from the unadjusted burst rupture data) released through a cladding breach. This characteristic of particle transport in a flowing gas stream supports the assumption that higher proportions of particulate present near a break are released relative to particulate present at large distances from the break location.

- The fraction of particle deposition increases with the size of the particle (Reference 2.2.5 [DIRS 106261], Table B). Thus, the larger fuel fines released in the burst rupture experiments, which comprise the vast majority of the mass of the released fuel, likely originated in the immediate vicinity of the cladding breach. For the full-length fuel rod, the larger diameter, high-density fuel fines are not likely to escape the fuel rod and hence, no significant change in the released mass from the burst rupture data is expected.[4] This further supports the reduction in the burst rupture release fractions.

- The internal gas pressure of a cool fuel rod is less than the pressure that occurred during the burst rupture tests. Thus at the onset of an event that breaches the fuel cladding, the 1-ft fuel rod segment exhibits a higher exhaust velocity than the full-length fuel rod.[5] Because velocity and the Reynolds number are directly proportional, this higher velocity results in a larger Reynolds number which, based on the general trends for turbulent flow through vertical tubes in Table B3 of ANSI N13.1-1969 (Reference 2.2.5 [DIRS 106261]), results in less particles being deposited. Thus, more particles are expected to be exhausted resulting in a higher release fraction for the 1-foot fuel rod segment.

---

[4] ANSI N13.1-1969 (Reference 2.2.5 [DIRS 106261], p.36) states that, for particles larger than those given in Table B3 (i.e., greater than 10 μm), significant re-entrainment is expected at higher flow rates. Neither the inner clad nor pellet surfaces, however, are expected to be smooth. In addition, the pressure transient time history is characterized by rapidly reducing pressure and flow. Hence, any particle that is deposited on internal surfaces is likely to remain adhered to it during the short duration of the pressure transient, making re-entrainment an insignificant consideration.

[5] In the worst-case condition of a large break or rupture (i.e., pinhole leaks or hairline cracks would not produce sufficient flow rate to promote particulate entrainment), the pressure difference between the full-length fuel rod and 1-ft fuel rod segment would be short-lived, as eventually both pressures would quickly equilibrate with the environment outside of the fuel rod.

- The flow paths in a fuel rod are not likely to be smooth and continuous. Fuel pellet irradiation-induced cracking produces non-smooth flow paths for the mixture of fill gases and fission gases. Pellet-to-clad interference is likely to occur randomly over the length of a fuel rod segment with particles entrained in those gases. Deposition is expected to increase per unit flow length through these paths because of the affinity of the larger particles to adhere to or plate-out on these surfaces.

The final argument for not dividing the experimental burst rupture release fractions by a factor of 10 is the likelihood of radionuclide releases from a guillotine break or a longitudinal split of a fuel rod that are equal to or larger than burst rupture. A guillotine break or a longitudinal split is not considered credible within the scope of this analysis (Assumption 3.2.1).

In SAND80-2124 (Reference 2.2.90 [DIRS 104724], p.11), an impact rupture is defined as a rupture of the cladding produced by bending or other deformation of a fuel rod; no mention is made of a guillotine break or longitudinal split. Intact irradiated fuel is considered quite rugged and capable of sustaining severe impact environments according to SAND80-2124 (Reference 2.2.90 [DIRS 104724], p.18). Based on these arguments, dividing the experimental burst rupture release fractions by a factor of 10 is justified based on regulatory precedents, physical trends evident in Table B3 of ANSI N13.1-1969 (Reference 2.2.5 [DIRS 106261]), and Assumption 3.2.1.

ISG-5 (Reference 2.2.66 [DIRS 160582], Table 7.1), NUREG-1617 (Reference 2.2.64 [DIRS 154000], Table 4-1), and NUREG/CR-6487 (Reference 2.2.4 [DIRS 145345], pp.30 to 31) provide release fractions to evaluate normal, off-normal, and hypothetical accident doses for storage casks. These release fractions for fuel fines are the average ARFs (corrected for fuel rod length) from the burst rupture tests in NUREG/CR-0722 (Reference 2.2.51 [DIRS 100990], Table 40) conservatively rounded-up (i.e., 2.4×10^{-5} is rounded up to 3×10^{-5}). This use of the burst rupture ARFs for both the transportation cask (Reference 2.2.64 [DIRS 154000], Table 4-1) and the storage cask (Reference 2.2.66 [DIRS 160582], Table 7.1) further demonstrates the applicability of these data to credible accidents involving commercial SNF.

NUREG/CR-6487 (Reference 2.2.4 [DIRS 145345], p.30) stated that strontium, cesium, and ruthenium are treated as volatiles in accidents involving transportation packages. For this analysis, with the exception of cesium and ruthenium, strontium is considered as fuel fines (Section 6.1.1.3). Event sequences involving fuel assemblies at the repository surface facilities are not expected to involve high enough temperatures for the melting or volatilizing of these elements to be of concern, unlike some potential transportation accidents, such as the fire described in 10 CFR 71.73(c)(4) (Reference 2.2.1 [DIRS 176575]). Thus, the ARF for ^{90}Sr should be linked to the fuel fines, instead of to volatiles during accidents at the repository.

Based on the above discussions and input data in Table 3, a single ARF value of 3×10^{-5} for the fuel fines and ^{90}Sr is recommended in this document to estimate the release of fuel fines and ^{90}Sr during an accident at the repository. The ARFs for fuel fines and ^{90}Sr from intact commercial SNF are summarized in Table 5.

6.1.5   ARF for Crud from Commercial SNF

Crud releases originate from the external surface of commercial SNF assemblies. In contrast to fuel fines, gases, and volatiles released from a fuel rod, the crud release fraction is not based on the fraction of fuel rods that are breached. The release mechanism involves surface spallation rather than leakage past fuel cladding barriers. Crud is primarily composed of iron-based compounds and some nickel, copper, cobalt, chromium, manganese, zinc, and zircalloy. The actual amount and type of crud varies from reactor to reactor and from cycle to cycle.

Crud becomes radioactive through neutron activation. The nuclear industry recognizes that excessive crud negatively affects fuel performance and it is making a concerted effort to control factors that contribute to crud formation. Thus, crud accumulation on older fuel rods is expected to be greater than the crud on fuel discharged over the last several years. The crud activity on older fuel rods, however, is less than that on freshly discharged fuel rods because of the relatively short half-life of the radionuclides that contribute to crud activity.

Crud can be classified into two general categories: (1) fluffy, easily removed crud composed mostly of hematite (Fe_2O_3), and (2) a tenacious crud that is tightly bound to the rods composed mostly of spinel ($NiFe_2O_4$). PWR crud is primarily of the second category while BWR crud is composed of both types. In general, PWR fuel has less crud activity than BWR fuel (Reference 2.2.73 [DIRS 103696], p.2).

Mishima and Olson (Reference 2.2.59 [DIRS 160588], p. 1134) examined measured data on crud spalling as a result of various mechanical forces during the fuel rod consolidation process and derived values of 4.1×10^{-4} for the CSF (crud spallation fraction) during rod consolidation and handling, and 2.2×10^{-7} for the fraction of crud airborne (i.e., CSF × ARF). This suggests that only a small fraction of the crud that spalls off rods becomes airborne during the rod consolidation process. The crud ARF is equal to 5.4×10^{-4} (= 2.2×10^{-7} / 4.1×10^{-4}). This value is bounded by an ARF of 0.1 for venting gases in a pressurized volume in which surface contamination composed of loose powder exists (Reference 2.2.24 [DIRS 103756], p. 5-22). The ARF of 0.1 is also a bounding value for the suspension of loose surface contamination by vibration shock (Reference 2.2.24 [DIRS 103756], Section 4.4.3.3.1).

Sandoval et al. (Reference 2.2.73 [DIRS 103696], pp.21 to 22, Table 1, p.I-50) provides measured release fractions for the crud located on the outer surface of fuel rods. Sandoval et al. (Reference 2.2.73 [DIRS 103696], Table 4 on p.24) provides spallation fractions for transportation conditions. The maximum crud spallation fraction for both PWR and BWR fuel occurs at elevated fuel temperatures (450°C) where a 0.15-m long region of crud is assumed to bubble up and spall off, resulting in a crud spallation fraction of 15 percent. The elevated fuel temperatures are caused by exposing fuel to a fire at a temperature of 800°C for 30 minutes. At lower temperature conditions (i.e., fuel rod surface temperature of 300°C), a maximum of 8 percent of the crud may spall off. Therefore, a bounding CSF value is 0.15, which is much larger than the CSF of 4.1×10^{-4} for the rod consolidation process.

The release fraction for crud found in SAND80-2124 (Reference 2.2.90 [DIRS 104724], p.34) was an estimate that has no experimental basis. This estimate was based on an assumption that 25 percent of the crud that plates out on spent fuel assemblies during reactor operation and

contaminates the transportation cask cavity surface is loosely adhering. The remainder adheres tightly and requires abrasion and chemical treatment for removal. SAND80-2124 (Reference 2.2.90 [DIRS 104724], p.34) assumes that this 25 percent release fraction includes not only the crud on the cladding surface, but also crud on the assembly structure and the cask interior. The report goes on to state that the 25 percent release fraction from the cask is comparable to the release of all the crud located on the surface of the fuel rod cladding (Reference 2.2.90 [DIRS 104724], p.34). Thus, the 25 percent crud release fraction from SAND80-2124 (Reference 2.2.90 [DIRS 104724], p. 34) equates to 100 percent release of the crud on the fuel rod cladding surfaces.

The input data for crud from commercial SNF are summarized in Table 3. Most reports suggest the value of 0.15 be used as the crud spallation fraction for normal operation and 1.0 to be used for an accident event, while NUREG-1536 provides a single value of 0.15. A crud spallation fraction of 1, which means that all of the crud on the surface of a fuel rod is released following an accident, is too conservative. It is based on an assumption made in NUREG/CR-6487 (Reference 2.2.4 [DIRS 145345], p.28), and no justification is given for this assumption in the documents listed in Table 3. Therefore, the CSF value of 0.15, instead of 1.0 is recommended for use at the repository.

The crud effective ARF for an event sequence can be calculated as:

$$CEARF = CSF \times ARF \qquad\qquad \text{Equation 3}$$

where

$CEARF$ = crud effective ARF (dimensionless)

CSF = crud spallation fraction, 0.15 (dimensionless)

ARF = airborne release fraction based on the suspension of loose surface contamination by vibration shock for crud, 0.1 (dimensionless).

The crud effective ARF is calculated from Equation 3 to be 0.015. This ARF value for crud is lower than the ARF suggested for vibration of loose surface contamination by NUREG/CR-6410 (Reference 2.2.69 [DIRS 103695], Table 3-1, Items 3.3.4.12a). Because the crud RF is taken as 1 (bounding) as recommended in Section 6.2.3, the crud respirable release fraction is also 0.015. This crud respirable release fraction is very conservative. The degree of conservatism is evident when it is compared to the crud respirable release fractions of 1.3×10^{-6} and 4.7×10^{-8} found in SAND99-0963 (Reference 2.2.52 [DIRS 104918], p.7). The SAND99-0963 (Reference 2.2.52 [DIRS 104918], p.7) crud respirable release fractions are not only orders of magnitude smaller, they are also calculated for sabotage attacks of rail casks employing devices with energy densities approximately one thousand times higher than that for potential cask drops at the repository.

The ARF for crud, which considers ^{60}Co and ^{55}Fe as the principal radionuclides present, is recommended in this document to be 0.015, and is summarized in Table 5. The crud surface activities are provided in Reference 2.2.13 ([DIRS 180185], Table 18).

6.1.6   Recommended ARFs for Intact Commercial SNF

Based on the previous discussions, the recommended values of ARFs for all groups of radionuclides considered in this document are summarized in Table 5.

Table 5. Recommended ARFs for Intact Commercial SNF

Radionuclide	ARF	In Section
^{3}H	0.3	6.1.2
^{85}Kr	0.3	6.1.2
^{129}I	0.3	6.1.2
^{134}Cs & ^{137}Cs	2×10^{-4}	6.1.3
^{90}Sr	3×10^{-5}	6.1.4
^{106}Ru	2×10^{-4}	6.1.3
Fuel Fines	3×10^{-5}	6.1.4
Crud	0.015	6.1.5

6.2   RESPIRABLE FRACTIONS FOR INTACT COMMERCIAL SNF

The definition of RF provided in DOE-HDBK-3010-94 (Reference 2.2.24 [DIRS 103756], p.xx) is the fraction of airborne radionuclides as particles that can be transported through air and inhaled into the human respiratory system and is commonly assumed to include particles 10 μm Aerodynamic Equivalent Diameter (AED) and less. The actual fraction of commercial SNF that is respirable depends on the particulate size distribution of the aerosolized commercial SNF.

Similar to the evaluation of ARFs, RFs are also categorized for four groups, i.e., gases, volatiles, fuel fines and crud. Radionuclides that are in the form of either a gas or a volatile are treated as if they were a gas and so are considered 100 percent respirable (RF=1). This is bounding. RFs for radionuclides in the form of fuel fines and crud are addressed in the subsections below.

6.2.1   Cut-off Diameters for Respirable Particulates

In order to determine the respirable fraction, the cut-off diameter for each type of respirable particle being considered must be determined. To that end, Attachment C provides a discussion of the historical definitions of respirable particles, derives the relationship between particle AED and cut-off diameter, and calculates the respirable cut-off diameters needed for this calculation.

The cut-off diameter ($d_{c/o}$) results from Attachment C are as follows:

- For commercial SNF, $d_{c/o}$ is about 3.5 μm,

- For oxidized fuel powder, $d_{c/o}$ is about 4.0 μm,

- For HLW, $d_{c/o}$ is about 7.0 μm, and

- For crud, $d_{c/o}$ is about 5.0 μm.

6.2.2   RF for Fuel Fines from Commercial SNF

Establishing the RF for commercial SNF fuel fines is limited to analyzing the same two primary groups of experimental data that produced the majority of the cited ARFs for commercial SNF (Table 2) as follows:

- Four experiments that burst ruptured highly irradiated commercial SNF rod segments in a flowing steam environment. These experiments quantified and characterized fission product release under conditions postulated for a spent-fuel transportation accident (Reference 2.2.51 [DIRS 100990]).

- Two single energy density impaction tests on three unconfined UO2 pellets. These tests characterized the size distribution and the RF of the fragments generated (Reference 2.2.58 [DIRS 158827]; Reference 2.2.41 [DIRS 116838]).

6.2.2.1   RF from Burst Rupture Tests

The first set of experimental data provides some characteristics of particle size distribution from the burst rupture tests. The tests indicated that more than 90% of mass of UO_2 fuel particles released was collected in the Furnace Tube with a typical particle size of about 150 μm, and less than 3% of mass of UO_2 fuel particles released was collected in the Filter Pack with a typical particle size of about 10 μm (Reference 2.2.51 [DIRS 100990], Table 20, Table 23, Table 25, Table 29 and Section 4.12.3).   This indicated that relatively large particles, which may not be able to be suspended in air for very long, were released during the burst rupture, likely due to a high pressure inside the fuel rod. Because the fuel particle releases are for total mass release, not just for airborne particle fraction, the release fraction from the experimental data could be much higher than the ARF. For this reason, the RF developed in this section is also considered for the fraction of respirable particles in the total mass released.   As the released particle size distribution is not specifically shown in the document, Assumptions 3.2.3 and 3.2.4 are used to interpret the values presented in the document. These data are then used to fit a particle size distribution.   The RF is determined using the distribution with the appropriate respirable diameter.

This method applies to the first data set from the burst rupture tests on irradiated commercial SNF rod segments in a flowing steam environment (Reference 2.2.51 [DIRS 100990]).   The interpretation of the data is in accordance with Assumptions 3.2.3 and 3.2.4: the MMD is equal to 150 μm, while 3% of cumulative mass released is less than a particle size of 12 μm.   The calculation of RF is performed using Mathcad software. The Mathcad file is named "*RF_FuelFines.xmcd*" as shown in Figure 1.

Aerosol particle sizes are generally described reasonably well by one of several mathematical distribution functions: the normal, lognormal, bimodal, and multimodal distribution functions (Reference 2.2.22 [DIRS 158805], p. 112). Particles of depleted UO_2 pellets from pulverization tests described in ANL-81-27 (Reference 2.2.58 [DIRS 158827], Figures 16 and 17) showed distributions that were characterized as lognormal functions with some departure from lognormal at the end of the spectrum. Other brittle materials (such as Pyrex Cylinders), from pulverization tests described in ANL-81-27 (Reference 2.2.58 [DIRS 158827], Figure 27) demonstrated

similar lognormal distributions, indicating that brittle materials often exhibit lognormal distributions when pulverized.

To fit the condition given above, a mass geometric standard deviation (MGSD) must be 3.83. With a lognormal distribution of particle mass at the MMD of 150 μm and MGSD of 3.83, the mass fraction of particles smaller than 3.5 μm, corresponding to respirable particles for commercial SNF as identified in Section 6.2.1 and Attachment C, is about 0.0026. As discussed previously, the RF developed in this analysis is based on total mass released. Therefore, the RF is the mass fraction of particles smaller than 3.5 μm, that is, 0.0026. To be conservative, the recommended value for the RF for fuel fines to be used for the burst rupture is selected as 0.005. A plot of particle size distributions for particle mass is shown in Figure 2 (taken from file "*RF_FuelFines.xmcd*"), which demonstrates a mass fraction of 0.5 at 150 μm (MMD = 150 μm), and a mass fraction of 0.03 at 12 μm.

Respirable Fraction For Fuel Fines

Purpose: to find respirable fraction for fuel fines at given conditions

Assumption: lognormal distribution for mass of particle size

Given conditions: mass median diameter (MMD) = 150 um,
                    cumulative mass fraction (12 um) = 0.03

Method: try a mass geometric standard deviation (MGSD) to fit given conditions

Calculations:

1. List the MMD and Try a MGSD:

$$MMD := 150 \qquad MGSD := 3.83$$

2. Define mass cumulative distribution (MCD), where x is partile size in um

$$mu := \ln(MMD) \qquad sig := \ln(MGSD)$$

$$MCD(x) := plnorm(x, mu, sig)$$

3. Verify given conditions:

$$MCD(MMD) = 0.5 \qquad MCD(12) = 0.03$$

4. Find cumulative mass fraction at a cutoff particle size for respirable portion:

$$MCD(3.5) = 2.568 \times 10^{-3}$$

Figure 1. Calculation of RF Based on Burst Rupture Data Using Mathcad
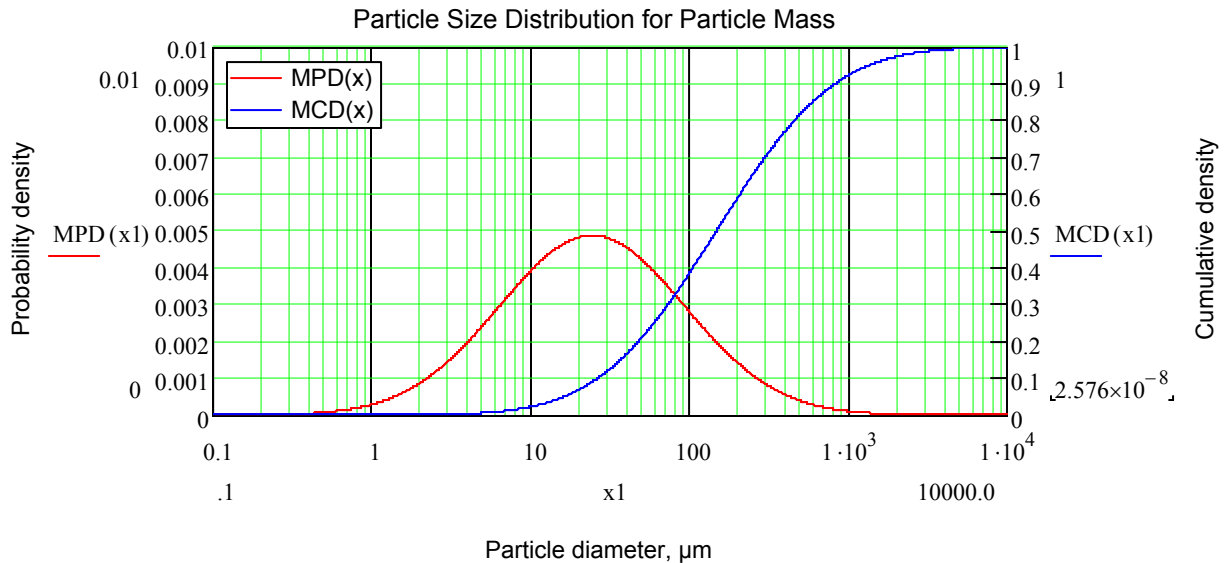
Figure 2. A Plot of Particle Size Distribution for Fuel Particle Mass Using Mathcad

6.2.2.2   RF from the Impact Rupture Tests

The second data set provides the mass fraction as a function of particle size from UO_2 fuel pellet drop tests. These are shown in Figure 3 and Figure 4, which are reproduced from ANL-81-27 (Reference 2.2.58 [DIRS 158827], Figures 16 and 17). In the tests, all debris was collected, and the sizes of the debris were measured. As shown in the figures, particles with a size smaller than a few millimeters are in a lognormal distribution (measured points are in a straight-line).   The mass percent of particles smaller than diameter D represents the release fraction for particles less than that particle size at the test condition. The impact rupture tests were conducted at Argonne National Laboratory, and documented in ANL-81-27 (Reference 2.2.58 [DIRS 158827]), as shown in Table 2. ANL-81-27 is considered a reliable source and the results are appropriate for the intended use at the Yucca Mountain repository. The experimental data show that RF mainly depends on material type, size of material, (Reference 2.2.58 [DIRS 158827], Table 2), and impact energy density (Reference 2.2.41 [DIRS 116838], Figure 13). RF is proportional to the impact energy density for a specific material (Reference 2.2.41 [DIRS 116838], Figure 13). The tests were conducted using UO_2 pellet drops with an impact energy density of 1.2 J/cm^3, which corresponds to a free fall from a height of 12 m for a pellet density of about 10 g/cm^3.

The test results from Figure 3 and Figure 4 are based on all potential particles, not just the particles that are released. Although the particle distributions for particles released to the environment may not be the same as the particle distribution for particles generated by drop,   the PULF, which represents the product of ARF × RF, was developed based on the test results (see Equation 1). This implies that these two distributions are the same because the respirable release fraction of 0.0002 was taken from the respirable particle diameter of 10 µm (see Figure 3 and Figure 4).

The respirable particle size, however, is 10 μm AED and less as defined and discussed in Section 4.3.1, Section 6.2.1, and Attachment C. The respirable cut-off diameter is 3.5 μm for UO_2 particles, which corresponds to a mass fraction of 0.00002 (0.002%), an order of magnitude lower than 10 μm UO_2 particles.

In addition, the airborne release corresponds to the particles that can be suspended in air. Airborne particles range in size from 0.001 to 500 μm, with most of the particulate mass in the range from 0.1 to 10 μm. Particles below 0.1 μm in size have a behavior similar to that of molecules and are characterized by large random motions caused by collisions with gas molecules. Particles larger than 1 μm but smaller than 20 μm tend to follow the motion of the gas in which they are borne. Particles larger than 20 μm have significant settling velocities; consequently, they are airborne for relatively short periods of time (Reference 2.2.18 [DIRS 158659], Section 3.2). For example, the settling velocity is approximately 30 cm per second for a particle size of 100 μm with a density of 1 g/cm^3. Therefore, it is reasonable to select 100 μm as the maximum particle size for airborne particulates of fuel fines and crud. The 100 μm cut-off diameter for airborne particles from spent fuel corresponds to about 300 μm AED, which is the high bound of the airborne particle size range, as discussed previously.

The mass percent of particles smaller than 100 μm, corresponding to airborne particulates, is about 0.2% for both Figure 3 and Figure 4 results. Based on the definition of RF presented in Section 4.3.1, the RF from the impact rupture tests is therefore equal to 0.01 (0.002% / 0.2%).
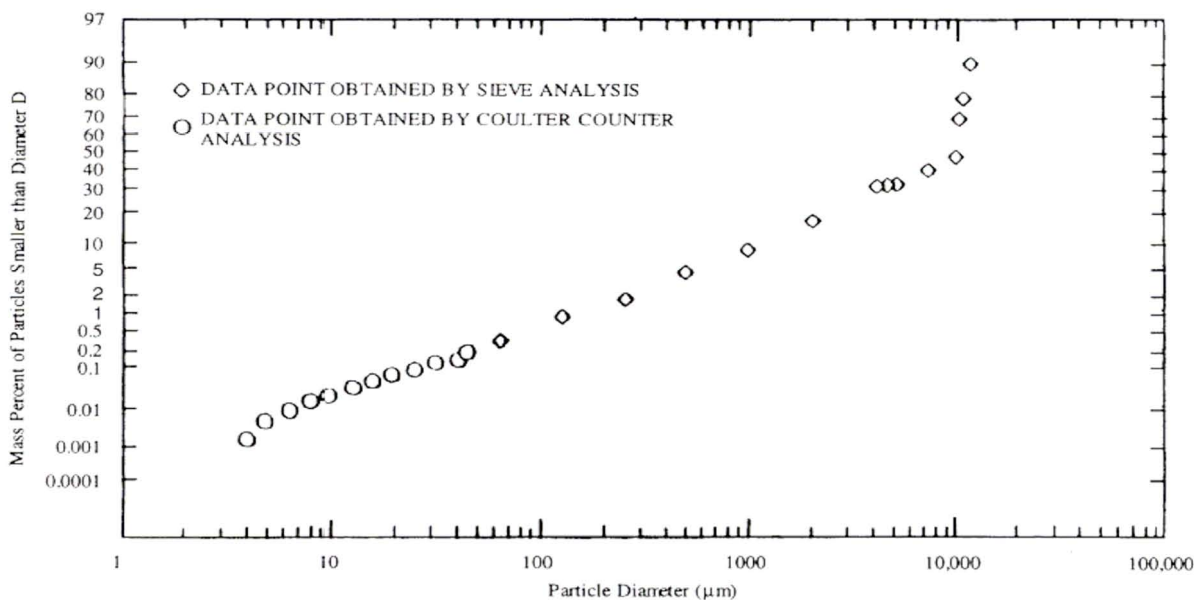
(Notes: for UO_2 Specimen No. 1 taken from Mecham et al. (Reference 2.2.58 [DIRS 158827], Figure 16)

Figure 3. Particle Size Distribution (No. 1) Measured with Drop Weight Impact of 1.2 J/cm^3
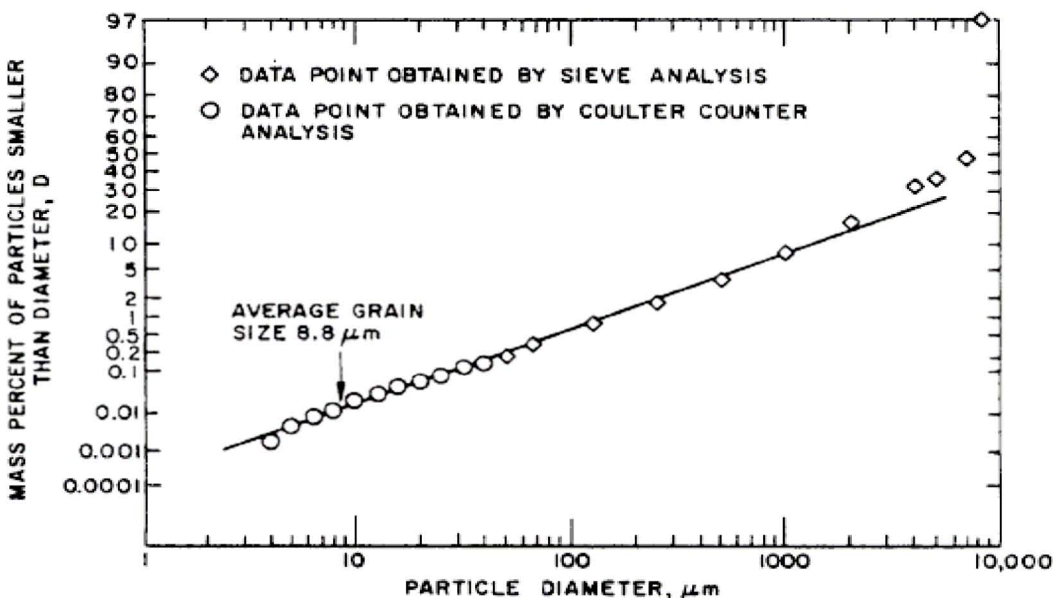
(Notes: for UO₂ Specimen No. 2 taken from Mecham et al. (Reference 2.2.58 [DIRS 158827], Figure 17)

Figure 4. Particle Size Distribution (No. 2) Measured with Drop Weight Impact of 1.2 J/cm^3

6.2.2.3 Comparison between Burst Rupture and Impact Rupture Distributions

From the previous two subsections, the RFs obtained from the two independent data sets do not vary significantly: 0.005 based on burst rupture tests vs. 0.01 based on impact rupture tests. Figure 5 compares the lognormal distributions produced for the burst rupture data (MMD = 150 μm, and MGSD = 3.8) from NUREG/CR-0722 (Reference 2.2.51 [DIRS 100990], p. 105 and Appendix C) and the impact rupture data (MMD = 18 mm and MGSD = 8.18) from ANL-81-27 (Reference 2.2.58 [DIRS 158827], Table 2). The resulting distributions show that, as expected, for commercial SNF particulates escaping through a hole in the clad produced by a burst rupture has fewer large particulates relative to the commercial SNF particulates produced by the impact of unclad fuel pellets. However, the shapes of the curves do not change significantly. Consequently, the respirable fractions from the two methods are similar. It should be noted that the data from the burst rupture tests are for all particles released from a segment of the fuel rod, while the data from the impact rupture tests are for all particles collected from the debris generated by the tests.

It is recommended in this document that the RF value of 0.005, which is based on the burst rupture tests, be used for intact commercial SNF. It is also recommended that the RF of 0.01, which is based on the impact rupture tests, be used for failed commercial SNF as discussed in Section 6.3.
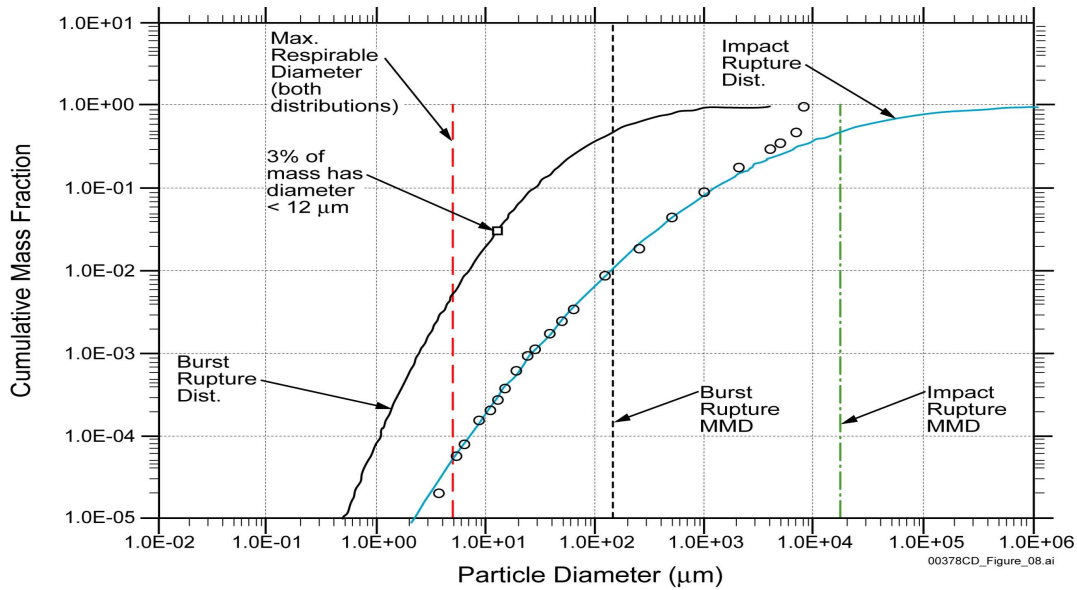
NOTE: Burst rupture data are from NUREG/CR-0722 (Reference 2.2.51 [DIRS 100990]) and impact rupture data are from ANL-81-27 (Reference 2.2.58 [DIRS 158827]).

Figure 5. Comparison of Cumulative Mass Fraction From Burst and Impact Ruptures

6.2.3   RF for Crud from Commercial SNF

Sandoval et al. (Reference 2.2.73 [DIRS 103696], p.II-5) reported that the measured distribution of crud particle sizes from a sample of Quad Cities fuel cladding had a lognormal distribution. This was determined from photographs using a scanning electron microscope. The mean geometric diameter (MGD) for the particle size distribution was 3.0 μm, with a geometric standard deviation (GSD) of 1.87.

The calculation of RF for crud is performed using the Mathcad software. The Mathcad file, "*RF_Crud.xmcd*", is shown in Figure 6. Using the input parameters for particle size, a probability distribution for particle size, NPD(x), is first defined. A probability distribution for particle mass, MPD(x), is calculated from the NPD(x). The mass fractions are then calculated using the cumulative distribution for particle mass. Because the particle size from crud is relatively small, all particles can become airborne, which is addressed by calculating the mass fraction of particles smaller than 100 μm as 1. The mass fraction of particles smaller than 5 μm, which corresponds to 10 μm AED respirable particles as discussed in Section 6.2.1 and Attachment C, is about 0.15. Based on the definition of the RF presented in Section 4.3.1, the RF for crud is the ratio of the respirable fraction to the airborne fraction, which is equal to 0.15.

Respirable Fraction For Crud

Purpose: to find respirable fraction for crud at given conditions

Assumption: lognormal distribution for both number and mass of particle size

Given conditions: geometric mean (GM) of particle number distribution = 3 um,
geometric standard deviation (GSD) for the distribution = 1.87

Method: convert the particle number distribution to mass distribution, and then find cumulative mass fraction at a cutoff particle size for respirable portion

Calculations:

1. Define probability distribution for number (NPD) where x is particle size in um

$$GM := 3 \qquad GSD := 1.87$$

$$mu := \ln(GM) \qquad sig := \ln(GSD)$$

$$NPD(x) := dlnorm(x, mu, sig)$$

2. Define cumulative distribution for particle number (NCD)

$$NCD(x) := plnorm(x, mu, sig)$$

$$NCD(GM) = 0.5$$

3. Calculate particle mass based on its size using density of 5.2 g/cm3

$$ro := 5.2$$

$$M(x) := \left(\frac{4}{3}\right)\pi\left(\frac{x}{2}\right)^3 ro$$

4. Define probability distribution for mass (MPD), where x is particle size in um

$$low := 0.01 \qquad high := 100$$

$$MPD(x) := \frac{M(x)\, NPD(x)}{\displaystyle\int_{low}^{high} M(x) \cdot NPD(x)\, dx}$$

5. Define cumulative distribution for particle mass (MCD), where y is the cutoff particle size

$$MCD(y) := \int_{low}^{y} MPD(x)\, dx$$

6. Calculate the mass fraction at cutoff particle size for respirable portion

$$MCD(5) = 0.144$$

$$MCD(100) = 1$$

Figure 6. Calculation of RF for Crud Using Mathcad

The plots of particle size distributions for both particle number and particle mass are shown in Figure 7 and Figure 8 (taken from Mathcad file "*RF_Crud.xmcd*"). The mass fraction to any particle size can be found from the cumulative mass distribution shown in Figure 8. However, the RF for crud is very sensitive to particle cut-off diameter. For example, the RF would be about 0.5 for a particle cut-off size of 10 μm. In addition, the measured crud particle size distribution is only for BWR fuel, and similar data are not available for PWR fuel. Therefore, a conservative assumption (Assumption 3.2.2) is adopted that 100% of crud particles are respirable (RF = 1) as a conservative approach (bounding).
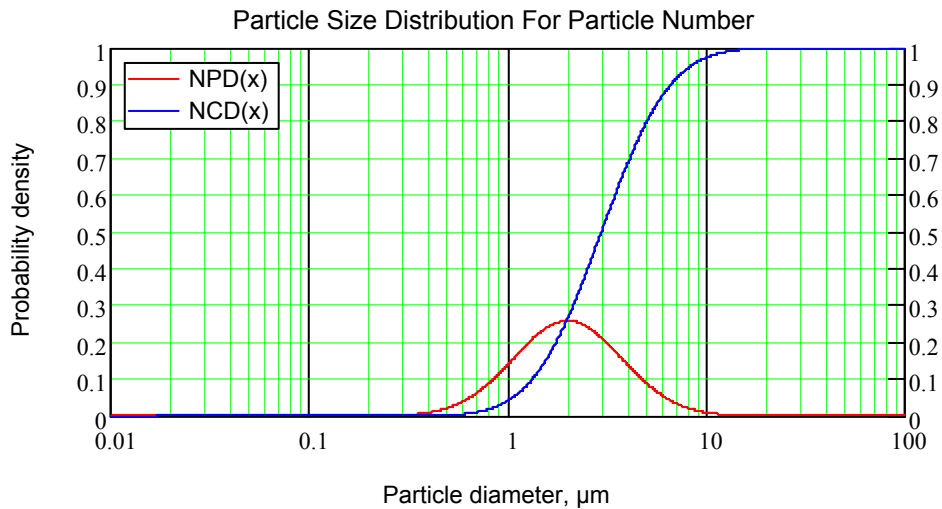

Figure 7. A Plot of Particle Size Distribution for Crud Particle Number Using Mathcad
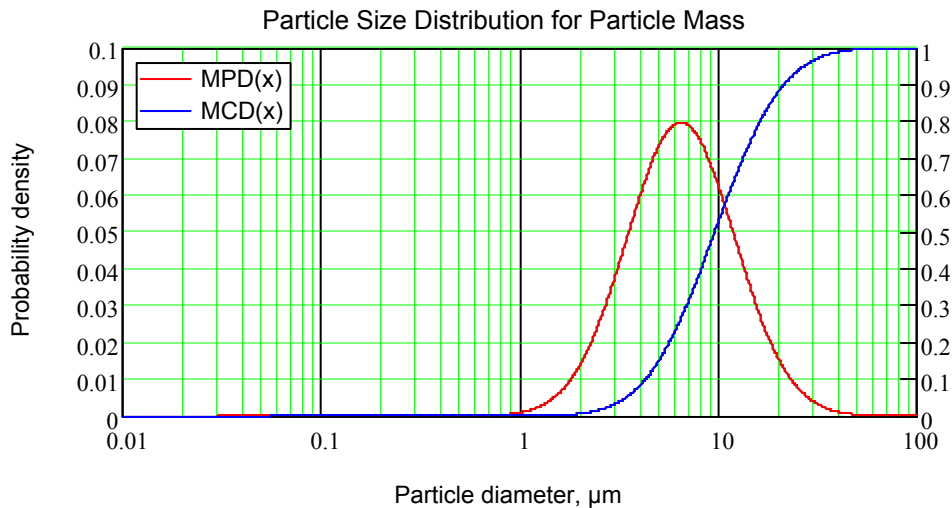
Figure 8. A Plot of Particle Size Distribution for Crud Particle Mass Using Mathcad

6.2.4   Summary of RFs for Intact Commercial SNF

For fuel fines from intact commercial SNF, an RF of 0.005 is recommended in this analysis. This value is based on the burst rupture tests as described in Section 6.2.2.1. For fuel fines from failed commercial SNF, an RF of 0.01 is recommended. This value is based on the impact rupture tests as described in Section 6.2.2.2. For crud from the cladding surface of commercial SNF, a conservative RF of 1.0 is recommended as discussed in Sections 6.2.3. For gases and volatiles, an RF of 1.0 is recommended.

6.2.5   Comparison of Respirable Release Fractions

The respirable release fractions (ARF × RF) have been calculated for rail casks and truck casks under hypothetical accident conditions in NUREG/CR-6672 (Reference 2.2.79 [DIRS 152476], pp.7-74 and 7-75). These values are compared in Table 6 with the values recommended for intact commercial SNF in this analysis.

Table 6. Respirable Release Fractions for Commercial SNF

Nuclide	Recommended Respirable Release Fractions (ARF × RF) [a]	Truck Casks [b]		Rail Casks [b]	
		PWR Release Fractions	BWR Release Fractions	PWR Release Fractions	BWR Release Fractions
^{3}H	0.3	1.4×10^{-1}	5.4×10^{-3}	1.8×10^{-1}	1.5×10^{-2}
^{85}Kr	0.3	1.4×10^{-1}	5.4×10^{-3}	1.8×10^{-1}	1.5×10^{-2}
^{129}I	0.3	4.1×10^{-9}	1.6×10^{-10}	5.4×10^{-9}	4.5×10^{-10}
^{134}Cs & ^{137}Cs	2×10^{-4}	4.1×10^{-9}	1.6×10^{-10}	5.4×10^{-9}	4.5×10^{-10}
^{90}Sr	1.5×10^{-7}	1.0×10^{-7}	4.0×10^{-9}	1.3×10^{-7}	1.1×10^{-8}
^{106}Ru	2×10^{-4}	1.0×10^{-7}	4.0×10^{-9}	1.3×10^{-7}	1.1×10^{-8}
Fuel Fines	1.5×10^{-7}	1.0×10^{-7}	4.0×10^{-9}	1.3×10^{-7}	1.1×10^{-8}
Crud (^{60}Co)	1.5×10^{-2}	1.4×10^{-3}	4.5×10^{-4}	1.8×10^{-3}	1.3×10^{-3}
Crud (^{55}Fe)	1.5×10^{-2}	1.4×10^{-3}	4.5×10^{-4}	1.8×10^{-3}	1.3×10^{-3}

NOTES: [a] Calculated based on ARF values in Table 5 and RF values in this section.

[b] NUREG/CR-6672 (Reference 2.2.79 [DIRS 152476], pp.7-74 and 7-75) Case 2 for truck casks and Case 5 for rail casks.

ARF = airborne release fraction; BWR = boiling water reactor; PWR = pressurized water reactor; RF = respirable fraction.

For gases, cesium, strontium, ruthenium, and fuel fines, the RF values recommended in this analysis are more conservative than the corresponding values given in NUREG/CR-6672 (Reference 2.2.79 [DIRS 152476], pp.7-74 and 7-75) for cases with impact speeds ranging from 30 to 60 mph and interior cask temperatures ranging from the ambient temperature to 350°C. The crud respirable release fraction of 0.015 recommended in Table 6 is also conservative

compared to the values given in NUREG/CR-6672 (Reference 2.2.79 [DIRS 152476], pp.7-74 and 7-75). It is concluded that the ARFs and RFs recommended in this document are appropriate based on the comparison shown in Table 6.

6.3 ARFs AND RFs FOR FAILED COMMERCIAL SNF

This section examines and establishes the ARFs and the RFs for failed commercial SNF. This section first examines the applicability of the ARFs and RFs established for intact commercial SNF in Sections 6.1 and 6.2 to those for failed commercial SNF. For cases where the intact commercial SNF values do not bound those of the failed commercial SNF, an estimate of bounding values for the failed commercial SNF is included.

According to the report *1999 Design Basis Waste Input Report for Commercial Spent Nuclear Fuel* (Reference 2.2.20 [DIRS 145022], p.C-1), there are four categories of "problematic" commercial SNF projected to be placed into disposable canisters (defined as canisters that can be placed into disposal containers without being repackaged). These four categories include:

1. *Mechanically and Cladding-Penetration Damaged SNF,* which includes: (1) fuel that is mechanically damaged such that it cannot be vertically lifted or fit within a standard dimension and/or (2) fuel that has lost containment as a result of cladding damage.

   For this evaluation, it is assumed that the fuel in this category is made-up of intact fuel assemblies and fuel pins/rods. The fuel pins/rods are held in some grid-like structure within a canister that provides the pins/rods with structural support equivalent to that of an intact assembly (Assumption 3.2.5).

2. *Consolidated/Reconstituted Assemblies*, which includes fuel that was disassembled and, when reassembled, has a form that is dimensionally different from the original.

   For this evaluation, it is assumed that the fuel in this category is also made-up of intact fuel assemblies. If the fuel assembly is a reassembled assembly, then its structural support is considered equivalent to an un-reassembled assembly (Assumption 3.2.5).

3. *Fuel Rods, Pieces, and Debris,* which includes variable-sized pieces of fuel and debris combining fuel and nonfuel materials.

   For this evaluation, it is assumed that the fuel in this category is in the form of loose fuel rods, fuel pieces, and debris and does not have any structural support system while in a canister (Assumption 3.2.5).

4. *Nonfuel Components,* which includes in-core assembly components physically separated from the assemblies and shipped separately.

Establishment of ARFs and RFs for the final category, Nonfuel Components, is outside the scope of this report; however, it is expected that the potential consequences resulting from an accident event involving this material are bounded by those from the other categories. This is due principally to the lack of fuel material included with the components of this category. The source term from this category is likely to be dominated by the surface crud source term.

The ARFs and RFs for specific isotopes identified in Sections 6.1 and 6.2 for intact commercial SNF involved in drop or impact events are examined to establish whether they bound the potential ARFs for each of the four categories of failed commercial SNF. The identified groups of specific isotopes are gases (^{3}H, ^{85}Kr, and ^{129}I), volatiles (^{134}Cs, ^{137}Cs, and ^{106}Ru), fuel fines (^{90}Sr, etc.), and crud (^{60}Co and ^{55}Fe). Crud also includes surface activity that is examined for each of these failed commercial SNF categories.

The failed fuel analyzed in this section is assumed to be contained within an annular canister with mesh screen caps at each end. Fuel handling at the repository does not involve removing this fuel from the canister. Fuel classified as failed but maintaining the form of an assembly or a group of fuel rods placed in some grid-like spacers provided within the canister (matrixed) are considered to withstand a drop or impact event without any pulverization (Assumption 3.2.5). This essentially means that the structural support of the fuel assembly/fuel rods and the canister wall act monolithically to mitigate any pulverization of the fuel. In other words, this failed commercial SNF acts the same as intact commercial SNF during normal operation because it is sealed and packaged within the canisters. During an accident, this failed commercial SNF is subject to the same impact energy as intact commercial SNF. Releases from intact fuel are larger than those from failed fuel because there is a higher gas pressure inside intact fuel rods that drives more radioactive material out. The following subsections provide the justifications for each ARF category considered in this document.

6.3.1   ARFs and RFs for Gases

As fuel is irradiated in a nuclear power reactor, fission product atoms, of which approximately 15 percent are inert gases, are produced and buildup internal to the cladding of the fuel rods. Release of these fission gases from the fuel matrix to the plenum and the gap region between the fuel and the cladding is directly related to fuel pellet swelling which is a strong function of linear power density. The primary fission gases released to this gap region for commercial SNF are noble gases, iodines, and tritium. The recommended ARF values for these gases for intact commercial SNF are based on Regulatory Guide 1.25 (Reference 2.2.68 [DIRS 107691], p.25.2), which states that the release fractions of these fission gases from the gap region of a fuel rod are conservatively assumed to consist of 30 percent of the ^{85}Kr, 10 percent of other noble gases, and 10 percent of the radioactive iodine. In addition, Regulatory Guide 1.25 (Reference 2.2.68 [DIRS 107691], p.25.2) states that 30 percent of the ^{127}I and ^{129}I inventory is to be assumed to be released for the purpose of sizing filters. These ARFs for gases are consistent with values used in many reference sources as shown in Table 3.

Discussions of ARFs for gases are provided for each type of failed commercial SNF in the following subsections. Similar to intact commercial SNF, the RF for gases is set equal to 1.0 in all cases (a bounding value) as 100 percent are considered respirable. Table 7 summarizes the following subsection results for the ARFs and RFs for gases associated with each category of failed commercial SNF. The ARFs and RFs for intact commercial SNF are also included in the table for reference.

Table 7. ARFs and RFs for Gases for Failed Commercial SNF

Fuel Category	ARF / RF		
	^{3}H	^{85}Kr	^{129}I
1. Mechanical/Cladding Damaged	0.3 / 1	0.3 / 1	0.3 / 1
2. Consolidated/Reconstituted	0.3 / 1	0.3 / 1	0.3 / 1
3. Other Fuel Rods, Pieces, and Debris	0.3 / 1	0.3 / 1	0.3 / 1
Intact Commercial SNF	0.3 / 1	0.3 / 1	0.3 / 1

NOTES: ARF = airborne release fraction; RF = respirable fraction; SNF = spent nuclear fuel.

6.3.1.1 Mechanically and Cladding-Penetration Damaged SNF

The release of fission gases from mechanically and cladding-penetration damaged SNF only occurs from the plenum and from the gap region between the cladding and the fuel of a fuel rod. An impact or drop event may result in the cladding of this failed fuel category being punctured, penetrated, or cracked resulting in the release of the gap fission gases. Fission gases from the fuel matrix, excluding the fraction considered released to the gap, are not expected to be released as a result of an impact or drop event. This is because the additional structural support provided to the assemblies or matrixed fuel rods by the canister mitigates the potential release of additional gases from the fuel matrix by preventing potential fuel pulverization caused by a drop or impact event.

For the mechanically and cladding-penetration damaged SNF category of failed fuel, the ARFs for fission gases are bounded by those established for intact commercial fuel (Table 5). This is clearly true for the cladding-penetrated commercial SNF where the majority of the fission gases originally in the gap have already been purged through the leak paths provided by the cladding penetrations prior to an impact or drop event. The penetration damage also ensures that no more fission gases have accumulated in the gap. The cladding of mechanically damaged commercial SNF prior to an impact or drop event may be either intact or failed. These leak paths also ensure little or no further fission gas accumulation in the gap. For the portion of damaged fuel that has intact cladding, it can be effectively treated as intact commercial SNF. Therefore, the ARFs for gases established for intact commercial SNF in Section 6.1 are considered bounding for the mechanically and cladding-penetration damaged commercial SNF, as shown in Table 7.

6.3.1.2 Consolidated/Reconstituted Assemblies

The release of fission gases from consolidated and reconstituted assemblies only occurs from the gap between the cladding and the fuel of a fuel rod. An impact or drop event may result in the cladding of this failed fuel category being punctured, penetrated, or cracked resulting in the release of the gap fission gases. Fission gases from the fuel matrix, excluding the fraction considered released to the gap, are not expected to be released as a result of an impact or drop event. This is because the additional structural support provided to the assemblies (or matrixed fuel pins) of this failed fuel category by the canister mitigates the potential release of additional gases from the fuel matrix by preventing potential fuel pulverization caused by a drop or impact event. Furthermore, the differences between this category of failed fuel and the fuel analyzed in Section 6.1 are insignificant with respect to the ARFs for fission gases. Thus, for the consolidated/reconstituted assembly category of commercial SNF failed fuel, the ARFs for the

fission gases are bounded by those established for intact commercial SNF in Section 6.1, as shown in Table 7.

6.3.1.3   Fuel Rods, Pieces, and Debris

Fuel rods, pieces, and debris do not have any assembly-like support structure while in a canister. Consequently, an impact or drop event can pulverize up to 20 percent of the fuel thereby releasing fission gases from the fuel matrix (see Assumption 3.2.5). There can also be a release of fission gases from the gap for a fuel rod in this category that still has intact cladding and that is then punctured, penetrated, or cracked.

For the fuel rods, pieces, and debris category of failed commercial SNF, the ARFs for the fission gases are bounded by the values of 0.3 listed in Section 6.1 for intact commercial SNF, as shown in Table 7. This is demonstrated as follows:

- For fuel rods in this group with intact cladding that are pulverized in the event of a drop or impact, the release fraction for the fission gases in the gap is less than 0.005 (Reference 2.2.51 [DIRS 100990], Tables 4 and 5). Adding that value to the fraction of the fuel matrix pulverized (0.2 per Assumption 3.2.5), yields a total that is less than the 0.3 value for intact commercial SNF.

- For fuel rods in this group with previously failed cladding, the fission gases in the gap would already have been released prior to the drop or impact event. Consequently, the fraction of fission gases released (i.e., the ARF) is limited to the amount assumed to be pulverized, or 0.2. This is less than the 0.3 value for intact commercial SNF.

- For fuel pieces and debris, these items are considered to be devoid of any intact cladding and thus do not have any gap fission gases to release in a drop or impact event. Consequently, the fraction of fission gases released (i.e., the ARF) is also limited to the amount assumed to be pulverized, or 0.2. This is less than the 0.3 value for intact commercial SNF.

The fraction of fuel assumed pulverized (see Section 6.3.2.3 does not include fission gases released from a fuel rod prior to the placement of the rods into a canister or the fission gases that remain in the particulates created by pulverization, which equate to about 30 percent of the total fission gas inventory.   Regulatory Guide 1.25 (Reference 2.2.68 [DIRS 107691], p.25.2) conservatively estimates that 30 percent of the fission gases are released to the gap. Considering this fraction and allowing for the fission gases that remain captured by the smaller particulates following pulverization, the use of a fission gas ARF of 0.3 is considered conservative.

6.3.2   ARFs and RFs for Volatiles and Fuel Fines

Fuel fines and volatiles found in the gap are liberated or created from fuel pellets because of the shaking of the rod and grinding action between fuel pellets that occurs during handling and transport of the fuel. Fuel fines exist as residue from the fuel manufacturing process and are also produced during irradiation from pellet cracking that is associated with thermal distortion caused

while the fuel was at high temperatures. In the latter case, the higher temperature at the center of a fuel pellet than at the periphery produces circumferential tensile stress that produce radial pellet cracks.

Some of the primary constituents that makeup fuel fines and volatiles of commercial SNF, as specifically noted in NUREG-1536 (Reference 2.2.63 [DIRS 101903], Table 7.1) and NUREG-1567 (Reference 2.2.65 [DIRS 149756], Table 9.2), are ^{90}Sr, ^{106}Ru, ^{134}Cs, and ^{137}Cs. As discussed in Section 6.1.3, the only volatiles potentially present in a potential accident at the repository are cesium and ruthenium. Volatiles are assumed to be 100 percent respirable (bounding).

The recommended ARF values for these nuclides, and fuel fines in Sections 6.1.3 and 6.1.4 are based on data collected from burst rupture tests in NUREG/CR-0722 (Reference 2.2.51 [DIRS 100990], Table 40). These ARFs are also consistent with values cited in NUREG/CR-6487 (Reference 2.2.4 [DIRS 145345], pp. 31 and 32) and NUREG/CR-6410 (Reference 2.2.69 [DIRS 103695], Table 3-1) for use in potential accident releases from intact fuel rods.

An extensive analysis of the RF in Section 6.2 for fuel fines released in the burst rupture tests reported in NUREG/CR-0722 (Reference 2.2.51 [DIRS 100990], p.105 and Appendix C), established an RF of 0.005. In addition, the experimental results reported in ANL-81-27 (Reference 2.2.58 [DIRS 158827]) as discussed in section 6.2.2.2 indicate that a RF value of 0.01 can be obtained from a drop or impact event that involves fuel pulverization. The applicability and details of these tests are described in detail in Sections 6.1 and 6.2. The ARFs were not produced from these experiments because the glass and UO$_2$ ceramic specimens being impacted by a dropped weight were unconfined (i.e., no cladding). These test data and their associated PULF (see Equation 2) were considered not appropriate for application to dropped or impacted intact commercial SNF assemblies. However, these data are considered applicable for failed commercial SNF because some of the failed fuel exists as small unclad fuel pieces and debris. Table 8 summarizes the ARFs and RFs for volatiles (i.e., cesium and ruthenium) and for fuel fines associated with each category of failed commercial SNF. The ARFs and RFs for intact commercial SNF are also included in the table for reference. Detailed discussions for volatiles and fuel fines for each type of failed commercial SNF are provided in the following subsections.

Table 8. ARFs and RFs for Volatiles and Fuel Fines for Failed Commercial SNF

Fuel Category	ARF / RF [a]		
	^{134}Cs & ^{137}Cs & ^{106}Ru	^{90}Sr	Fuel Fines
1. Mechanical/Cladding Damaged	2×10^{-4} / 1	3×10^{-5} / 5×10^{-3}	3×10^{-5} / 5×10^{-3}
2. Consolidated/Reconstituted	2×10^{-4} / 1	3×10^{-5} / 5×10^{-3}	3×10^{-5} / 5×10^{-3}
3. Fuel Rods, Pieces, & Debris	2×10^{-4} / 1	3×10^{-5} / 0.01	3×10^{-5} / 0.01
Intact Commercial SNF	2×10^{-4} / 1	3×10^{-5} / 5×10^{-3}	3×10^{-5} / 5×10^{-3}

NOTES: [a] These values assume a cask drop from 7 meters (see discussion in Section 6.3.2.3).
ARF = airborne release fraction; RF = respirable fraction; SNF = commercial spent nuclear fuel.

6.3.2.1   Mechanically and Cladding-Penetration Damaged SNF

The release of volatiles and fuel fines from mechanically and cladding-penetration damaged SNF occurs from the fuel surface and from the gap between the cladding and the fuel. An impact or drop event may result in the cladding of this failed fuel category to be punctured, penetrated, or cracked resulting in the release of the volatiles and fuel fines through entrainment by the exhausting gases in the gap. Volatiles and fuel fines in the fuel matrix are not expected to be released as a result of an impact or drop event because the additional structural support provided by the canister prevents fuel pulverization (see Assumption 3.2.5).

Thus, for the mechanically and cladding-penetration damaged SNF category of failed fuel, the ARFs for the volatiles and fuel fines on the surface of the fuel and in the gap are bounded by those established in Table 5. This is clearly true for the cladding-penetrated commercial SNF where the majority of the fission gases originally in the gap have already been purged through the leak paths provided by the cladding penetrations prior to an impact or drop event, thereby removing the motive force contributing to the expulsion of these fission products from the irradiated fuel.

For the mechanically damaged commercial SNF, the ARFs are bounded for the same reasons the intact commercial SNF is bounded by these ARFs: high deposition through narrow, often long, and tortuous paths to the breach point, especially for larger particulates which constitute a majority of the total mass released. Furthermore, the canister walls increase the amount of surface area where local deposition of fuel fines/volatiles can take place, effectively increasing the tortuous paths they must pass through prior to escaping to the environment. These characteristics provide sufficient justification that the fuel fine and volatile ARFs for intact commercial SNF bound the same ARFs for this category of failed commercial SNF, as shown in Table 8.

6.3.2.2   Consolidated/Reconstituted Assemblies

The release of volatiles and fuel fines from consolidated and reconstituted assemblies only occurs from the fuel surface and from the gap between the cladding and the fuel. An impact or drop event may result in the cladding of this failed fuel category to be punctured, penetrated, or

cracked resulting in the release of the volatiles and fuel fines through entrainment by the exhausting gases in the gap. Volatiles and fuel fines in the fuel matrix are not expected to be released as a result of an impact or drop event because the additional structural support provided by the canister prevents fuel pulverization (see Assumption 3.2.5).

Thus, for the consolidated/reconstituted assembly category of commercial SNF failed fuel, the ARFs for the volatiles and fuel fines in the gap are bounded by those established in Table 5. This is because of the same reasons the intact commercial SNF is bounded by these ARFs: high deposition through narrow, often long, and tortuous paths to the breach point especially for larger particulates which constitute a majority of the total release mass (see Section 6.2). The canister walls also increase the amount of surface area where local deposition of fuel fines/volatiles can take place, effectively increasing the tortuous paths the fuel fines/volatiles must pass through prior to escaping to the environment. These characteristics provide justification that the fuel fine and volatile ARFs for intact commercial SNF bound the same ARFs for this category of failed commercial SNF, as shown in Table 8.

6.3.2.3   Fuel Rods, Pieces, and Debris

The release of fuel fines and volatiles from fuel rods, pieces, and debris occurs from the fuel matrix and, for fuel rods with intact cladding, from the gap. An impact or drop event may result in the cladding of a fuel rod in this failed fuel category to be punctured, penetrated, or cracked resulting in the release of the volatiles and fuel fines through entrainment by the exhausting gases in the gap. In addition, because this category of failed fuel is not considered to have any assembly-like structure while in a canister, an impact or drop event may pulverize some fraction of the fuel, thereby releasing fuel fines and volatiles from the fuel matrix (see Assumption 3.2.5).

Thus, for the fuel rods, pieces, and debris category of failed commercial SNF, the product of the ARF and the RF for the fuel fines is conservatively assumed equal to the PULF as discussed in Section 4.3.4. Because the PULF equation (Equation 2) was derived from data involving small specimens (i.e., three pellets), there may be a large degree of conservatism built into this equation when its use is extrapolated to masses greater than a few pellets. This conservatism is due in a large part to a cushioning effect created by the pulverization of the fuel at the bottom of a stack of fuel (e.g., pellets in a fuel rod). The fuel at the bottom of the dropped stack is pulverized into a powder and then acts as a cushion to the fuel dropping above it. In addition, this equation does not take into account the structural credit provided by the presence of cladding or the canister.

As discussed in Section 4.3.4, in an attempt to correct for some of this conservatism, SAND84-2641 (Reference 2.2.53 [DIRS 104779], pp.5-24 to 5-26) modified the PULF correlation by including an EPF. Unfortunately, values for EPF are not available from analysis or experiment; however, SAND84-2641 (Reference 2.2.53 [DIRS 104779], pp.5-24 to 5-26) assumed that this factor is conservatively 0.2. This is equivalent to assuming that approximately only 20 percent of the total fuel is pulverized, most likely the bottom 20 percent.

Not all of the pulverized fuel will be released into environment, because all failed commercial SNF are in a canister based on Assumption 3.2.5. The canister reduction factor (RED) is not available experimentally. Therefore, an analog analysis is provided below to estimate this factor.

DOE-HDBK-3010-94 (Reference 2.2.24 [DIRS 103756], pp.4-85 – 4.87) provides experimental data from three rocks (1.29 kg, 1.17 kg, and 1.82 kg) dropped from a height of 3.7 m either (1) onto sand held in an open-lid steel quart can in a vented metal box placed on a plywood sheet or (2) onto unconfined sand placed on a plywood sheet. Two experiments were performed using sand screened to be less than 500 μm in diameter with 1.8 percent less than 25 μm. The measured ARF and RF for the confined sand were 3.0×10^{-4} and 0.07, respectively, while the ARF and RF for the unconfined sand were 8.7×10^{-4} and 0.36 (Reference 2.2.24 [DIRS 103756], Table 4-15), respectively. The experiments showed that the can reduces the sand release significantly. The RED can be estimated by:

$$\text{RED} = \frac{(ARF \times RF)_{confined}}{(ARF \times RF)_{unconfined}} = \frac{3.0 \times 10^{-4} \times 0.07}{8.7 \times 10^{-4} \times 0.36} = 0.067 \qquad \text{Equation 4}$$

A failed fuel canister would be expected to provide the same degree or better confinement than on open-lid can. Although applicability of the experimental data to failed commercial SNF may be questioned, it clearly indicates that the canister used for failed fuel can reduce the release of pulverized particulates into the environment by at least one order of magnitude. Therefore, a conservative value for the RED of 0.1 is used for a failed fuel canister.

In addition, the respirable fraction for particulates is based on the mass of particles less than 10 μm physical diameter, not the 10 μm AED in ANL-81-27 (Reference 2.2.58 [DIRS 158827], Figures 16 and 17, Table 2). As discussed in Section 6.2.1 and Attachment C, for uranium oxide particles with a density of 10.96 g/cm^3, the respirable size is about 3.5 μm. In a 1.2 J/cm^3 drop-weight impact on a set of three UO$_2$ pellets, the fractions of particles smaller than 10 μm and 3.5 μm are 2×10^{-4} and 2×10^{-5}, respectively (Reference 2.2.58 [DIRS 158827], Figures 16 and 17). Because the PULF equation is based on a respirable particle size of 10 μm physical diameter, the PULF value can logically be reduced by a respirable correction factor (RCF) of 0.1 ($= 2 \times 10^{-5} / 2 \times 10^{-4}$) to correct for the fraction of respirable fuel fines.

Based on above discussion, the corrected PULF for failed fuel rods, pieces, and debris can be written as:

$$\text{PULF}_{corrected} = EPF \times RED \times RCF \times A \times \rho \times g \times h \qquad \text{Equation 5}$$

where

EPF = the energy partition factor, 0.2
RED = the canister reduction factor, 0.1
RCF = the respirable correction factor, 0.1.

The design of the repository surface facilities, such as the CRCF, limits the maximum lift heights to less than 7 meters. This lift height is provided in *Basis of Design for the TAD Canister-Based Repository Design Concept* (Reference 2.2.12 [DIRS 182131], Section 4.2.1.9.22), but it does not specifically mention for the TAD canister. However, the facility is designed for all canisters. It would be too complicated to change the configuration every time to deal with different waste

canisters. Therefore, the maximum lift height provided for a HLW canister or other canisters is also valid for the TAD canister. Using Equation 5 with input values for Equation 2, a correct PULF can be calculated:

$$PULF_{corrected} = 0.2 \times 0.1 \times 0.1 \times 2 \times 10^{-11} \times 10.96 \times 980 \times 700 = 3 \times 10^{-7} \qquad \text{Equation 6}$$

This calculated corrected PULF value is the product of ARF × RF. The RF from the impact rupture test data is 0.01 as discussed in 6.2.2.2. Therefore, the ARF is calculated from Equation 6 to be 3×10^{-5}, which is the same as the ARF for intact commercial SNF. The PULF value is the release fraction from a drop event, and it does not include the releases of fuel fines from the gas when cladding breaches during the drop event. However, the contribution from the fuel fines from the gaps is at least one order of magnitude lower because of the canister reduction factor discussed above. The ARF and RF for the category of fuel rods, pieces, and debris under failed commercial SNF are shown in Table 8.

For the volatile radionuclides released from failed fuel in the category of fuel rods, pieces, and debris, the use of the intact commercial SNF ARF/RF of $2 \times 10^{-4} / 1$ is also conservative because a portion of volatile radionuclides was already released when fuel rods, pieces and debris were formed at the reactor site. The ARF/RF values of $2 \times 10^{-4} / 1$ are bounding for the release of cesium isotopes from failed fuel, as shown in Table 8.

6.3.3 ARFs and RFs for Crud

Crud releases originate from the surface of a fuel rod and associated components (e.g., grid spacers). In contrast to the fuel fines, gases, and volatiles released from a fuel rod, the crud release fraction is not based on the fraction of fuel rods that are breached and the release mechanism involves surface spallation rather than leakage past fuel cladding barriers. Crud is primarily composed of iron-based compounds and some nickel, copper, cobalt, chromium, manganese, zinc, and zircalloy. The actual amount varies from reactor to reactor and cycle to cycle. Crud has become radioactive through neutron activation and has a relatively short half-life. In general, pressurized water reactor fuel is found to have less crud activity than boiling water reactor fuel (Reference 2.2.73 [DIRS 103696], p.2).

From Section 6.1.5, the crud effective ARF for intact commercial SNF fuel assemblies is 0.015, which is also recommended for use for failed commercial SNF categories with cladding. Similarly, the RF for crud is conservatively established in Section 6.2.3 to be equal to 1, which is also recommended for use for failed commercial SNF categories. Additional discussion for each category of failed fuel is provided in the following subsections.

Table 9. ARFs and RFs for Crud for Failed Commercial SNF

Fuel Category	ARF / RF	
	^{60}Co	^{55}Fe
1. Mechanical/Cladding Damaged	0.015 / 1	0.015 / 1
2. Consolidated/Reconstituted	0.015 / 1	0.015 / 1
3. Other Fuel Rods, Pieces, and Debris	0.015 / 1	0.015 / 1
Intact Commercial SNF	0.015 / 1	0.015 / 1

NOTES: ARF = airborne release fraction; RF = respirable fraction; SNF = spent nuclear fuel.

6.3.3.1 Mechanically and Cladding-Penetration Damaged SNF

A crud effective ARF of 0.015 and an RF of 1 applied to this failed fuel category are considered bounding, because this fuel is unlikely to have crud characteristics significantly different from intact commercial SNF.

6.3.3.2 Consolidated/Reconstituted Assemblies

Application of a crud effective ARF of 0.015 and an RF of 1 is clearly conservative for the consolidated/reconstituted assemblies because a significant amount of crud on the surfaces of the fuel pins would have been removed when the pins were pulled through the grid structures. Any remaining crud on the pin surfaces is likely to be tightly adhering and unlikely to flake off during a drop or impact event.

6.3.3.3 Fuel Rods, Pieces, and Debris

For fuel rods, pieces, and debris, a crud effective ARF of 0.015 and an RF of 1 are conservative. Fuel rods would likely have been pulled through grid structures, which would have removed the majority of loosely adhering crud leaving only tightly adhering crud. Similarly, pieces and debris are likely to have only a small amount of crud or no crud depending on the origin of fuel. For example, fuel pellets that have only been exposed to a spent fuel pool environment are likely to have no crud on their surfaces.

6.3.4 Summary of ARFs and RFs for Failed Commercial SNF

The discussions in Sections 6.3.1 to 6.3.3 indicate that the ARFs and RFs developed for intact commercial SNF are reasonable and conservative for use with failed commercial SNF. The ARFs for intact commercial SNF shown in Table 5 and the RFs summarized in Section 6.2.4 are applicable to failed commercial SNF, as shown in Table 7 and Table 8. The only exception is the RF for fuel rods, debris and pieces, which is selected based on impact rupture test data, is higher by a factor of two (0.01) than the value from burst rupture test data (0.005). However, a drop of fuel rods, debris and pieces is not an accident scenario considered in preclosure consequence analyses, because the radionuclide inventory associated with fuel rods, debris and pieces is much lower than a spent fuel assembly.

6.4 ARFs AND RFs FOR FUEL OXIDATION

Based on the TAD canister-based repository design concept (Reference 2.2.12 [DIRS 182131], Section 4.2.1.9.8), the CRCF and the TAD canister are designed to maintain the cladding temperature for commercial SNF below 400ºC during normal operations and 570ºC during off-normal and accident conditions (Reference 2.2.12 [DIRS 182131], Section 33.2.2.27 and 33.2.2.28). Within these cladding temperature limitations, oxidation of fuel pellets can occur only if the fuel pellets are exposed to air. This can occur if a canister is breached during an accident because the fuel rods are also likely to be breached, thereby exposing the fuel pellets to air. The oxidation process, which occurs on the air-exposed fuel surface, is dependent on the temperature of the fuel surface.

Once an accident occurs, air can freely reach the fuel pellets through the breached canister and cladding without restriction (Assumption 3.2.6). These assumptions are bounding because not all rods may be damaged by the event and because the defect size may inhibit the access of oxygen through the cladding to the fuel. The oxidation process starts at the area of breached cladding, which then causes additional stress on the cladding due to fuel pellet volume increase. This volume increase leads to unzipping of cladding until all fuel materials are oxidized to U_3O_8 powder.

The particle size distribution of oxidized U_3O_8 depends strongly on temperature. A higher temperature oxidizes UO_2 quickly but creates relatively large particles. For example, a particle size of 600 μm was reported from a test at a temperature of 900°C; 80 μm at 700°C; 16 μm at 500°C; and 7.5 μm at 300°C (Reference 2.2.49 [DIRS 172864], p.5). The reference temperature for spent fuel is 400°C. The temperature limit of 570ºC during off-normal and accident conditions (Reference 2.2.12 [DIRS 182131], Section 33.2.2.28) is not used for evaluating fuel oxidation because this temperature limit was set for accidents involving transportation casks involved in a fire. Therefore, based on the tests cited above (Reference 2.2.49 [DIRS 172864], p.5), oxidized fuel particles are expected to be in a range of about 10 μm when oxidation occurs at a temperature of 400°C.

Literature data indicate that UO_2 oxidizes into U_3O_8 powder completely in a few hours at a temperature of 400°C (Reference 2.2.39 [DIRS 172518], p. 48). Only 3% of the mass has a particle size larger than 44 μm, and 10% of mass has a particle size between 10 μm and 44 μm (Reference 2.2.39 [DIRS 172518], Figure 1). This demonstrates that it is appropriate to conservatively treat all oxidized fuel particles as being capable of becoming airborne.

This section considers the fuel oxidation for the low burnup fuel (less than about 45 GWd/MTU). Because high burnup fuel has different characteristics from low burnup fuel, the fuel oxidation process may also be different. The fuel oxidation for high burnup fuel (up to 80 GWd/MTU) is discussed in Section 6.6.

6.4.1 Fuel Oxidation

As discussed in Section 4.3.5, a two-step process ($UO_2{\rightarrow}UO_{2.4}{\rightarrow}U_3O_8$) is commonly used to model the oxidation of spent fuel in air. The first step depends on fuel temperature only, while the second step depends on both fuel temperature and burnup. In this section, the maximum

allowed temperature for stainless steel clad assemblies (400°C) and average burnup is used to estimate the oxidation fraction of damaged spent fuel.

This section reviews current methods available to calculate UO_2 and U_3O_8 oxidation rates, describes the key fuel parameters for oxidation including crack propagation rates, estimates the fraction of oxidation in a damaged fuel rod, and determines the time for complete oxidation of the damaged fuel rod. These are then used in Section 6.4.2 through Section 6.4.4 to determine the ARFs and RFs for oxidation after an accident.

6.4.1.1 Incubation Time

The extent of oxidation is dependent on both the temperature of the fuel and the time that the fuel is exposed to air. As discussed above, fuel first oxidizes to $UO_{2.4}$, and then to U_3O_8. As the fuel is converted to U_3O_8, its volume increases producing stress on the cladding that can lead to clad unzipping. The time between the onset of oxidation and the time of U_3O_8 formation is defined as the incubation time, as discussed in BSC 2005 (Reference 2.2.11 [DIRS 173261], Section 5.1.1). The incubation time is a function of the pellet/cladding gap at the onset of oxidation, the time for the fuel in any local region to oxidize to $UO_{2.4}$, and the time for a fraction of the fuel to react to U_3O_8.

The calculation methods used to determine the time to oxidize to $UO_{2.4}$ are given in several references including NUREG-1565 (Reference 2.2.3 [DIRS 101547], Equation 1), PNNL-11929 (Reference 2.2.34 [DIRS 101672], Equation 2.3), and BSC 2005 (Reference 2.2.11 [DIRS 173261], Equation 5-1). The general equation is as follows:

$$t_{2.4} = k_{2.4} \times \exp\left(\frac{Q_{2.4}}{RT}\right) \qquad \text{Equation 7}$$

where

$t_{2.4}$ = time that UO_2 oxidizes to $UO_{2.4}$, hour or year

$k_{2.4}$ = empirically derived coefficient, hour or year

$Q_{2.4}$ = activation energy, kJ/mol or kcal/mol

R = universal gas constant, J/(mol K) or cal/(mol K)

T = absolute temperature, K.

Table 10 summarizes the coefficients for Equation 7 from the three reference sources. The differences between these coefficients are relatively insignificant. The calculated time for oxidizing UO_2 to $UO_{2.4}$ is less than 2 hours when the fuel temperature is 673 K (400°C). Therefore, this process is very rapid when there is sufficient air available.

Table 10. Comparison of Coefficients and Results for Equation 7

	NUREG-1565 (Reference 2.2.3 [DIRS 101547], Equation 1)	PNNL-11929 (Reference 2.2.34 [DIRS 101672], Equation 2.3)	BSC 2005 (Reference 2.2.11 [DIRS 173261], Equation 5.1)	Notes
$k_{2.4}$, coefficient	2.97×10^{-13} yr (2.6×10^{-9} hr)	2.6×10^{-9} hr	1.40×10^{-8} hr (nominal) 2.93×10^{-9} hr (bounding)	Similar
$Q_{2.4}$, activation energy	26.6 kcal/mol (111 kJ/mol)	111 ± 29 kJ/mol	105 kJ/mol	Similar
R, universal gas constant	1.9872 cal/mol/K (8.314 J/mol/K)	8.314 J/mol/K	8.314 J/mol/K	Same
$t_{2.4}$, hour @ 673 K	1.1	1.1	2.0 (nominal) 0.4(bounding)	Similar

The calculation methods used to determine the time to oxidize $UO_{2.4}$ to U_3O_8 are also given in several references, including NUREG-1565 (Reference 2.2.3 [DIRS 101547], Equation 5), PNNL-11929 (Reference 2.2.34 [DIRS 101672], Equation 5.5), and BSC 2005 (Reference 2.2.11 [DIRS 173261], Equation 5.2). The general equation for incubation time can be expressed as:

$$t_{inc} = t_{2.4} + \lambda_{inc} k_{7.5} \times \exp\left(\frac{Q_{7.5} + \alpha B}{RT}\right)$$

Equation 8

where

t_{inc} = incubation time, hr or yr

$k_{7.5}$ = empirically derived coefficient, hr or yr

$Q_{7.5}$ = activation energy, kJ/mol or cal/mol

α = constant for the burnup correction, (J/mol)/(GWd/MTU)

B = burnup in GWd/MTU

λ_{inc} = correction term defined in BSC 2005 (Reference 2.2.11 [DIRS 173261], Equation 5.3) as:

$$\lambda_{inc} = 1 - \frac{r_{11}}{r_{01}}$$

Equation 9

where

r_{11}/r_{01} = ratio defined in BSC 2005 (Reference 2.2.11 [DIRS 173261], Equation 5.4) as:

$$\frac{r_{11}}{r_{01}} = \left[\frac{(1+x)^3(1+s)^3 - z_1 z_2}{z_1 - z_1 z_2}\right]^{1/3}$$
Equation 10

where

x = percentage of the initial fuel pellet gap to fuel pellet radius ratio

s = percent strain necessary to initiate splitting

z_1 = ratio of volume for UO_2 to $UO_{2.4}$

z_2 = ratio of volume for U_3O_8 to $UO_{2.4}$.

Because the above four parameters depend on fuel rod type, the incubation time is different for PWR and BWR fuel if other conditions are the same. The fuel used in the tests reported by EPRI (Reference 2.2.28 [DIRS 127313]) was characterized and the fuel to cladding gap was measured. Due to cladding creep, the measured gap ranged from 0.25 mm at the rod ends to 0.03 mm at the rod center (Reference 2.2.28 [DIRS 127313], p. 2-10). The rod diameter was also measured as a function of rod length. The EPRI report (Reference 2.2.28 [DIRS 127313], Figure 2-2) states that a rod diameter of 10.64 mm is representative. Using a cladding thickness of 0.62 mm and a minimum gap thickness of 0.03 mm, a value of 0.64 percent (0.03 mm/[(10.64 mm / 2) − (0.62 mm + 0.03 mm)] × 100) is determined for x in Equation 10. As discussed in BSC 2005 (Reference 2.2.11 [DIRS 173261], Section 5.1.1), the percent strain s necessary to initiate splitting varies from about one to 6.5 percent. For the purposes of determining the consequences from normal operations, a conservative strain value of one percent – the low end of the strain range – is used. The ratio of volume z_1 is 0.9929 and z_2 is 1.3709/0.9929 = 1.3807.

Using Equation 8 to Equation 10 and the input parameters discussed above, the results are presented in Table 11. The table shows that the calculated total incubation time at 400°C for a representative fuel burnup of 50 GWd/MTU (see Table 1) is between 1.4 and 11 hours. For a lower burnup fuel of 40 GWd/MTU, the calculated incubation time can be as low as 0.9 hour (0.9 to 3.4 hr). The relatively short incubation times at these conditions indicates that fuel oxidation must be considered after an accident when spent fuel could be exposed to air. In addition, looking at the Table 11 results for BSC 2005 (Reference 2.2.11 [DIRS 173261]), it can be seen that high burnup fuel takes longer to oxidize than low burnup fuel (11 hours vs. 3.4 for the nominal case; 3.0 hours vs. 0.9 for the bounding case). Oxidation at a low temperature also takes longer than at a high temperature. For example, the incubation time can be an order of magnitude longer at 350°C than at 400°C based on the calculation performed in the Excel file "*CSNF_RF_Cal.xls*". Using representative burnup fuel to estimate the incubation time is considered to be a reasonably conservative approach.

Table 11. Comparison of Coefficients and Results for Equation 8

	NUREG-1565 (Reference 2.2.3 [DIRS 101547], Equation 5)	PNNL-11929 (Reference 2.2.34 [DIRS 101672], Equation 5.5)	BSC 2005 (Reference 2.2.11 [DIRS 173261], Equation 5.2)	Notes
$k_{7.5}$, **coefficient**	1.56×10^{-19} yr (1.37×10^{-15} hr)	Not given	4.84×10^{-14} hr (nominal) 1.48×10^{-14} hr (bounding)	Different
λ_{inc}, **coefficient**	1	1	See Equation 9	Similar
$Q_{7.5}$, **activation energy**	44.1 kcal/mol (184.5 kJ/mol)	155-211 kJ/mol	150 kJ/mol	Similar
α, **constant for burnup**	0	1.2 (J/mol)/(GWd/MTU)	1.0 (J/mol)/(GWd/MTU)	Different
$t_{2.4}$, **hour @ 673 K**	1.1	1.1	2.0/0.4	Similar
t_{inc}, **hour @ 673 K and 40 GWd/MTU**	1.4	-	3.4 (nominal) 0.9 (bounding)	Similar
t_{inc}, **hour @ 673 K and 50 GWd/MTU**	1.4	-	11 (nominal) 3.0 (bounding)	Similar

Source: the attached Excel file *CSNF_RF_Cal.xls*

The calculations described in this section are performed in the Excel spreadsheet file "*CSNF_RF_Cal.xls*". The worksheet "*Oxidation*" in the file contains the equations and inputs shown above. The worksheet "*Comparison*" in the file contains the calculation results cited in Table 10 and Table 11. The calculations are self-explained, and the results quoted in the text are highlighted. This electronic file is provided in Attachment E of this document.

6.4.1.2 Crack Propagation

Crack propagation is measured by the oxide formation front velocity or clad unzipping velocity. Equation 11 is the general expression for the clad unzipping velocity.

$$V = V_0 \times \exp\left(\frac{-Q}{RT}\right)$$

Equation 11

where

V = unzipping velocity, cm/min

V_0 = fitted coefficient, cm/min

Q = fitted coefficient, J/mol or cal/mol

R = universal gas constant, 8.314 J/mol/K, or 1.9872 cal/mol

T = absolute temperature in K.

This equation requires two fitted coefficients. There are some experimental data available and published during the 1980's. They are reported in EPRI NP-4524 (Reference 2.2.28 [DIRS 127313], Table 3-3), and other data including Novak et al. (Reference 2.2.61 [DIRS 125697], p. 263), Boase and Vandergraaf (Reference 2.2.10 [DIRS 117977], Fig. 14), Kohli et al. (Reference

2.2.44 [DIRS 126191], p.197), and Einziger and Cook (Reference 2.2.26 [DIRS 126202], p. 69). Using all of the above experimental data as inputs, the fitted coefficients based on Equation 11 are listed in Table 12. The equation coefficients are fitted in the Excel file, *oxidation.xls*, which contains three worksheets: *Splitting Rate Data, Splitting Rate Figure, and Splitting Rate Correlation*. The worksheet *Splitting Rate Data* contains all the experimental input data from the above five references. The worksheet *Splitting Rate Figure* contains a graphical presentation of all the experimental input data, as well as a curve fitting equation. The worksheet *Splitting Rate Correlation* contains the conversion of fitted coefficients from *Splitting Rate Figure* into the format of Equation 11. This electronic file is provided in Attachment E of this document.

In addition, Novak et al. (Reference 2.2.61 [DIRS 125697], Equation 1) provided the same fitted formula as Equation 11 with different coefficients as shown in Table 12. Einziger (Reference 2.2.27 [DIRS 166177], Equation 1) also provided the same fitted formula as Equation 11, with the coefficients listed in Table 12.

Table 12 summarizes the coefficients from the three sources discussed above. The table shows that, for a fuel temperature of 673 K (400°C), the calculated clad unzipping velocities range from a low of 6.2×10^{-3} (Novak et al.) to a high of 3.7×10^{-2} cm/min (Einziger). The calculated crack propagation velocity at 360°C is about 3.2×10^{-3} cm/min using the coefficients from BSC 2005 (see Table 12). This value is a factor of 1.4 higher than the measured rate (2.3×10^{-3} cm/min) shown in EPRI NP-4524 (Reference 2.2.28 [DIRS 127313], Table 3-3). This indicates that Einziger's formula, which yields the highest unzipping velocity in Table 12, may overestimate the clad unzipping velocity.

Table 12. Comparison of Coefficients and Results for Equation 11 and Equation 12

	Einziger (Reference 2.2.27 [DIRS 166177], Equation 1)	Novak et al. (Reference 2.2.61 [DIRS 125697], Equation 1)	Fitted equation using published experimental data in this report	Notes
V_0, coefficient	4.98E6 cm/min	2.18 m/s (1.31×10^4 cm/min)	2,217 cm/min	Input
Q, activation energy	25,043 cal/mol (104.8 kJ/mol)	81.5 kJ/mol	70.87 kJ/mol	Input
V, cm/min @ 673 K	3.7×10^{-2}	6.2×10^{-3}	7.0×10^{-3}	Result from Equation 11
L, cm @ t_{inc} = 0 hr	1590	268	303	Result from Equation 12
Time required for splitting a 300 cm fuel rod (hr)	140	810	710	-

Source: the attached Excel files *CSNF_RF_Cal.xls* for the calculation and *Oxidation.xls* for the equation fitting in Column 4

The length of cladding unzipped due to oxidation can then be calculated using the unzipping time, which is the difference between total air exposure time and incubation time defined in Equation 8:

$$L = V \times (t_{air} - t_{inc})$$ Equation 12

where

L = length of cladding unzipped, cm

V = unzipping velocity, cm/min (from Table 12 using Equation 11)

t_{air} = total air exposure time, min (720 hrs, per Assumption 3.2.7)

t_{inc} = incubation time, min (from Table 11 using Equation 8).

The total air exposure time (720 hrs) is much longer than the incubation time (<11 hrs) calculated in Table 11. This allows the incubation time to be set to 0 without introducing excessive conservatism into the analysis. The calculated lengths of cladding unzipped when t_{inc} = 0 hr range from 268 to 1590 cm as shown in Table 12. This range covers the total length of a BWR fuel rod (300 cm) or a PWR fuel rod (360 cm). The time required for splitting a 300 cm fuel rod is also calculated and shown in Table 12.

The Table 12 results demonstrate that almost an entire 300 cm fuel rod would be oxidized after 720 hours under the assumed conditions. As a conservative approach, this analysis presumes that a damaged fuel rod is completely oxidized in 30 days (720 hours), and that U_3O_8 powder is available for release into the air beginning approximately one hour after an accident. Based on this, the recommended ARFs and RFs due to fuel oxidation for gases, volatiles and fuel fines are developed in Section 6.4.2 to Section 6.4.4.

The calculations described in this section and the results shown in Table 12 are also performed in Excel spreadsheet file "*CSNF_RF_Cal.xls*". The calculations are self-explained, and the results quoted in the text are highlighted. The Excel file also includes the input data for the cladding split data, and clad unzipping velocity discussed in this section.

6.4.2   Gaseous Radionuclide Release from Fuel Oxidation

The release of fission product gases from oxidation has been determined in several reports including Colle et al. (Reference 2.2.17 [DIRS 179470], pp.229-242), Einziger (Reference 2.2.27 [DIRS 166177], p. 95), and Lorenz et al. (Reference 2.2.51 [DIRS 100990], Tests HBU-5 and HBU-6). The reported releases of fission gases, such as krypton and xenon, are measured using small-irradiated fuel samples within a device that controls temperature. The condition ensures that the entire sample is oxidized and the release of fission gases is from U_3O_8.

Colle et al. (Reference 2.2.17 [DIRS 179470], pp.229-242) reported fission product releases from BWR fuel with burnup up to 65 GWd/MTU, which supports the release from high burnup fuel as discussed in Section 6.6.2. Einziger (Reference 2.2.27 [DIRS 166177], p. 95) indicates that approximately 7 percent to 30 percent of the [85]Kr inventory is released from the fuel upon oxidation to U_3O_8 for advanced gas-cooled reactor fuel. Einziger (Reference 2.2.27 [DIRS 166177], p. 95) states that although no similar tests have been done for light water reactor fuel, it is expected that the trends would be similar.

Lorenz et al. (Reference 2.2.51 [DIRS 100990]) in test HBU-5 reported that 0.53 percent of the [85]Kr was released due to oxidation. The test rod segment was used previously in a test where

0.63 percent was released. Lorenz et al. (Reference 2.2.51 [DIRS 100990], Figure 11) indicates that ^{85}Kr releases ended after about 4 hours. Lorenz et al. suggest that this is due to plugging of the defect hole. As can be seen in Lorenz et al. (Reference 2.2.51 [DIRS 100990], Figure 11), even if plugging did not occur, the release of ^{85}Kr was reaching an upper limit. Therefore, no more than 0.6 percent of the total ^{85}Kr would have been released due to oxidation. In test HBU-6, which was performed at 700°C instead of 500°C, a fresh rod segment was used. Total release of ^{85}Kr during the experiment time (5 hours for 700°C) was no more than 1.2 percent.

Finally, it is conservative to assume all ^{3}H is released as water vapor because the experimental results of voloxidation indicated that ^{3}H was totally released once spent fuel was heated to about 500°C (Reference 2.2.30 [DIRS 180520], Reference 2.2.31 [DIRS 180519], and Reference 2.2.80 [DIRS 180521]). As discussed in Section 6.1.2, 30% of the total ^{3}H is released in the initial burst; therefore, the ARF for ^{3}H due to fuel oxidation is the remaining 70%. Voloxidation experiments indicate that the process of oxidation of UO_2 to U_3O_8 essentially removed all of the tritium, 17 to 22 percent of the ^{14}C, 7 to 17 percent of the ^{85}Kr, and less than 8 percent of the ^{129}I (Reference 2.2.80 [DIRS 180521], p.570).

Based on the above discussion, an ARF value of 0.3 is conservative for ^{85}Kr, ^{14}C, and ^{129}I fission gases due to oxidation after fuel is exposed in air. For ^{3}H, an ARF value of 0.7 is recommended. The respirable fraction for all gases is taken to be 1 because gases are considered to be 100% respirable as discussed in Section 6.2.

6.4.3 Volatile Radionuclide Release from Fuel Oxidation

NUREG/CR-6672 (Reference 2.2.79 [DIRS 152476], p.7-45) discusses the releases of iodine, cesium, and ruthenium from fuel following oxidation. The data used by Sprung et al. in NUREG/CR-6672 (Reference 2.2.79 [DIRS 152476]) come from experiments performed by Lorenz et al. (Reference 2.2.51 [DIRS 100990]) on highly irradiated fuel at 700°C. Sprung et al. (Reference 2.2.79 [DIRS 152476], p. 7-45) indicate that the releases of cesium, iodine, and ruthenium increased by factors of 54.6, 22.4, and 20,200, respectively, when the experimental atmosphere was dry air rather than steam. The experiments by Lorenz et al. (Reference 2.2.51 [DIRS 100990]) were performed for various temperatures in both steam and dry air atmospheres. There were three steam tests (HBU-1, HBU-2, and HBU-4) and two dry air tests (HBU-5 and HBU-6). The release rate of cesium in the steam atmosphere was found to be highly dependent on temperature, suggesting a diffusional release mechanism from the fuel matrix. This release rate was significantly enhanced in the dry air atmosphere at 700°C (Reference 2.2.51 [DIRS 100990], Test HBU-6); however, the release rate was not appreciably different at 500°C (Reference 2.2.51 [DIRS 100990], Test HBU-5). The cladding temperatures expected at the repository are well below the temperatures used in these tests; therefore, it is expected that the release of cesium would be much lower. Conservatively assuming the release rate at 500°C represents the expected release rate at the repository, the total release fraction of cesium after 100 hours of oxidation would be approximately 1.3×10^{-7}. The release rates of ruthenium were all well below the release rates for cesium except for test HBU-6, where the release of ruthenium was approximately a factor of 2 lower than cesium. These ARFs are at least one order of magnitude smaller than the value of 2×10^{-4} recommended in Section 6.1.3.

Because the measured release fraction for ^{137}Cs for fuel oxidation is much smaller than for fuel fines (see Section 6.4.4), the ARF for volatile radionuclides, which could be the sum of the evaporation and particles release, is taken as the same value for fuel fines, 2×10^{-3}. However, the RF for volatiles of 1 is used as discussed in Section 6.2. It is therefore concluded that an ARF of 2×10^{-3} and an RF of 1 are reasonable conservative values for volatile radionuclides due to oxidation after fuel is exposed in air.

6.4.4 Fuel Fines Release from Fuel Oxidation

Davis et al. (Reference 2.2.21 [DIRS 103711], p. 9) determined the ARF of particles from powder due to the oxidation of UO_2 pellets in air. The recommended ARF value of 0.12 was based on the particle size distribution of oxidized UO_2 powder measured by Iwasaki et al. (Reference 2.2.39 [DIRS 172518]). The ARF value recommended by Davis et al. (Reference 2.2.21 [DIRS 103711], p. 9) is overly conservative and may not be applicable to an accident in a repository facility. It may be reasonable to apply this value to an aircraft accident that Davis et al (Reference 2.2.21 [DIRS 103711]) tried to evaluate because the oxidized UO_2 powder could eventually be picked up by the wind and dispersed in the open air. However, in a repository accident, oxidized UO_2 powder is likely to stay in the facility, and only a small fraction would be picked up by airflow even if the ventilation system were operating.

As estimated in Section 6.4.1, an entire fuel rod could be oxidized to U_3O_8 powder from UO_2 pellets within 30 days when both the cladding and TAD canister are breached after an accident. An accident, such as a TAD canister drop into a transport cask or a waste package, could occur while transferring the TAD canister from a transport cask into a waste package. It is likely that the failed fuel assemblies would be in a relatively confined environment and would have a very low chance of being disturbed. Nevertheless, the oxidized U_3O_8 powder produced as a result of the event can be suspended into the air when there is airflow. It is expected that the two parameters most important to the release of powder into the environment are the airflow velocity and the powder size distribution.

Based on the *Basis of Design for the TAD Canister-Based Repository Design Concept* (Reference 2.2.12 [DIRS 182131], Section 22.2.1.4), the air flow velocity for the underground work areas is at least 30 ft per minute (about 0.15 m/s). The flow rates in the surface facilities (such as CRCF, and WHF) range from 3 to 20 m^3/s, and facility cross section areas range 3000 to 4000 m^2 (Reference 2.2.14 [DIRS 180308], Tables 3 and 4). This indicates that linear airflow velocity in the surface facilities should be much lower than 0.1 m/s. Another powder suspension mechanism is the airflow from a high temperature object (the oxidized powder) to a low temperature one (the environment). It is expected that any airflows caused by such a temperature difference are relatively small compared to those from the building ventilation and can be ignored without a loss of conservatism.

As mentioned in Section 6.4, the particle size distribution of oxidized U_3O_8 depends strongly on temperature. A higher temperature oxidizes UO_2 quickly, but creates relatively large particles. Based on the results from Reference 2.2.49 ([DIRS 172864], p.5), oxidized fuel particles should be in a range of about 10 μm if oxidation does occur at the temperature of 400°C.

Among the limited available literature information, the relevant measurements of ARFs were performed by Mishima et al. (Reference 2.2.24 [DIRS 103756], Section 4.4.1). The experiments were conducted by heating various plutonium-based particles including plutonium oxide, partially oxidized plutonium oxalate, plutonium oxalate, and plutonium fluoride. In the experiments, temperatures ranged from ambient to 1,000°C and airflows from 0.1 m/s to 1.2 m/s. Some relevant results as well as test conditions are shown in Table 13.

Table 13. ARFs measured by Mishima et al. (Reference 2.2.24 [DIRS 103756], Section 4.4.1)

Material	Airflow rate (m/s)	Temperature (°C)	Particle size (μm)	ARF
PuO_2	0.1	Ambient	15-150	6.1×10^{-6}
PuO_2	0.1	800-900	15-150	5.6×10^{-6}
Partially oxidized Pu oxalate	0.1	Ambient	MMD = 32	5.6×10^{-4}
Partially oxidized Pu oxalate	0.1	1000	MMD = 32	2.7×10^{-3}
Pu oxalate	0.1	Ambient	MMD = 50	$< 8.0 \times 10^{-5}$
Pu oxalate	0.1	700	MMD = 50	9.0×10^{-5}
Pu fluoride	0.1	Ambient	MMD = 38	$< 8.0 \times 10^{-5}$
Pu fluoride	0.1	1000	MMD = 38	$< 8.0 \times 10^{-5}$

Source: Reference 2.2.24 [DIRS 103756], Section 4.4.1

It is calculated that the lower air velocity (0.1 m/s) can carry particles as large as 17 μm. That is barely above the lower size of the powder used, and a low ARF value would be anticipated (Reference 2.2.24 [DIRS 103756], Section 4.4.1.1). Although the plutonium-based particles have different behaviors from uranium-based particles, the release fraction of the powder mainly depends on the particle size and airflow rate. It is expected that the results are comparable in terms of powder release. In Table 13, the highest value (2.7×10^{-3}) is for partially oxidized Pu oxalate at a temperature of 1,000°C. Using linear interpolation between ambient temperature and 1,000°C, an ARF of about 1.5×10^{-3} can be estimated for a temperature of 400°C.

Besides the results from Mishima et al. (Reference 2.2.24 [DIRS 103756], Section 4.4.1), other generic ARFs and RFs are reported in the DOE handbook (Reference 2.2.24 [DIRS 103756]). Those relevant to oxidized powder release include the vibration or shock release of powder contamination in which the bounding ARF and RF were determined, respectively, to be 1×10^{-3} and 1 (Reference 2.2.24 [DIRS 103756], Section 4.4.3.3.1). However, the bounding RF for agglomerated particles was considered to be 0.1. For complete oxidation of uranium metal at temperatures greater than 500°C, the bounding ARF and RF were determined, respectively, to be 1×10^{-3} and 1 (Reference 2.2.24 [DIRS 103756], pp. 4-2 and 4-3). These additional ARFs are comparable to the results based on the measured ARFs from plutonium-based powder. For conservatism, this value is doubled so that an ARF value of 2×10^{-3} is recommended for fuel fines oxidation releases.

The RFs are strongly dependent on the particle size distribution. It is reported that powders at rest are difficult to deagglomerate and their dispersion often requires substantial mixing in suspensions to attain their original size distribution (Reference 2.2.24 [DIRS 103756], Section

4.4.3.3). An RF value of 0.01 was recommended as a reasonable, conservative value consistent with other measured RFs (Reference 2.2.24 [DIRS 103756], Section 4.4.1.1). However, based on the previous discussions for the vibration and oxidation of uranium metal, it is recommended that an RF value of 0.1 be used for fuel fines oxidation releases.

6.4.5   Summary of ARFs and RFs for Fuel Oxidation

ARFs and RFs for crud are not considered for fuel oxidation because the release of crud particles is already considered during a drop event. As mentioned by Einziger (Reference 2.2.27 [DIRS 166177], p.97), additional crud spallation due to oxidation of the cladding is insignificant. Therefore, the radionuclide release from crud after the accident is less important than during the accident and can be ignored without loss of conservatism.

A summary of ARFs and RFs for gases, volatiles, and fuel fines for low burnup fuel (<45 GWd/MTU) due to fuel oxidation is shown in Table 14 based on the discussions in Section 6.4.2 to Section 6.4.4. These ARFs and RFs for fuel oxidation are for radionuclide releases after an accident; they are in addition to the releases occurring during an accident, whose release fractions were developed in Sections 6.1 and 6.3.

Table 14. Recommended ARFs and RFs for Low Burnup Fuel Oxidation After an Accident

Radionuclide	ARF / RF	In Section
^{3}H	0.7 / 1	6.4.2
^{85}Kr	0.3 / 1	6.4.2
^{129}I	0.3 / 1	6.4.2
^{134}Cs & ^{137}Cs	2×10^{-3} / 1	6.4.3
^{90}Sr	2×10^{-3} / 0.1	6.4.4
^{106}Ru	2×10^{-3} / 1	6.4.3
Fuel Fines	2×10^{-3} / 0.1	6.4.4
Crud	N/A	N/A

6.5   ARFs AND RFs FOR HIGH BURNUP FUEL

6.5.1   High Burnup Fuel Characteristics

When the cross-section averaged burnup exceeds about 40 GWd/MTU, the surface microstructure of a UO_2 fuel pellet (known as the rim structure) changes. The thickness of the rim increases dramatically with the burnup. There are also several characteristics in the rim region (or rim zone) that become more significant as burnup increases. These include smaller grain size (0.1-0.3 μm), higher porosity (up to more than 20%); and larger pore size (a few microns). Burnup varies with the distance to the surface in a fuel pellet, with the highest on the surface (Reference 2.2.56 [DIRS 178776], p.170). Une et al. (Reference 2.2.82 [DIRS 178780], p.62) reported that the pellet size and fission rate hardly influence the rim structure formation. Several characteristics of high burnup fuel are discussed below.

Rim Properties – The properties of UO_2 fuel pellets in the rim zone of high burnup fuel are compared with low burnup fuel in Table 15 (Reference 2.2.42 [DIRS 178782], p.11).

Table 15. Comparison of Properties in the Rim Zone and Typical Low Burnup UO_2 Fuel

Fuel material property	Rim zone	Low-burnup fuel
Density (kg/m^3)	9670	10,250
Porosity (volume fraction)	0.10	0.04
Grain size (μm)	0.3	10
Intergranular bubble size (nm)	2.0	20

Rim Thickness – Johnson et al. (Reference 2.2.43 [DIRS 178773], pp.56-65) provided a summary of the rim thickness as a function of average burnup based on a literature review. This is shown in Figure 9. There are three equations in the figure representing the different aspects of the rim thickness calculation. The best fit, labeled as Eq. (1) in Figure 9, is represented by (Reference 2.2.45 [DIRS 178774], Eq.1):

$$R_t = 3.55 \times BU_R - 185 \qquad\qquad \text{Equation 13}$$

where R_t is the rim thickness in μm and BU_R is the rim burnup in GWd/MTU.

The bounding case, labeled as Eq. (2) in Figure 9, is given as (Reference 2.2.45 [DIRS 178774], Eq.2):

$$R_t = 5.28 \times BU_R - 178 \qquad\qquad \text{Equation 14}$$

Johnson et al. (Reference 2.2.43 [DIRS 178773], p.59) proposed a pessimistic expression to correct the bounding case in the range of 30 GWd/MTU, which was inconsistent with microstructural studies. The equation, labeled as Eq. (3) in Figure 9, is:

$$R_t = 5.44 \times BU_R - 281 \qquad\qquad \text{Equation 15}$$

The calculated rim thicknesses are 193 μm, 384 μm, and 298 μm using Equation 13, Equation 14, and Equation 15, respectively, for an average burnup of 80 GWd/MTU, which is converted to the mean local burnup within the entire rim region using a factor of 1.33 proposed by Johnson et al. (Reference 2.2.43 [DIRS 178773], p.60). The above three equations are in a linear relationship, while Lassmann et al. (Reference 2.2.47 [DIRS 119370], Figure 8) suggested an exponential relationship between the burnup and rim thickness, which is also shown in Figure 9.

SKI Report 2005:16 (Reference 2.2.42 [DIRS 178782], p.11) provides the following equation for commercial PWR fuel rods:

$$w_{Rim} = \begin{cases} 0 & E_{av} \le 35 \, GWd \, / \, MTU \\ 0.0427(E_{av} - 35)^{2.41} & 35 < E_{av} < 70 \, GWd \, / \, MTU \end{cases} \qquad \text{Equation 16}$$

where w_{Rim} = the width of the rim zone in μm and E_{av} = the pellet radial average burnup in GWD/MTU. At the highest valid average burnup of 70 GWd/MTU, the rim thickness is about 225 μm.

Based on above discussion, the rim thickness should be no more than 300 μm using the pessimistic expression proposed by Johnson et al. (Reference 2.2.43 [DIRS 178773], p.59), for the high burnup fuel of 80 GWd/MTU, which is the highest burnup spent fuel expected to be received at the Yucca Mountain repository.
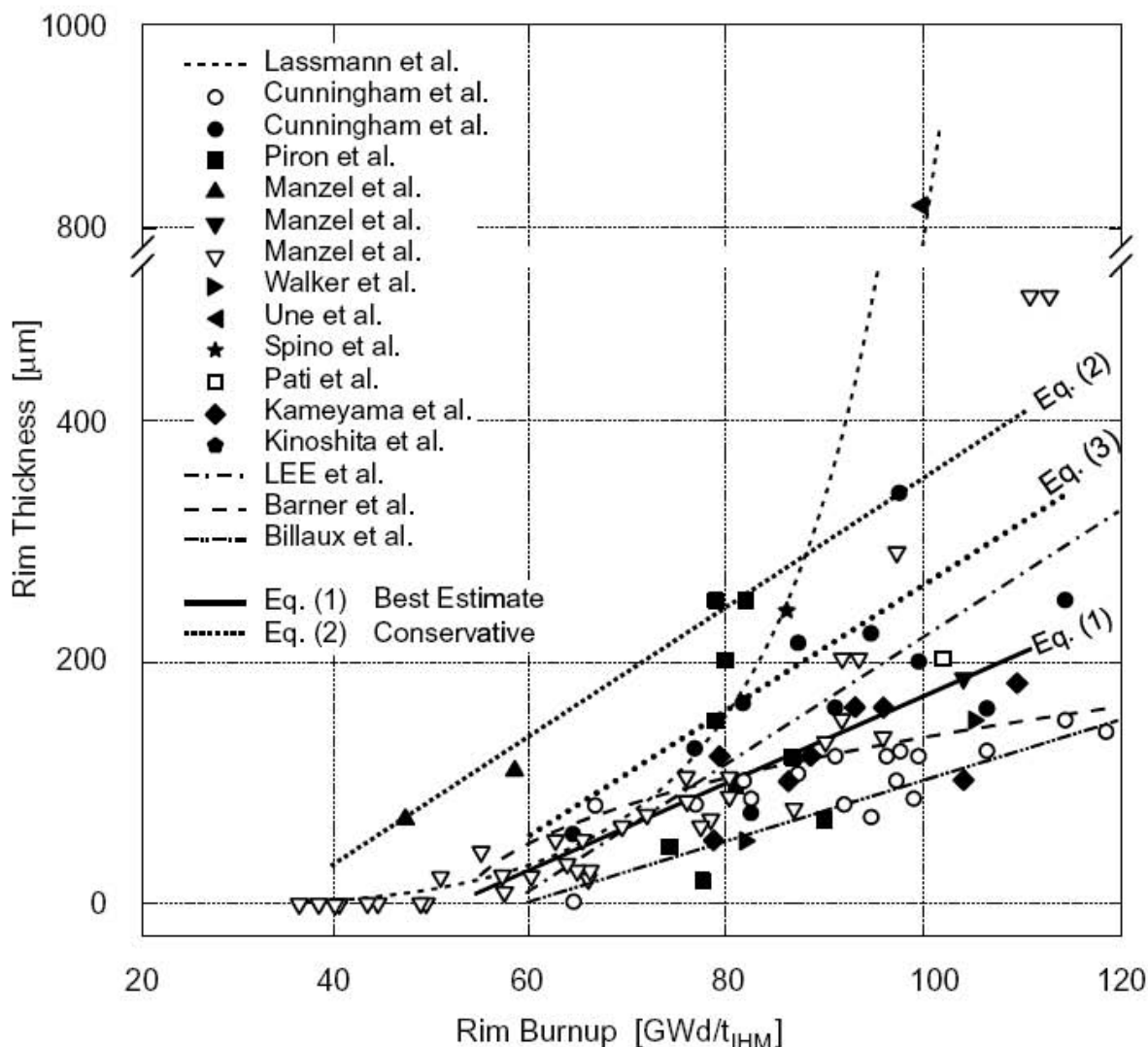
(Note: taken from Johnson et al. (Reference 2.2.43 [DIRS 178773], Fig.2)

Figure 9. Rim Thickness as a Function of Burnup (GWd/MTU)

Grain Size Change – Based on Spino et al. (Reference 2.2.77 [DIRS 178778], 66-84), a UO_2 fuel pellet has an initial grain size of 9-12 μm. After irradiation, the grain size distribution in the rim between the different burnups (67 vs. 98 GWd/MTU) is very similar, being only slightly wider for the case of the high burnup, as shown in the left side figures in Figure 10 (Reference 2.2.77 [DIRS 178778], Figure 11). Comparison of the grain size distribution at different radial positions for the fuel with 98 GWd/MTU average burnup shows the distribution widening (grain-growth) towards the center of the pellet, as shown right side of figures in Figure 10. It should be noted that, although both positions (r/r_0 = 0.7 and 0.55) are not considered part of the rim, the grain size is in the submicron range. It can therefore be concluded from Figure 10 that the grain size decreases to the submicron range when local burnup exceeds burnup of 88 GWd/MTU.
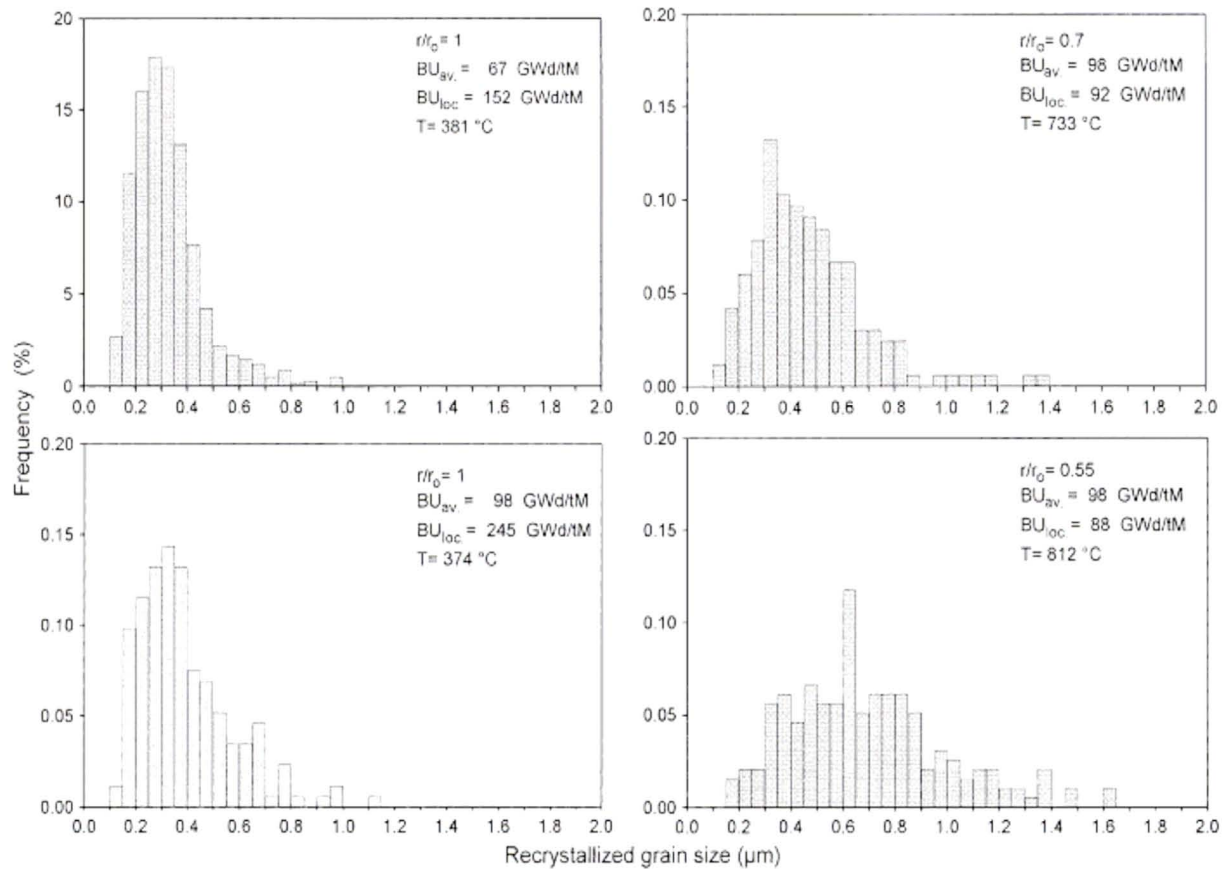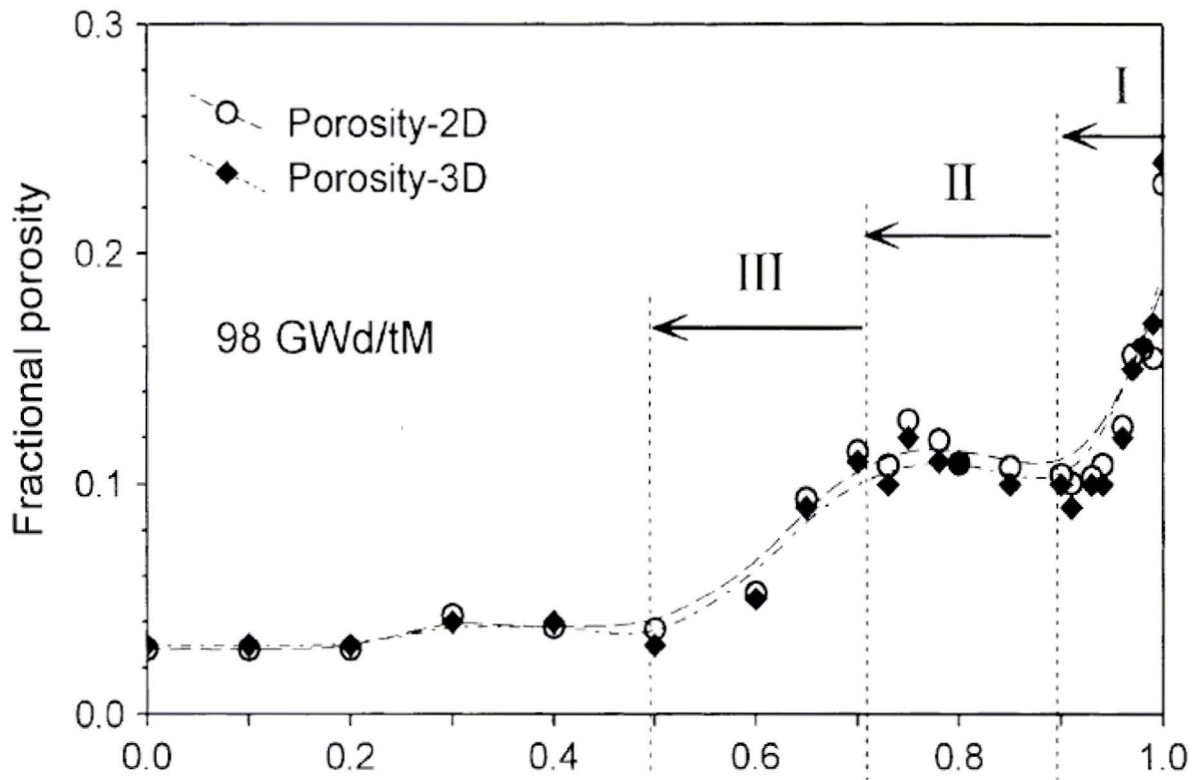
(Note: taken from Spino et al. (Reference 2.2.77 [DIRS 178778], Figure 11))

Figure 10. Comparison of Grain Size Distributions at Various Positions and Burnups

Rim Porosity – The most important characteristic in the rim is the porosity because high porosity can lead to significant gas releases resulting in rod overpressurization and the lifting of fuel cladding. Spino et al. (Reference 2.2.77 [DIRS 178778], Figure 3) provided the rim porosity as a function of radial position for the 98 GWd/MTU average burnup, as shown in Figure 11. The porosity increases towards the surface of a pellet from 3% in the center to 24% in the edge. In terms of porosity as a function of local burnup, Spino et al. (Reference 2.2.77 [DIRS 178778], Figure 5) reported that the porosity increases with local burnup increase, as shown in Figure 12. The local burnup depends on the radial position with the highest local burnup occurring on the edge. It can be seen from Figure 12 that the rim burnup can be as high as 245 GWd/MTU, which is 2.5 times the average burnup of 98 GWd/MTU.

In addition, Spino et al. (Reference 2.2.77 [DIRS 178778], p. 66) suggested that no clusters of interconnected pores were observed even at the maximum pore fraction of 0.24 (which was observed at the pellet surface for the 98 GWd/MTU burnup fuel). Koo et al. (Reference 2.2.46 [DIRS 178775], pp. 249–255) concluded that it is rim porosity rather than pore size distribution or rim thickness that determines the fraction of open pores connected to the pellet surface.

(Note: taken from Spino et al. (Reference 2.2.77 [DIRS 178778], Figure 3)

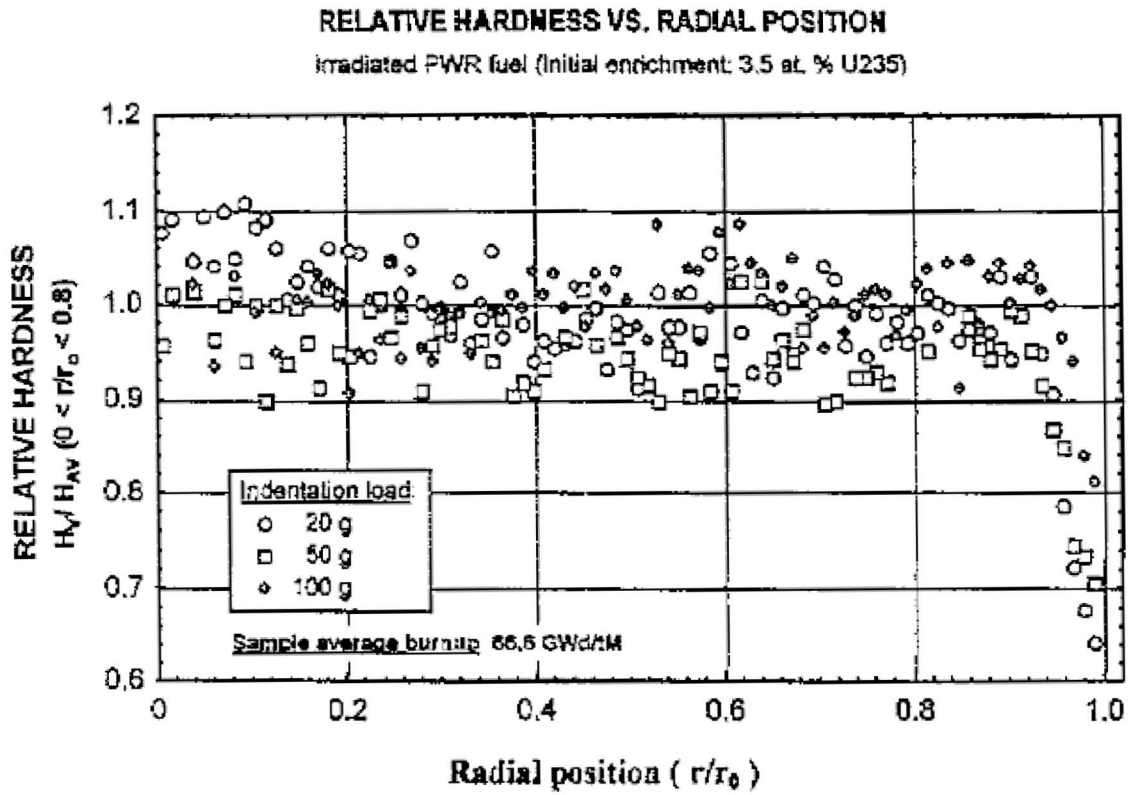Figure 11. Fractional Porosity as a Function of Radial Position
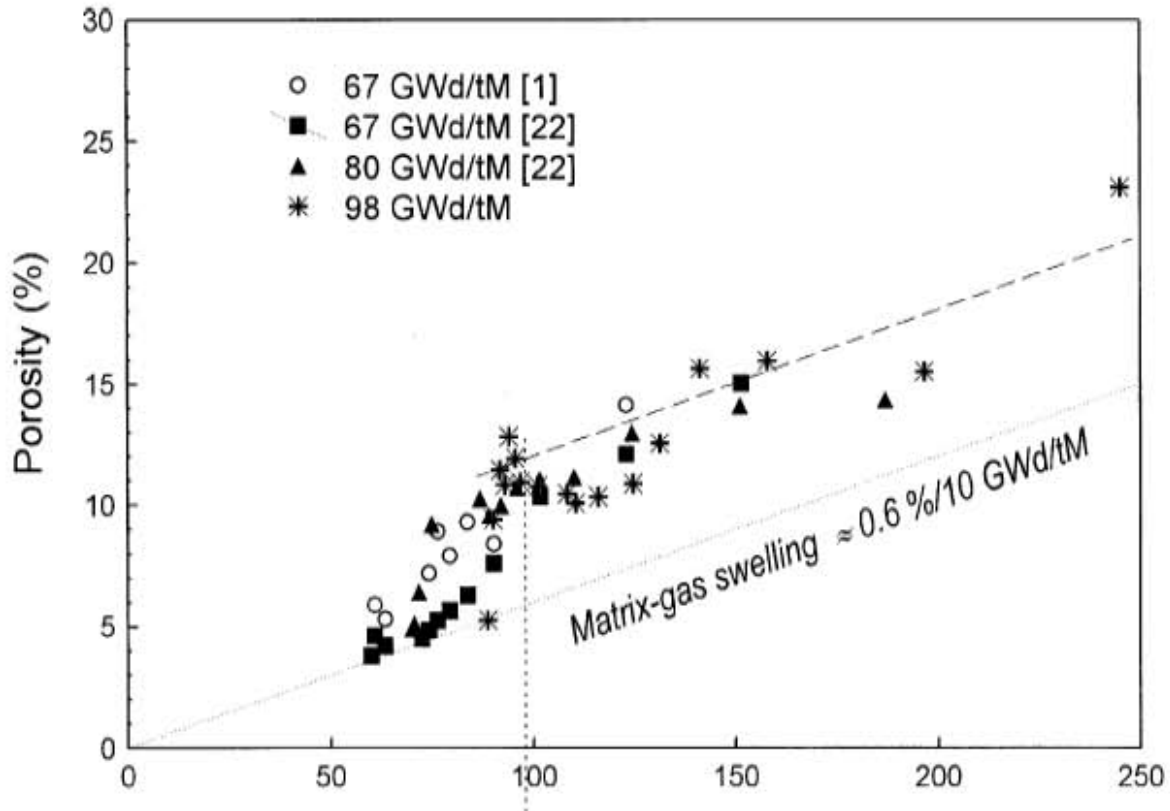
(Note: taken from Spino et al. (Reference 2.2.77 [DIRS 178778], Figure 5)

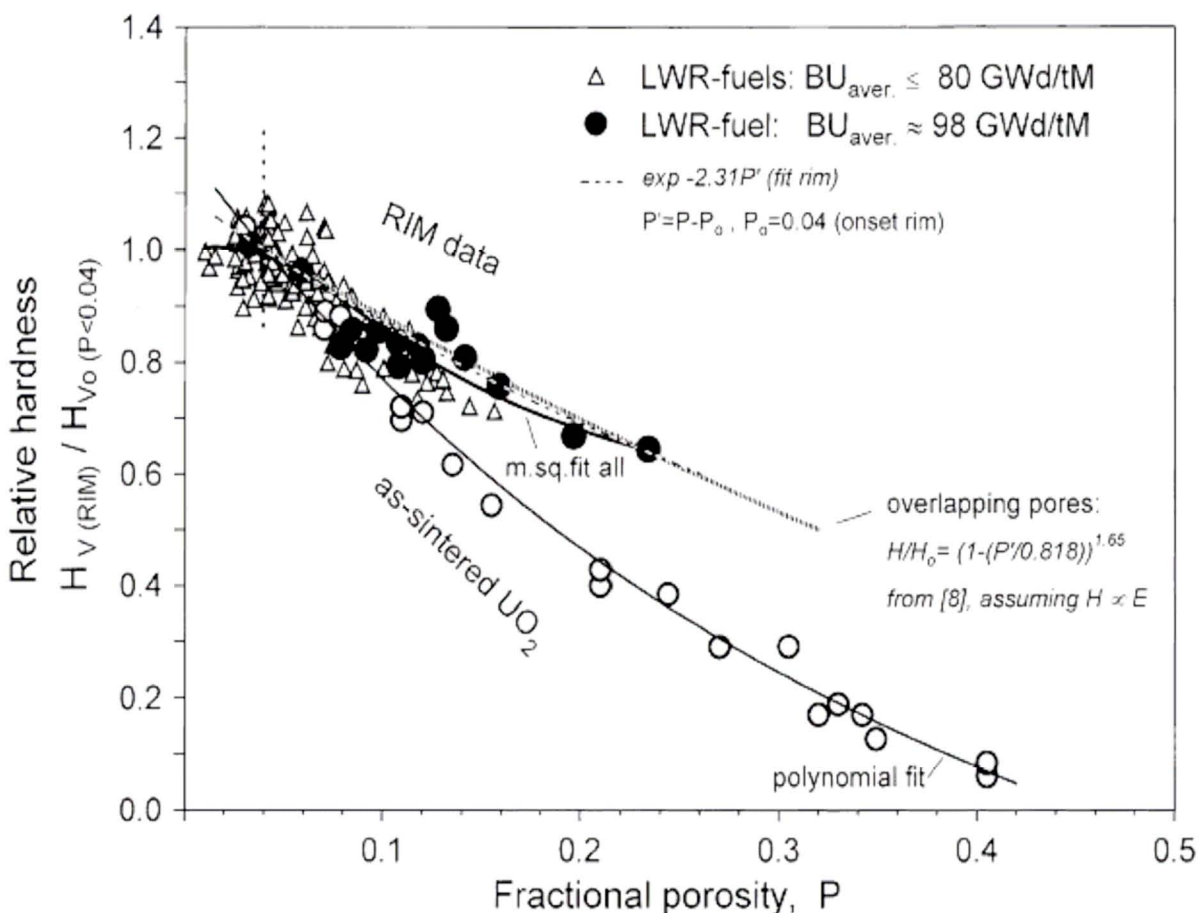Figure 12. Porosity as a Function of Local Burnup

The number of rim pores that connect with each other and form release channels in the rim increases very rapidly above the threshold porosity of around 24%. When the rim porosity is less than 24%, only a small number of rim pores located within 20 μm from the pellet surface contribute to a gas release resulting in a very low gas release. Once the rim porosity exceeds a threshold value, however, extensive release channels would be developed and considerable gas release would occur in the rim leading to fuel rod over-pressurization and then to clad lift-off (Reference 2.2.46 [DIRS 178775], p. 254). The maximum rim porosity observed for an average burnup of 80 GWd/MTU is 14.3% (Reference 2.2.77 [DIRS 178778], Table 2). This indicates that even the bounding spent fuel assemblies (80 GWd/MTU) do not achieve a rim porosity high enough to form extensive release channels.

Rim Hardness – Matzke and Spino (Reference 2.2.56 [DIRS 178776], p.176) reported that the relative hardness remains constant along most of the pellet radius, and then decreases towards the fuel pellet edge where the rim structure exists, as shown in Figure 13 (Reference 2.2.56 [DIRS 178776], Figure 7). Recent testing demonstrates that relative hardness decreases with fraction porosity (Reference 2.2.77 [DIRS 178778], Figure 9). At a porosity of about 0.15, which corresponds to the highest porosity for an average fuel pellet burnup of 80 GWd/MTU (see previous section), the relative hardness is about 0.7 to 0.8, as shown in Figure 14 (Reference

(Note: taken from Matzke and Spino (Reference 2.2.56 [DIRS 178776], Figure 7)

Figure 13. Relative Hardness as a Function of Radial Position

1.4

1.2

1.0

0.8

0.6

0.4

0.2

0.0

$\triangle$ LWR-fuels: $BU_{aver.} \leq$ 80 GWd/tM

$\bullet$ LWR-fuel: $BU_{aver.} \approx$ 98 GWd/tM

---- exp -2.31P' (fit rim)

$P'=P-P_o$, $P_o=0.04$ (onset rim)

RIM data

Relative hardness $H_{V\,(RIM)}$ / $H_{Vo\,(P<0.04)}$

m.sq.fit all

as-sintered UO_2

overlapping pores:

$H/H_o = (1-(P'/0.818))^{1.65}$

from [8], assuming $H \propto E$

polynomial fit

0.1   0.2   0.3   0.4   0.5

Fractional porosity, P

(Note: taken from Spino et al. (Reference 2.2.77 [DIRS 178778], Figure 9)

Figure 14. Relative Hardness as a Function of Fractional Porosity

Rim Toughness – Matzke and Spino (Reference 2.2.56 [DIRS 178776], p.176) reported that the fracture toughness of the central parts of the fuel roughly corresponds to the range of values for unirradiated UO_2, while the fracture toughness of the rim zone can be twice as large, as shown in Figure 15 (Reference 2.2.56 [DIRS 178776], Figure 9). The improvement in fracture toughness at the rim is mainly caused by the grain refinement (Reference 2.2.78 [DIRS 174080], p.186). The results indicate that, although the rim contains smaller grains and more pores, it is not as easy to break into small grain particles as the lower burnup central fuel. Based on these results, the release fraction of fine particles from high burnup fuel would be expected to be lower than from low burnup fuel. This is because the rim structure of high burnup fuel is tougher than the overall pellet for both high and low burnup fuels, which would prevent high burnup spent fuel pellets from breaking into smaller pieces.
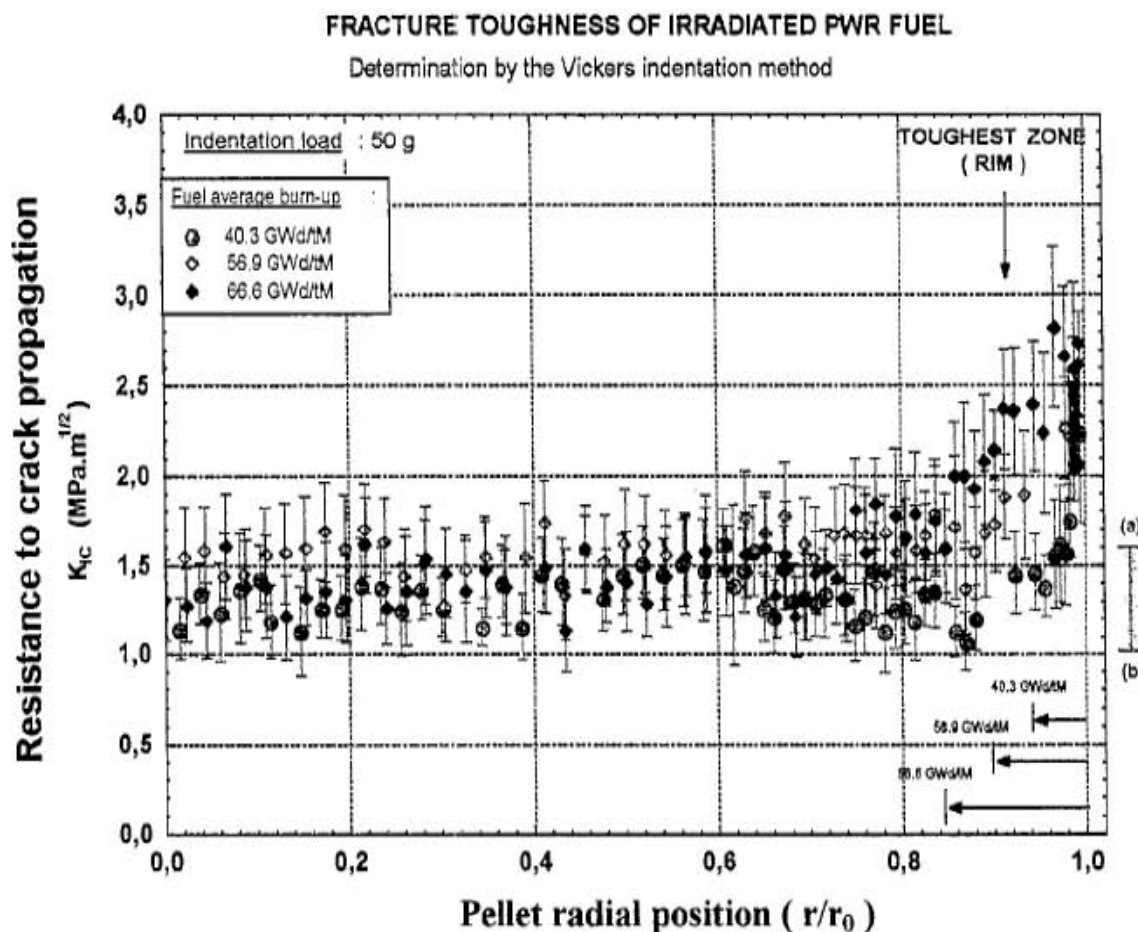
(Note: taken from Matzke and Spino (Reference 2.2.56 [DIRS 178776], Figure 9)

Figure 15. Fracture Toughness as a Function of Radial Position

6.5.2 Gaseous Radionuclide Release from High Burnup Fuel

Fission gas release has been measured and modeled in a number of reports. It is a key phenomenon that must be assessed for fuel rod design and licensing as it contributes to the fuel rod internal pressure, with the associated risks of fuel thermal degradation and cladding failure (Reference 2.2.9 [DIRS 178772], p.125). Under normal reactor operating conditions, a fraction of the fission gas is released into the gap between the fuel and cladding. At low burnups, the measured fission gas releases into the gap are less than 1% for rod-average burnup of 30 GWd/MTU of ATM-103 spent fuel (Reference 2.2.33 [DIRS 109205], p.iii), and about 10% for a rod-average burnup 43 GWd/MTU of ATM-106 spent fuel (Reference 2.2.32 [DIRS 109206], p.iii).

Bernard et al. (Reference 2.2.9 [DIRS 178772], p.128) show less than 1% fission gas releases for low burnup (40 GWd/MTU) and an increase of fission gas release with increasing burnup due to either a thermal effect or a rim effect or both, as shown Figure 16 (Reference 2.2.9 [DIRS 178772], p.128). Johnson et al. (Reference 2.2.43 [DIRS 178773], Figure 1) provide similar

fission gas release results, as shown in Figure 17. CNWRA 2004-08 (Reference 2.2.40 [DIRS 178808], p.3-5) reported that the measured fission gas release fraction from PWR fuel rods was about 10% for an average burnup of 50 GWd/MTU and 25% for 98 GWd/MTU, as shown in Figure 18 (Reference 2.2.40 [DIRS 178808], Figure 3-6). These measured fission gas release fractions appear lower than the measured data from ATM-103 and ATM-106. There are many reasons that could cause the different fission gas releases including the fuel rod manufacturing process. Pre-pressurization of the fuel rods with helium typically leads to a reduction in the fission gas release by as much as an order of magnitude, as shown in CNWRA-93-006 (Reference 2.2.54 [DIRS 101719], Figure 3-5).
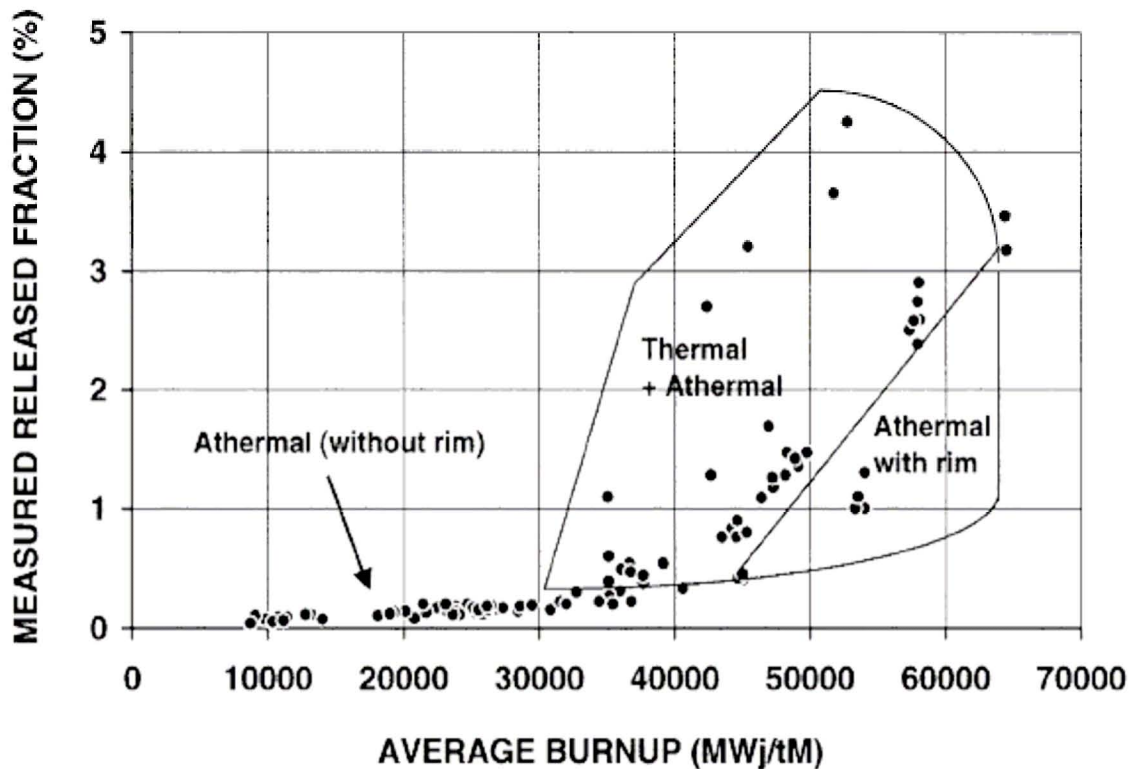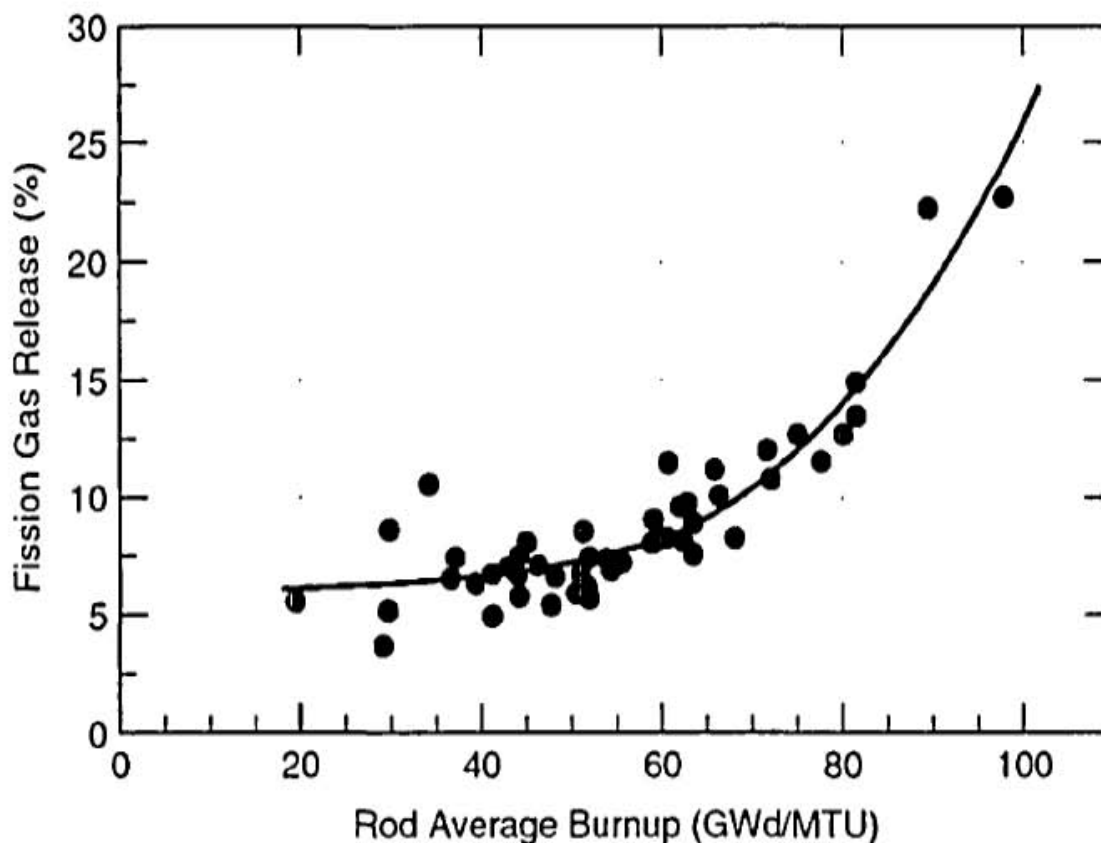

(Note: taken from Bernard et al. (Reference 2.2.9 [DIRS 178772], Figure 4)

Figure 16. Fission Gas Release as a Function of Average Burnup
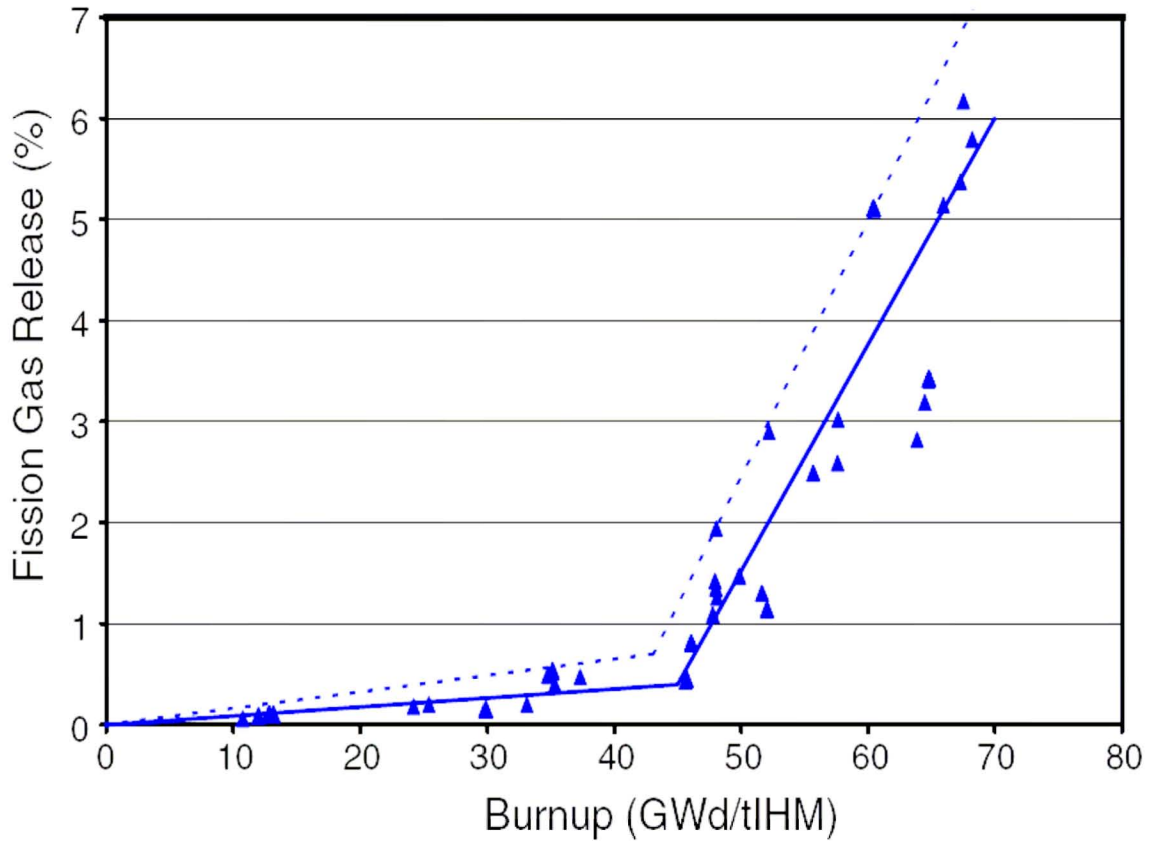
(Notes: taken from Johnson et al. (Reference 2.2.43 [DIRS 178773], Figure 1);
solid line – best fit; dashed line – bounding or pessimistic estimate)

Figure 17. Fission Gas Release from PWR Fuel as a Function of Burnup

(Note: taken from CNWRA 2004-08 (Reference 2.2.40 [DIRS 178808], Figure 3-6)

Figure 18. Percentage of Fission Gas Released to the Rod-Free Volume

Fission gas is also retained in the rim pore structure. The fission gas in this region can be considered as released from the fuel matrix even though it is not released to the void space in the fuel rod (Reference 2.2.43 [DIRS 178773], p.60). The fraction of fission gas present in the rim region (pore + grains) is estimated to be 16.5% using a pessimistic expression of rim thickness (see Equation 15) at a burnup of 75 GWd/MTU (Reference 2.2.43 [DIRS 178773], Table 2). Combining the fission gas in the gap and in the rim region, the total potential fission gas release into the environment can be up to 25% for a fuel burnup of 75 GWd/MTU (Reference 2.2.43 [DIRS 178773], Figure 1 and Table 2).

Based on the above, it is concluded that only a few percent of the total fission gas is available for release into the environment when the cladding of high burnup spent fuel is breached . Another 10-20% fission gas is retained in the rim region but is not released unless the rim region is fully broken. The worst release fraction for fission gas from high burnup fuel (a few percent plus 20%) is lower than the 30% conservatively selected for low burnup spent fuel in Section 6.1.2. Therefore, the ARF for gases from high burnup fuel is bounded by the 0.30 ARF value for intact commercial SNF gases as shown in Table 16.

6.5.3   Volatile Radionuclide Release from High Burnup Fuel

Cesium is usually categorized as a volatile element because it behaves similarly to xenon at temperatures above 1,200°C, at which temperature both are gaseous. Moreover, similar percentages of cesium and xenon are released from UO_2 grains. However, at the rim of high burnup fuel where the microstructure has been transformed, the release behavior of cesium is very different from that of xenon. In this case, cesium appears to be retained completely, although a large percentage of fission gases are released from the restructured fuel. The difference in the release behavior exhibited by xenon and cesium from the rim region of high burnup fuel can be attributed to their physical state. Below 1,200°C, cesium is a liquid, whereas xenon is a gas. As a result they react differently at the grain boundaries. Xenon forms nanometer size interconnected bubbles, which feed into the faceted pores and thereby drain the new grain structure of gas. Cesium, in contrast, is relatively immobile and this forms a film on the grain faces (Reference 2.2.87 [DIRS 143273], p.42).

Based on the above discussion, volatile radionuclides behave as fine particles unless they are at a high temperature which could cause their evaporation. Because high burnup fuel contains more radionuclides that release more heat than low burnup fuel, it is expected that the surface temperature of fuel pellets would be higher than for low burnup fuel. Therefore, the ARF for volatiles in high burnup fuel would also be expected to be higher. Johnson et al. (Reference 2.2.43 [DIRS 178773], Table 6) provided the gap and grain boundary inventory estimates for various radionuclides for PWR UO_2 fuel in a burnup range of 37 to 75 GWd/MTU. These estimates clearly show that the radionuclide inventory in the gap and grain boundary increases with fuel burnup. For volatile radionuclides such as cesium, the inventory in the gap and grain boundary is about one order of magnitude higher for high burnup fuel at 75 GWd/MTU than low burnup fuel at 37 GWd/MTU. Consequently, it is recommended that the ARF for volatile radionuclides from high burnup fuel be established at one order of magnitude higher than the ARF developed for low burnup fuel in Section 6.1.3.

Therefore, the ARF for volatile radionuclides, such as ^{134}Cs, ^{137}Cs, and ^{106}Ru, released from high burnup fuel is 2×10^{-3}, which is one order of magnitude higher than the value 2×10^{-4} used for intact commercial SNF as discussed in Section 6.1.3. The RF for volatile radionuclides released from high burnup fuel is conservatively established at 1.0, the same as the RF for gases (bounding). The ARF and RF values for volatiles released from high burnup fuel are shown in Table 16.

6.5.4   Fuel Fines Release from High Burnup Fuel

During an accident, the airborne release fraction of fine particles from high burnup fuel is not expected to be higher than that from low burnup fuel (as discussed in Section 6.1.4). This is because the toughness on the rim is almost twice as high as the toughness at the center of a high burnup fuel pellet, which, in turn, is close to the toughness of the fuel surface of low burnup fuel (see Figure 15). The improvement of fracture toughness is mainly caused by the grain refinement (Reference 2.2.78 [DIRS 174080], p.186). The high toughness on the rim prevents a fuel pellet from breaking into small pieces during a drop event, as discussed in Section 6.5.1.

The relative hardness of a fuel pellet can impact the release of fuel fines. The relative hardness decreases towards the fuel pellet edge where the rim structure exists (see Figure 13). With a porosity less than 15%, which corresponds the highest porosity from an average fuel pellet burnup of 80 GWd/MTU, the relative hardness decreases about 20-30% (see Figure 14). The low relative hardness could have a negative impact on releases of fuel fines due to an accident. However, the increase of the toughness on the rim is higher than the decrease of the hardness on the fuel pellet edge. Above discussions indicate that, although the rim contains smaller grains and more pores, it is not as easy to break into small grain particles as unirradiated fuel.

In addition, the total release fraction for fuel fines after an accident may be restricted by the size of the breach or the amount of damage to the fuel cladding and canisters. Although high burnup fuel may have a higher fuel cladding fragility, release fraction for fuel fines remains the same as that for low burnup fuel, as a guillotine break or a longitudinal split of a fuel rod is not considered credible in a repository accident (Assumption 3.2.1).

The respirable fraction depends on the size distribution of particles released. The smaller the particle size, the higher the RF. As the grain size of particles on the rim surface is much smaller ($0.1 - 0.3$ μm) than those particles from low burnup fuel (about $8 - 10$ μm), the RF value for high burnup fuel would be expected to be higher than for low burnup fuel. Because no measured respirable fractions from high burnup fuel have been identified, a bounding value of 1.0 is selected as the most conservative approach.

Therefore, the ARF value of 3×10^{-5} for fuel fines (including ^{90}Sr, which is considered to be in particulate form) developed for low burnup intact commercial SNF in Section 6.1.4 is valid for use with high burnup fuel. The RF for fuel fines released from high burnup fuel is conservatively selected as 1.0. The ARF and RF values for fuel fines released from high burnup fuel are shown in Table 16.

6.5.5 Crud Release from High Burnup Fuel

Crud surface activities might be higher as fuel burnup increases because the fuel has spent longer in the reactor environment. However, current improvements in water chemistry may actually reduce the crud activity present on high burnup fuel. In any case, the ARFs and RFs for crud are considered to be the same for both low burnup fuel and high burnup fuel because the crud particles are on the outside of the fuel cladding and the mechanisms that cause the particles to be released into the environment do not depend on either fuel burnup or total crud activity.

From Section 6.1.5, the ARF value for crud released from intact commercial SNF is 0.015. From Section 6.2.3, the RF value for crud released from intact commercial SNF is 1.0. These values are used as the ARF and RF for crud released from high burnup fuel and are shown in Table 16.

6.5.6 Summary of ARFs and RFs for High Burnup Fuel

A summary of ARFs and RFs for gases, volatiles, fuel fines, and crud for high burnup fuel are shown in Table 16 based on the discussions in Section 6.5.2 to Section 6.5.5. This information applies to both intact and failed high burnup fuel assemblies. As discussed in Section 6.3 for low

burnup fuel, ARFs developed for failed commercial SNF are bounded by those established for intact commercial SNF. The discussions for failed commercial SNF of low burnup fuel in Section 6.3 are valid for failed commercial SNF of high burnup fuel.

Table 16. Recommended ARFs and RFs for High Burnup Fuel

Radionuclide	ARF / RF	In Section
^{3}H	0.3 / 1	6.5.2
^{85}Kr	0.3 / 1	6.5.2
^{129}I	0.3 / 1	6.5.2
^{134}Cs & ^{137}Cs	2×10^{-3} / 1	6.5.3
^{90}Sr	3×10^{-5} / 1	6.5.4
^{106}Ru	2×10^{-3} / 1	6.5.3
Fuel Fines	3×10^{-5} / 1	6.5.4
Crud	0.015 / 1	6.5.5

## 6.6   ARFs AND RFs FOR OXIDATION OF HIGH BURNUP FUEL

6.6.1   Oxidation of High Burnup Fuel

The model discussed in Section 6.4.1 indicates that the fuel oxidation process is slower for high burnup fuel, although the model may not be sufficiently accurate to adequately predict the oxidation for high burnup fuel.

6.6.2   Gaseous Radionuclide Release from Oxidation of High Burnup fuel

Colle et al. (Reference 2.2.17 [DIRS 179470], pp.229-242) recently reported fission product releases from BWR fuel with burnups up to 65 GWd/MTU. The report states that "if the oxidation temperature does not exceed 750 K (477°C), most fission products are entirely retained in the matrix. Even the fission gas precipitated in-pile in grain boundary pores did not escape in a significant amount during the low temperature oxidation. This was corroborated by monitoring ^{85}Kr release during oxidation: only 2-5% of the gas initially present in the fuel was released (Reference 2.2.17 [DIRS 179470], p.231)."

Of the three conditions tested by Colle et al. (Reference 2.2.17 [DIRS 179470]), Experiment C (oxidation of irradiated samples in a furnace in air and subsequent thermal annealing in the Knudsen cell) is considered to be closest to the conditions of a repository accident. The release fraction results for ^{129}I, ^{136}Xe, and ^{137}Cs are presented in Figure 19 (Reference 2.2.17 [DIRS 179470], Figure 10). The figure shows that less than 10% of the fission gas (^{136}Xe) and ^{129}I is released at a temperature of 400°C (673K). Higher release fractions, about 30% of the fission gas (^{136}Xe), and 20% of ^{129}I, are released at a temperature of 570°C (843K).
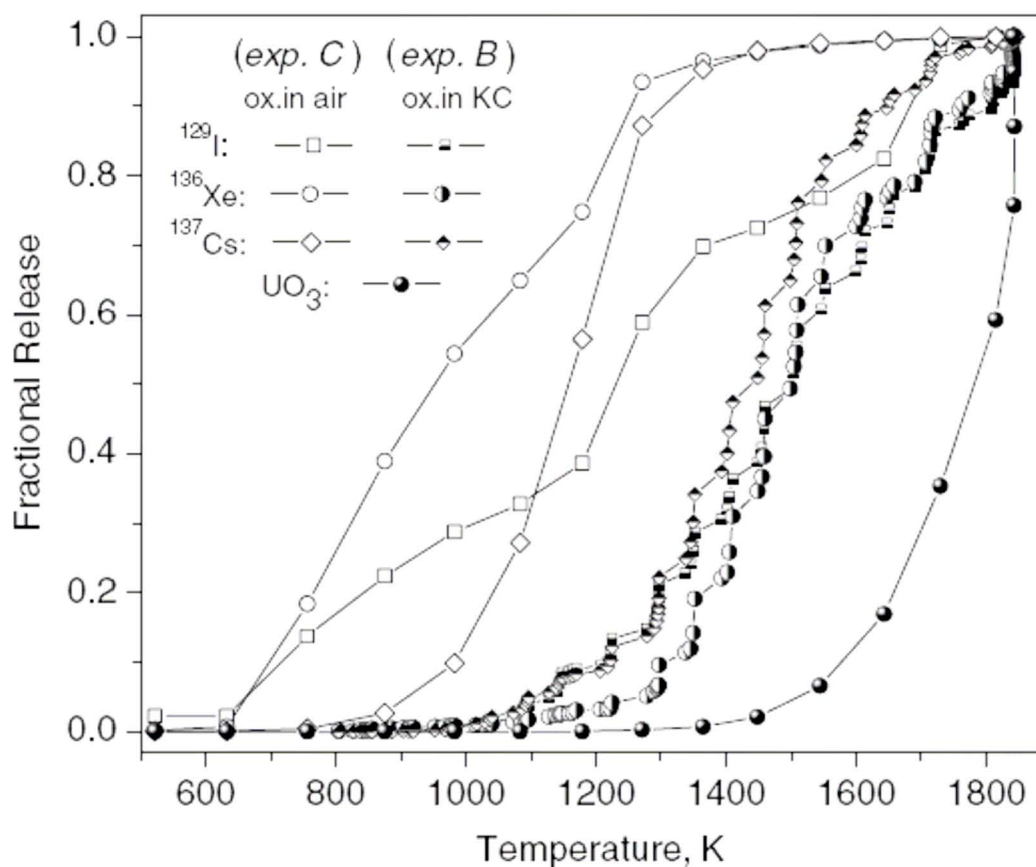
(Notes: Taken from Colle et al. (Reference 2.2.17 [DIRS 179470], Figure 10)

Figure 19. Release of Fission Gases and Volatiles in Experiments B and C

Based on the above, the ARF value of 0.30 for gases developed for oxidized low burnup fuel in Section 6.4.2 is considered valid for oxidized high burnup fuel. Similar to oxidized low burnup fuel, it is conservative to assume that all ^{3}H is released as water vapor because the experimental results for voloxidation indicate that ^{3}H was totally released once spent fuel was heated to about 500°C (see Section 6.4.2). The RF for gases is conservatively established at a value of 1.0 (bounding) as has been done for other fuel conditions. The ARF and RF for gases for high burnup fuel oxidation after an accident are shown in Table 17.

6.6.3   Volatile Radionuclide Release from Oxidation of High Burnup Fuel

Figure 19 also shows the experimental results of release fraction tests for volatile radionuclides such as ^{137}Cs. The value of fractional release is less than 0.001 at a temperature of 400°C. Other experiments conducted by Colle et al. indicate that the release fraction for ^{137}Cs is less than 0.001 until about 900-1000 K as shown on a log scale plot (Reference 2.2.17 [DIRS 179470], Figures 5 and 9). Therefore, it is considered conservative to use a release fraction of 0.001 for ^{137}Cs releases from fuel oxidized at a temperature of 673 K. It is expected that the release fractions for other volatile radionuclides are less than ^{137}Cs, as discussed in Section 6.1.3.

This reported release fraction (1×10^{-3}) for ^{137}Cs from high burnup fuel is lower than the selected release fraction (2×10^{-3}) for volatile radionuclides from low burnup fuel established in Section 6.4.3. Therefore, for conservatism, an ARF of 2×10^{-3} and an RF of 1.0 is recommended in this analysis for volatile radionuclides released due to the oxidation of high burnup fuel exposed to air. The ARF and RF for high burnup fuel oxidation after an accident are shown in Table 17.

6.6.4 Fuel Fines Release from Oxidation of High Burnup Fuel

The ARF for fuel fines from the oxidation of high burnup fuel after an accident are expected to be similar to the ARF for low burnup fuel. This is primarily because the particle size distributions of the oxidized powder (as measured by PNNL) are very similar for both low burnup and high burnup fuel (Assumption 3.1.1). Attachment D provides the justification for this assumption which requires verification because it is based on preliminary PNNL test results (see Figure 20, taken from file *Test Results Comp.xls* as attached in Attachment E). In addition, as shown in Section 6.4.1.1, the incubation time at a given temperature increases with increasing burnup (i.e., high burnup fuel oxidizes more slowly than low burnup fuel). Therefore, it is conservative to assume that all high burnup fuel is oxidized and that the ARF value is the same as the ARF for low burnup fuel developed in Section 6.4.4.
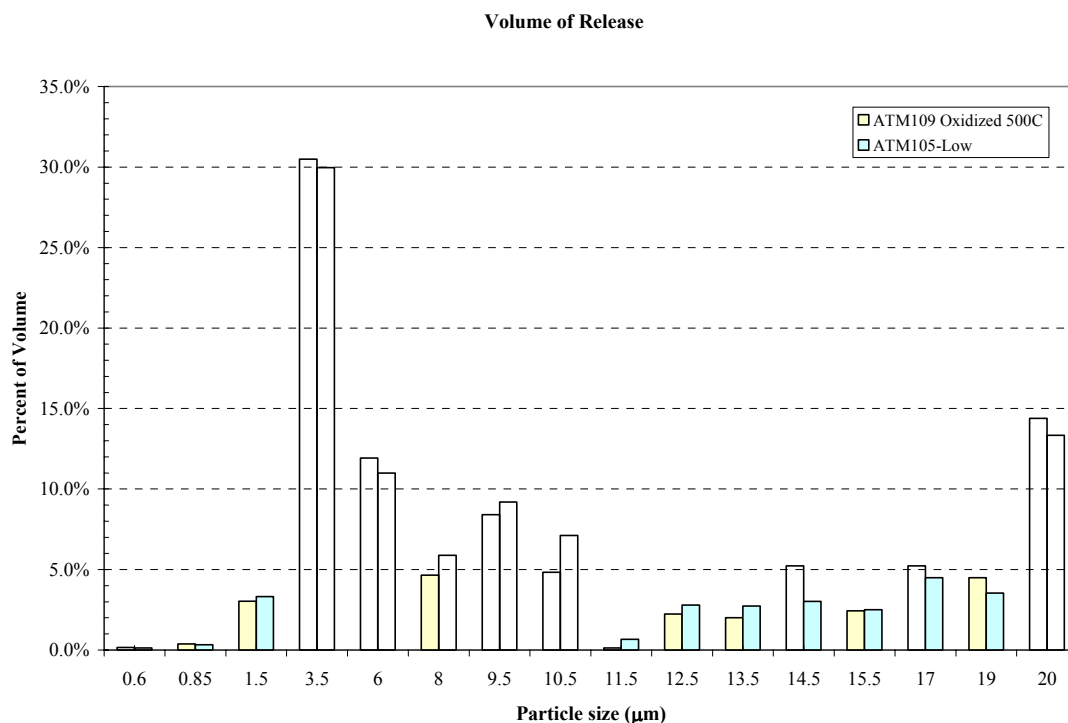

Figure 20. Oxidized Powder Particle Size Distributions for High and Low Burnup Fuel

As shown in Figure 20, approximately 35% of the particle volume is less than 3.5 μm in diameter. As calculated in Section 6.2.1 the respirable cut-off diameter for oxidized fuel powder

is 4 µm. Therefore, the RF for fuel fines from fuel oxidation of high burnup fuel may be 0.35. However, to account for uncertainties in the test data, the RF is selected to be 1 as a conservative bound.

The ARF and RF for fuel fines (including ^{90}Sr) for high burnup fuel oxidation after an accident are shown in Table 17.

6.6.5 Summary of ARFs and RFs for Oxidation of High Burnup Fuel

ARFs and RFs for crud are not considered for high burnup fuel oxidation because the release of crud particles is already considered during a drop event. As mentioned by Einziger (Reference 2.2.27 [DIRS 166177], p.97), additional crud spallation due to oxidation of the cladding is insignificant. Therefore, the radionuclide release from crud after the accident is less important than during the accident and can be ignored without loss of conservatism.

A summary of ARFs and RFs for gases, volatiles, and fuel fines for oxidation of high burnup fuel is shown in Table 17 based on the discussions in Section 6.6.2 to Section 6.6.4. These ARFs and RFs for high burnup fuel oxidation are for radionuclide releases after an accident; they are in addition to the releases occurring during an accident.

Table 17. Recommended ARFs and RFs for High Burnup Fuel Oxidation After an Accident

Radionuclide	ARF / RF
^{3}H	0.7 / 1
^{85}Kr	0.3 / 1
^{129}I	0.3 / 1
^{134}Cs & ^{137}Cs	2×10^{-3} / 1
^{90}Sr	2×10^{-3} / 1
^{106}Ru	2×10^{-3} / 1
Fuel Fines	2×10^{-3} / 1
Crud	NA

6.7 ARFs AND RFs FOR HIGH-LEVEL RADIOACTIVE WASTE

High-level radioactive waste (HLW) is generated as a result of the reprocessing of SNF. HLW is received at the repository in sealed stainless steel canisters in the form of vitrified glass. During normal repository operation, no radionuclides are expected to be released to the environment from HLW canisters. However, in an accident, such as a canister drop that causes the canister to breach, the vitrified glass inside the canister can fracture and small pieces of glass containing radionuclides could be released to the environment. All radionuclides that could be released to the environment from a breached HLW canister are in the form of particulates. There are no radionuclides in the form of gases, volatiles, or crud associated with HLW.

ANSI/ANS-5.10-1998, *Airborne Release Fractions at Non-Reactor Nuclear Facilities* (Reference 2.2.6 [DIRS 103755], p.15) recommends using DOE-HDBK-3010-94 (Reference 2.2.24 [DIRS 103756], Section 4.3.3) to calculate the release fraction from an impact breach of a HLW canister. The empirical equation is based on experimental measurements of impact tests

on UO2, ceramic and glass-simulated waste forms. Small-scale laboratory tests established each correlation for the percentage of respirable size release fractions created during impacts. The formula for the PULF from a drop event, that is, the release fraction of respirable airborne particulates (particles with a physical diameter <10 μm) is shown as Equation 2 in Section 4.3.4.

Lift heights of loaded casks and canisters in the IHF are less than 40 feet (12.2 m) (Reference 2.2.15 [DIRS 182031], Section 7). This represents the worst possible height for a HLW canister drop event. Using this height and HLW density of about 2.7 g/cm^3 (Reference 2.2.23 [DIRS 102812], Table 3.3.1), the PULF is calculated using Equation 2 to be:

$$\text{PULF} = 2 \times 10^{-11} \times 2.7(g/cm^3) \times 980(cm/s^2) \times 1220(cm) = 6.5 \times 10^{-5} \qquad \text{Equation 17}$$

SAND84-2641 (Reference 2.2.53 [DIRS 104779], p.5-23) recommends using the PULF value of 2×10^{-4} for all scenarios involving dropped HLW canister because of uncertainty in the accuracy and applicability of the PULF equation for glass waste. This recommendation is deemed too conservative because it does not consider the relatively lower impact energy density for glass than for UO$_2$ at the same drop height. The impact energy density for glass dropped from a height of 12.2 m can be calculated using the formula discussed in Section 4.3.4.

$$\frac{E}{V} = \rho \times g \times h = 2.7 \times 10^{-3}(kg/cm^3) \times 9.8(m/s^2) \times 12.20(m) = 0.32(J/cm^3) \qquad \text{Equation 18}$$

This calculated impact energy density is three times lower than 1 J/cm^3 that is used as basis for the recommendation in SAND84-2641 (Reference 2.2.53 [DIRS 104779], p.5-23). In addition, the experimental results with an impact energy density of 0.41 J/cm^3 in ANL-81-27 (Reference 2.2.58 [DIRS 158827], Table 3) show that the respirable fractions (<10 μm) range from 2.5×10^{-5} to 4.2×10^{-5} for the tested Pyrex cylinders. The results for the tested Pyrex cylinders are shown in Figure 21 from ANL-81-27 (Reference 2.2.58 [DIRS 158827], Figure 27). The figure shows the measured data points are all above 100 μm when the data are fitted within a lognormal distribution. The respirable fractions (<10 μm) are less than 5×10^{-5}.

As mentioned previously, the PULF represents the product of the ARF and RF. By using the same method as used for estimating the RF for impact rupture tests on three unconfined UO$_2$ pellets in Section 6.2.2.2, an RF for HLW glass can be estimated. As shown in Figure 21, the mass percent of particles smaller than 100 μm, corresponding to airborne particulates, is about 0.2%, while the mass percent of particles smaller than 7 μm, corresponding to respirable particles as discussed in Section 6.2.1 and Attachment C for HLW, is about 0.002%. This makes the RF equal to about 0.01 (0.002% / 0.2%) based on the definition of RF presented in Section 4.3.1.
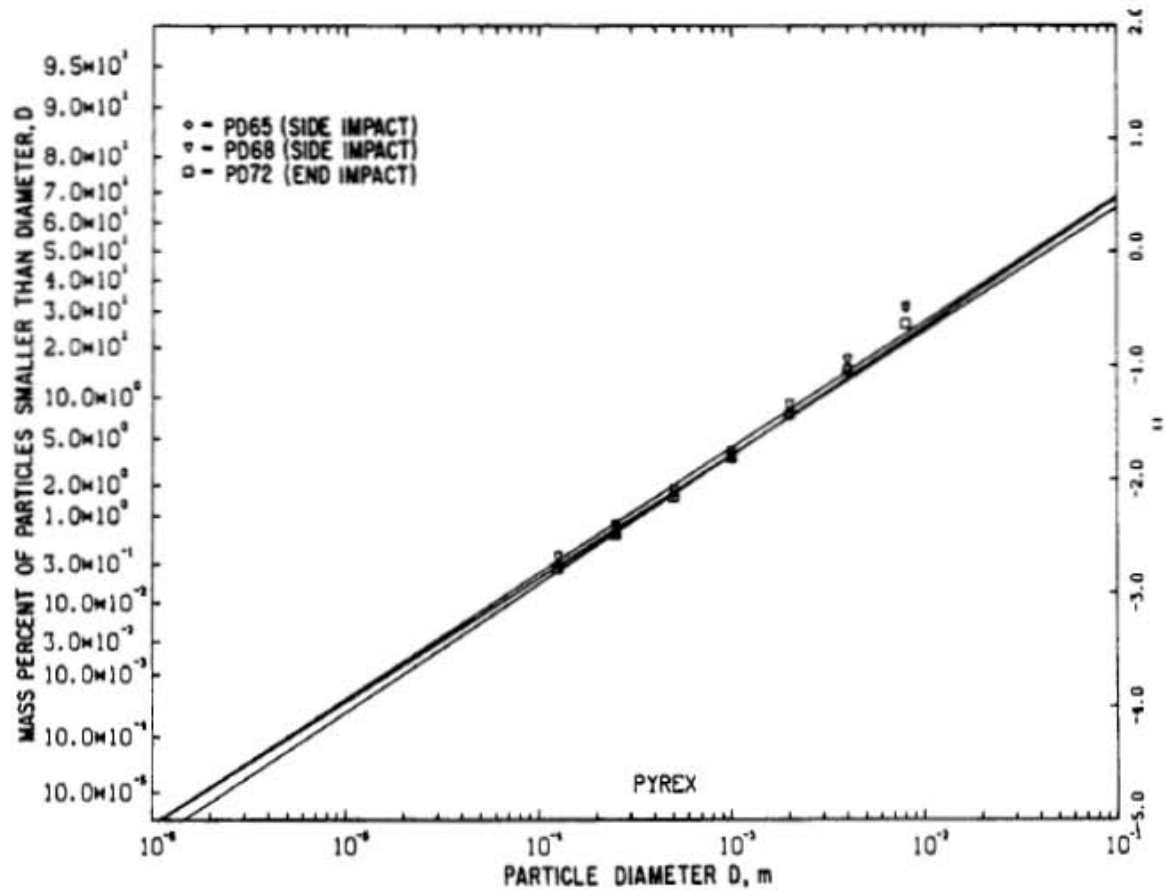
(Note: for solid Pyrex cylinders taken from Mecham et al. (Reference 2.2.58 [DIRS 158827], Figure 27)

Figure 21. Particle Size Distribution Measured with Drop Weight Impact of 0.41 J/cm^3

The PULF for HLW glass, calculated in Equation 17, is 6.5×10^{-5}, which is rounded up to 7×10^{-5} for conservatism. The respirable fraction for glass is estimated above to be 0.01. Therefore, the ARF is 0.007 (7×10^{-5} / 0.01). Based on this, it is recommended that an ARF of 0.007 and an RF of 0.01 (or the product of ARF $\times$ RF = 7×10^{-5}) be used for the radionuclide release resulting from a HLW canister accident. The calculated PULF is considered conservative because it is based on a bounding drop height at 40 feet and because the particle size used for the respirable fraction is 10 μm physical diameter (about 14 μm AED), which corresponds to a higher PULF value. As discussed previously, the release from a damaged HLW canister is in the form of particulate materials only, with no gases, volatiles radionuclides, or crud present.

7. RESULTS AND CONCLUSIONS

This analysis specifies and documents the airborne release fractions and respirable fractions for radioactive materials that could be released during an accident at the repository involving commercial SNF or high-level radioactive waste in a dry environment. The radionuclides would be released from the inside of breached fuel rods (or pins), from the detachment of radioactive material (crud) from the outside surfaces of fuel rods and other fuel assembly components, or from the crushing of high-level radioactive waste glass. The definitions of airborne release fraction and respirable fraction are given in Section 4.3.1.

The ARFs and RFs established for commercial SNF in Sections 6.1 and 6.2 may be applied to drop or impact accidents involving either a bare unconfined fuel assembly or a confined fuel assembly contained in a shipping cask, canister, or waste package. This analysis does not take credit for any container that confines a fuel assembly even though the container would provide an additional barrier against radioactive material releases during an accident. Therefore, applying the ARFs and RFs from this analysis to confined commercial SNF assemblies is a conservative approach.

The ARFs and RFs for failed commercial SNF under repository accident conditions are discussed in Section 6.3, and the use of the same values as for intact commercial SNF are justified. Because failed commercial SNF is received at the repository in a canister (Assumption 3.2.5), the ARFs and RFs established for failed commercial SNF take credit for the protection afforded to the failed fuel by the canister.

The ARFs and RFs for fuel oxidation after a drop event are developed in Section 6.4. The radionuclide releases due to fuel oxidation are in addition to the releases for intact or failed commercial SNF.

A fraction of commercial SNF comes from high burnup fuel, i.e., fuel with a burnup higher than 45 GWd/MTU. The highest burnup considered in this document is 80 GWd/MTU. The ARFs and RFs for high burnup fuel under repository accident conditions are analyzed in Section 6.5, and are the same values as for intact commercial SNF.

Discussions regarding the oxidation of high burnup fuel after a drop event accident are provided in Section 6.6. Again, the radionuclide releases due to fuel oxidation are in addition to the releases for intact or failed commercial SNF.

The ARF and RF for a HLW canister drop event are discussed and documented in Section 6.7.

Table 18 summarizes the recommended ARFs and RFs associated with commercial SNF, with post-accident oxidation, and with a dropped HLW canister. The content of this summary table provides the results of the ARFs and RFs values at various conditions, which are specified in the purpose of this document (Section 1.1).

Table 18. ARFs and RFs for Commercial SNF and HLW

| Radio-nuclides | ARF / RF | | | | |
| | Low Burnup Fuel | | High Burnup Fuel | | High Level Waste |
	Intact & Failed Commercial SNF Assembly	Fuel Oxidation After an Accident	Intact & Failed Commercial SNF Assembly	Fuel Oxidation After an Accident	
Located in	Table 5, Table 7, Table 8, Table 9	Table 14	Table 16	Table 17	Section 6.7
^{3}H	0.3 / 1	0.7 / 1	0.3 / 1	0.7 / 1	N/A
^{85}Kr	0.3 / 1	0.3 / 1	0.3 / 1	0.3 / 1	N/A
^{129}I	0.3 / 1	0.3 / 1	0.3 / 1	0.3 / 1	7×10^{-3} / 0.01
^{134}Cs & ^{137}Cs	2×10^{-4} / 1	2×10^{-3} / 1	2×10^{-3} / 1	2×10^{-3} / 1	7×10^{-3} / 0.01
^{90}Sr	3×10^{-5} / 5×10^{-3}	2×10^{-3} / 0.1	3×10^{-5} / 1	2×10^{-3} / 1	7×10^{-3} / 0.01
^{106}Ru	2×10^{-4} / 1	2×10^{-3} / 1	2×10^{-3} / 1	2×10^{-3} / 1	7×10^{-3} / 0.01
Fuel Fines	3×10^{-5} / 5×10^{-3}	2×10^{-3} / 0.1	3×10^{-5} / 1	2×10^{-3} / 1	7×10^{-3} / 0.01
Crud (^{60}Co & ^{55}Fe)	0.015 / 1	NA	0.015 / 1	NA	N/A

Note: radionuclides are categorized as gas (such as 3H, 85Kr and 129I), volatiles (134Cs, 137Cs, and 106Ru), fuel fines (including 90Sr) and crud (such as 60Co and 55Fe). See details in Section 6.1.1.3.

ATTACHMENT A

Gravitational Deposition Confirmatory Analysis

NUREG/CR-0722 (Reference 2.2.51 [DIRS 100990], p. 105), states that a small fraction of fuel particles ejected from a burst fuel pin were carried out of the furnace tube into the thermal gradient tube and filter pack. At the time of rupture, the velocity of the steam flowing past the rupture point, through the furnace tube, and down through the filter pack was 15 cm/s. Thus, for particles to settle out before reaching the thermal gradient tube, they would have to fall at a rate of about 3 cm/s (the terminal settling velocity). NUREG/CR-0722 (Reference 2.2.51 [DIRS 100990], p. 105) states that particles with diameters greater than 12 to 15 μm would fall at this rate. This has been confirmed by sampling (albeit somewhat randomly and sparsely) some of the particulates collected in the filters with a scanning electron microscope and determining that these particulates had diameters typically equal to 10 μm (Reference 2.2.51 [DIRS 100990], p. 105 and Appendix C). To confirm that particles with diameters greater than 12 to 15 μm settle out before reaching the thermal gradient tube, gravitational deposition methods, presented in Appendix B of ANSI N13.1-1969 (Reference 2.2.5 [DIRS 106261]), are applied.

The first step is to confirm the terminal settling velocity. According to ANSI N13.1-1969 (Reference 2.2.5 [DIRS 106261]), the length for 100 percent deposition (cm) is:

$$L_{100} = \frac{8rV}{3u_t} \qquad \text{(Eq. A-1)}$$

where

L_{100} is the length for 100 percent deposition (cm)

r is the radius of the tube (cm)

V is the average velocity in the tube (cm/s)

u_t is the terminal settling velocity (cm/s).

The 100 percent deposition length in this case is assumed to be approximately the length of the furnace tube (i.e., 44 cm). The actual length may be somewhat shorter depending on where the actual rupture point occurred. The average velocity in the tube is stated to be approximately 15 cm/s and the radius of the furnace tube is approximately 3.5 cm based on NUREG/CR-0722 (Reference 2.2.51 [DIRS 100990], Figure 4 on p. 105). Thus, the Equation A-1 can be solved for the terminal settling velocity:

$$u_t = \frac{8rV}{3L_{100}} = \frac{8(3.5\,cm)(15\,cm/s)}{3(44\,cm)} \qquad \text{(Eq. A-2)}$$
$$= 3.18\,cm/s$$

This velocity is very close to the 3 cm/s in NUREG/CR-0722 (Reference 2.2.51 [DIRS 100990], p. 105).

With the terminal settling velocity now calculated, the diameter of the particles settling at this velocity can be calculated from Stoke's Law (ANSI N13.1-1969 (Reference 2.2.5 [DIRS 106261]), p. 34):

$$u_t = \frac{g d_p^2 \left(\rho_p - \rho_g \right)}{18 \mu} K_m \qquad \text{(Eq. A-3)}$$

where

      g is the gravitational constant (980 cm/s^2)
      d_p is the diameter of the particle (cm)
      ρ_p is the density of the particle (g/cm^3)
      ρ_g is the density of the steam (g/cm^3)
      μ is the steam viscosity (g/cm-s)
      K_m is the Cunningham correction for slip (unitless).

This equation can be solved for the diameter of the particle.

The terminal velocity has already been shown to be approximately 3 cm/s, the particle density is taken to be 10.96 g/cm^3 (see Section 6.2.2), the Cunningham correction factor has been shown to be nearly unity (see Figure 1), and the density of steam and viscosity of steam at 900ºC are approximately 1.8×10^{-4} g/cm^3 and 2.8×10^{-4} g/cm-s, respectively.[1] Thus, the particle diameter can be calculated from:

$$d_p^2 = \frac{18 \mu u_t}{g \left(\rho_p - \rho_g \right) K_m} \qquad \text{(Eq. A-4)}$$

---

[1] The steam density is from *Fundamentals of Classical Thermodynamics* (Reference 2.2.83 [DIRS 108881], p. 641). The steam viscosity is from *Flow of Fluids Through Valves, Fittings, and Pipe* (Reference 2.2.19 [DIRS 149707], p. A-2).

$$d_p = \sqrt{\frac{18\,\mu\,u_t}{g\left(\rho_p - \rho_g\right)K_m}}$$

$$d_p = \sqrt{\frac{18(2.8\times10^{-4}\ g/cm-s)(3.0\ cm/s)}{(980\ cm/s^2)\left(10.96\ g/cm^3\right)(1)}}$$

$$d_p = \sqrt{1.41\times10^{-6}\ cm^2}$$

$$d_p = 11.9\ \mu m$$

This value is essentially equal to the smallest diameter presented in NUREG/CR-0722 (Reference 2.2.51 [DIRS 100990], p. 105) as having settled before reaching the thermal gradient tube (i.e., 12 μm). If shorter 100 percent deposition lengths were considered in this analysis, then the terminal settling velocities would increase, which in turn results in a larger diameter. This larger diameter is likely near the 15-μm diameter noted in NUREG/CR-0722 (Reference 2.2.51 [DIRS 100990], p. 105).

Thus, both the terminal settling velocity of 3 cm/s and the diameter of the fuel particles that settled out before reaching the thermal gradient tube are confirmed from NUREG/CR-0722 (Reference 2.2.51 [DIRS 100990], p. 105) using methods presented in Appendix B of ANSI N13.1-1969 (Reference 2.2.5 [DIRS 106261]).

INTENTIONALLY LEFT BLANK

ATTACHMENT B

Summary of Release Fractions from Other NRC Licensed Facilities/Casks

Safety analysis reports (SARs) for cask systems and independent spent fuel storage installations (ISFSIs) provide valuable information on values of release fractions used in consequence analyses approved by the NRC. The values of these release fractions, which are given in Table 19 through Table 21, are provided for information only; they do not impact the analysis performed in this calculation.

Each of the following documents is found in the NRC's Public Document Room, 2120 L Street, NW, Lower Level, Washington, DC 20555-0001. They are cross-referenced by the following numbers in Table 19, Table 20, and Table 21.

(1) *Fort St. Vrain Independent Spent Fuel Storage Installation Safety Analysis Report, Revision 2* (Reference 2.2.38 [DIRS 155101]).

(2) *North Anna Power Station Independent Spent Fuel Storage Installation, License Application* (Reference 2.2.86 [DIRS 158884]).

(3) "Docket No. 72-11, Rancho Seco Independent Spent Fuel Storage Installation, Revision 1 to the Rancho Seco Independent Spent Fuel Storage Installation License Application and Safety Analysis Report" (Reference 2.2.74 [DIRS 157601]) for the Sacramento Municipal Utility District (SMUD).

(4) *Safety Analysis Report for the INEL TMI-2 Independent Spent Fuel Storage Installation, Revision 0* (Reference 2.2.37 [DIRS 103308]).

(5) *Trojan Independent Spent Fuel Storage Installation, Safety Analysis Report* (Reference 2.2.67 [DIRS 103449])

(6) *10 CFR 72 Topical Safety Analysis Report for the Holtec International Storage, Transport and Repository Cask System (HI-STAR-100 Cask System)* (Reference 2.2.35 [DIRS 131475], Reference 2.2.2 [DIRS 176577]).

(7) *Safety Analysis Report Large On-Site Transfer and On-Site Storage Segment, CLIN 0004PC* (Reference 2.2.89 [DIRS 130528]).

(8) *Safety Analysis Report for the NUHOMS®-MP187 Multi-Purpose Cask* (Reference 2.2.85 [DIRS 105288]).

(9) *Safety Analysis Report for the Standardized NUHOMS® Horizontal Modular Storage System for Irradiated Nuclear Fuel* (Reference 2.2.84 [DIRS 157643]).

(10) *TN-24 Dry Storage Cask Topical Report* (Reference 2.2.81 [DIRS 158882]).

(11) *Safety Analysis Report for the TranStor™ Storage Cask System* (Reference 2.2.75 [DIRS 150946]).

(12) *Final Design Package Babcock & Wilcox BR-100, 100 Ton Rail/Barge Spent Fuel Shipping Cask* (Reference 2.2.7 [DIRS 104439]).

(13) *Safety Analysis Report for the NAC Legal Weight Truck Cask* (Reference 2.2.60 [DIRS 158874]).

(14) *Safety Analysis Report for the TranStor™ Shipping Cask System* (Reference 2.2.76 [DIRS 141465]).

Independent Spent Fuel Storage Installations

Table 19 summarizes the release fractions used in the SARs of the various ISFSIs. For each ISFSI, a hypothetical loss of confinement accident was analyzed. In each case, 100 percent of the fuel cladding was assumed ruptured and the cask breached in such a manner that the release fraction from the cask to the environment was equal to unity. In nearly each case, except for the Fort St. Vrain and INEL TMI-2 ISFSIs, ^{85}Kr was either the only analyzed radionuclide or the only radionuclide that significantly contributed to the dose at the site boundary. It is also noted in the INEL TMI-2 SAR that the fraction of particulates and solids that were released from the cask to a filtration system was approximately 1 percent. This value is expected to be high compared to releases from originally intact fuel assemblies because most of the TMI-2 fuel was no longer confined by cladding. The release fractions for the gases ^{3}H and ^{129}I spanned the whole spectrum (i.e., a release fraction between 0 and 1). The release fraction for the gas ^{85}Kr ranged from 0.25 to 1.00, with an equal number selecting 0.3 and 1.0.

Storage Cask Systems

Table 20 summarizes the release fractions used in the SARs of the various storage cask systems. For each storage cask, a hypothetical loss of confinement accident was analyzed. In each case, 100 percent of the fuel cladding was assumed ruptured and the cask breached in such a manner that the release fraction from the cask to the environment was equal to unity. In each case, ^{85}Kr was either the only analyzed radionuclide or the only radionuclide that significantly contributed to the dose at the site boundary. No particulate releases were considered in any of these SARs, as the particulates were expected to locally deposit near their release point. The release fractions for the gases ^{3}H and ^{129}I ranged from 0 to 0.3. The release fraction for the gas ^{85}Kr was nearly always equal to 0.3 for the storage casks with the exception of the ^{24}TN cask system, which used a release fraction of 0.1.

Transportation Cask Systems

Table 21 summarizes the release fractions used in the SARs of various transportation cask systems. In each case, 100 percent of the fuel cladding was assumed ruptured and the cask breached in such a manner that the release fraction from the cask to the environment was equal to unity. In each case, ^{85}Kr was the only radionuclide that significantly contributes to the dose at the site boundary. No particulate releases were considered in any of these SARs, as the particulates were expected to locally deposit near their release point. However, the Sierra TranStor cask did consider 100 percent of the crud (^{60}Co) to be released from the fuel rod surfaces and 100 percent of this to be aerosolized. The release fractions for tritium ranged from 0.1 to 0.3. The release fraction for ^{129}I ranged from 0 to 0.3, but its contribution to the dose was nearly always ignored. The release fraction for the gas ^{85}Kr was always equal to 0.3.

Table 19. Release Fractions Used in SARs for Independent Spent Fuel Storage Installations

Name (Ref. No.)	NRC Docket Number	Release Fractions				Source Page Numbers
		Particulate	Fission Gases			
		Co, Cs, Ru, Sr	H-3	Kr-85	I-129	
INEL Fort St. Vrain (1)	72-0009	1.00×10^{-5}	0.50	1.00	0.00	A8-9/2
VEPCO North Anna (2)	72-0016	0.00 [a]	1.00	1.00	0.00 [a]	8.3-2
SMUD Rancho Seco (3)	72-0011	0.00 [a]	0.30	0.30	0.30	I 8-32
INEL TMI-2 (4) [b]	72-0020	1.00×10^{-3}	0.00 [a]	0.10	0.00 [a]	7.2-2
PGE Trojan (5)	72-0017	0.00 [a]	0.30	0.30	0.30	8-8

[a] Based on the dose calculations performed in these SARs, these radionuclides were not included and hence, their release fractions are assumed to be zero. In actuality, the release fractions are likely to be relatively small compared to fission gases; however, other factors (e.g., local deposition, respirability) are assumed to make their dose contributions negligible.

[b] Values for the INEL TMI-2 ISFSI are for damaged fuel from Three Mile Island Unit 2. Hence, fission gases liberated from the fuel are assumed to have escaped. In addition, much of the material stored is made up of filters that contain a large number of particulates.

Table 20. Release Fractions Used in SARs for Storage Cask Systems

Name (Ref. No.)	NRC Docket Number	Release Fractions				Source Page Numbers
		Particulate	Fission Gases			
		Co, Cs, Ru, Sr	H-3	Kr-85	I-129	
Holtec HI-STAR (6)	72-1008	0.00	0.30	0.30	0.30	11.2-6
Westinghouse Large MPC (7)	-	0.00	0.30	0.30	0.30	7.3-1
Vectra NUHOMS (9)	72-1004	0.00 [a]	0.30	0.30	0.30	8.2-40
TN-24 (10)	-	0.00 [a]	0.10	0.10	0.00 [a]	8.1-4
SNC TranStor™ (11)	72-1023	0.00	0.30	0.30	0.30	11-17

[a] Based on the dose calculations performed in these SARs, these radionuclides were not included and hence, their release fractions are assumed to be zero. In actuality, the release fractions are likely to be relatively small compared to fission gases, however other factors (e.g., local deposition, respirability) are assumed to make their dose contributions negligible.

Table 21. Release Fractions used in SARs for Transportation Cask Systems

Name (Ref. No.)	NRC Docket Number	Release Fractions				Source Page Numbers
		Particulate	Fission Gases			
		Co, Cs, Ru, Sr	H-3	Kr-85	I-129	
B&W BR-100 Shipping Cask (12)	71-9230	0.00 [a]	0.10	0.30	0.00 [a]	II 4-10
Holtec HI-STAR (6)	71-9261	0.00	0.30	0.30	0.30	11.2-6
NAC Legal Weight Truck (13)	71-9225	0.00 [a]	0.10	0.30	0.00 [a]	4.3-1
Westinghouse Large MPC (7)	-	0.00	0.30	0.30	0.30	7.3-1
Vectra NUHOMS®MP-187 (8)	71-9255	0.00 [a]	0.30	0.30	0.30	4-5
SNC TranStor™ (14)	71-9268	0.00 (100% crud)	0.30	0.30	0.30	4-15

[a] Based on the dose calculations performed in these SARs, these radionuclides were not included and hence, their release fractions are assumed to be zero. In actuality, the release fractions are likely to be relatively small compared to fission gases, however other factors (e.g., local deposition, respirability) are assumed to make their dose contributions negligible.

ATTACHMENT C

Respirable Particle Definition and Calculation of Cut-off Diameter

Definition of Respirable Particles

According to DOE-HDBK-3010-94 (Reference 2.2.24 [DIRS 103756], pp.1-4 to 1-6), several definitions of respirable particles have been presented by various groups at different times, as follows:

- Particles with terminal velocities equal to that of a 5-μm diameter particle were considered "respirable dust" by the British Medical Research Council in 1952.

- Particles with a 50 percent respirable cut-size of 3.5-μm AED were considered "respirable dust" by the U.S. Atomic Energy Commission.

- Particles with a 50 percent respirable cut-size of 2-μm AED were considered "respirable dust" by the American Conference of Governmental Industrial Hygienists.

- Particles with a 50 percent respirable cut-off at 15-μm AED were considered "inhalable dust" (particles entering the upper respiratory airway and entering the thorax) by the EPA.

- Particles with a 50 percent respirable cut-size at 10-μm AED were considered "inhalable dust" (particles entering the nasal or oral passages) by the International Standards Organization - Europe.

From the above definitions, the first three sources define respirable particles as less than 5-μm AED, while the last two sources define inhalable particles as less than 15-μm AED. This indicates that the respirable particles are smaller than the inhalable particles. An AED of 10 μm adequately represents the cut-off diameter for respirable particulate (Reference 2.2.24 [DIRS 103756], pp.1-4 to 1-6). This value is further supported by ANSI/ANS-5.10-1998 (Reference 2.2.6 [DIRS 103755], Appendix B2.1.4, p.19), which states that the respirable fraction "is commonly assumed to include particles 10 μm Aerodynamic Equivalent Diameter (AED) and less as a conservative approximation." Accordingly, use of a 10-μm AED cut-size for respirable particles is considered conservative, and may even be overly conservative since the mass is a cube function of particle diameter (Reference 2.2.24 [DIRS 103756], p.1-5).

According to DOE-HDBK-3010-94 (Reference 2.2.24 [DIRS 103756], p.xviii), the AED is equivalent to the diameter of a sphere of density 1 g/cm^3 that exhibits the same terminal velocity as the particle in question. In this case, the particle in question represents the cut-off diameter for respirable particles ($d_{c/o}$).

Relationship Between AED and Cut-off Diameter

The terminal settling velocity is determined from Stoke's solution for the drag on a sphere in creeping flow with correction factors for particulate shape and slip (Reference 2.2.73 [DIRS 103696], p.11):

$$v_{term} = \frac{\rho \times g \times d^2 \times C(Kn)}{18 \times \mu_{air} \times \kappa}$$

Equation 19

where

ρ = aerosol particulate density (g/cm^3)

g = gravitational acceleration (980 cm/s^2)

d = aerosol diameter (cm)

$C(Kn)$ = Cunningham-Knudsen-Weber slip correction factor (dimensionless)

Kn = Knudsen number (dimensionless)

μ_{air} = bulk gas viscosity (g/(cm-s)

κ = dynamic shape factor (dimensionless). $\kappa = 1$ for a unit density sphere.

To calculate the cut-off diameter for respirable particles ($d_{c/o}$), the terminal settling velocity (v_{term}) for the AED is set equal to that for $d_{c/o}$.

$$\frac{\rho_{AED} \times g \times AED^2 \times C(Kn)_{AED}}{18 \times \mu_{air} \times \kappa_{AED}} = \frac{\rho_p \times g \times d_{c/o}^2 \times C(Kn)_p}{18 \times \mu_{air} \times \kappa_p}$$

Equation 20

The Cunningham-Knudsen-Weber correction factor as a function of particulate diameter at a temperature of 300 K and a pressure of 10^5 Pa is shown in Figure 22, which is taken from Sandoval et al. (Reference 2.2.73 [DIRS 103696], p. II-5). Except for particulates with diameters less than 2 μm, the Cunningham-Knudsen-Weber correction factor is nearly equal to unity and hence, the ratio of $C(Kn)_p$ to $C(Kn)_{AED}$ is approximately unity. Using the ρ_{AED} as a unit density of 1 g/cm^3 and $\kappa_{AED} = 1$ for a sphere, the relationship between the AED and $d_{c/o}$ can be written as:

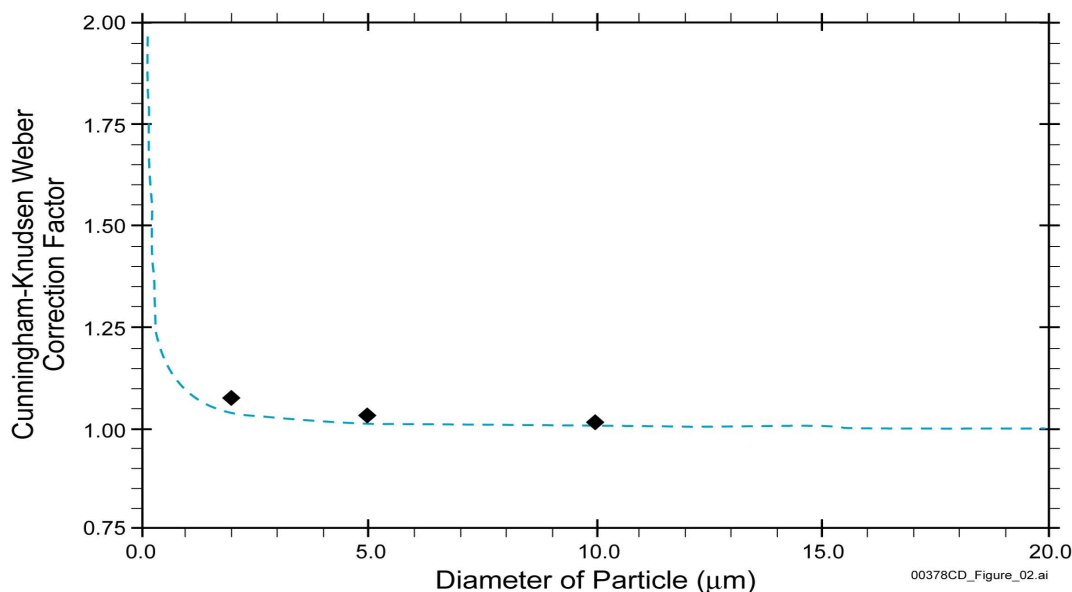$$AED = d_{c/o} \times \sqrt{\frac{\rho_p}{\kappa_p}}$$

Equation 21

where

ρ_p = density of the particulate in the aerosol, g/cm^3

κ_p = dynamic shape factor for the particulate in the aerosol (dimensionless)

AED = aerodynamic equivalent diameter for respirable particulate, 10 μm

$d_{c/o}$ = cut-off diameter in units of μm with particle density of ρ_p and dynamic shape factor of κ_p.

NOTE: The three diamonds in this figure represent points presented in ANSI N13.1-1969 (Reference 2.2.5 [DIRS 106261], Table B3).

Figure 22. Cunningham-Knudsen-Weber Slip Correction Factor in Air at 300 K and 10^5 Pa

Calculation of Respirable Cut-off Diameter

The dynamic shape factor measures particle spherical shape. The dynamic shape factor for a sphere is defined as 1. A higher value increases the drag experienced by particles of non-spherical shape. From a visual examination of the Quad Cities crud sample, and from measurements of the factor on model aerosol particle systems, a value of 1.3 is a reasonable choice (Reference 2.2.73 [DIRS 103696], p.II-5). As this reference is a reliable source, it is appropriate for the intended use at the Yucca Mountain repository.

This value for the dynamic shape factor is also used for aerosols from commercial SNF, based on a comparison between the scanning electron microscope pictures in NUREG/CR-0722 (Reference 2.2.51 [DIRS 100990], Appendix C), and Sandoval et al. (Reference 2.2.73 [DIRS 103696], pp.I-37 and I-38). Pictures produced by the scanning electron microscope show that commercial SNF particles and crud particles do not significantly differ in shape. In addition, a default value of particle shape factor of 1.5 was used for the human lung model for the dose coefficients in the ICRP Publication 66 (Reference 2.2.36 [DIRS 153705], p.49). The shape factor of 1.3 implies compact, angular shaped particles. This value is close enough to unity that it does not play a decisive role (Reference 2.2.73 [DIRS 103696], p.II-5). It is clear that particles from commercial SNF and crud are never perfectly spherical. A dynamic shape factor of 1.3 is appropriate to account the different shape of particles in air.

The fuel particle density when it is released into air is normally considered to be equal to the theoretical density of UO_2, which is 10.96 g/cm^3 (Reference 2.2.88 [DIRS 127163], p.B-151). This value is used in many documents that describe the UO_2 particle density such as DOE-HDBK-3010-94 (Reference 2.2.24 [DIRS 103756], p.4-52). However, when a UO_2 particle is suspended in air, it starts to oxidize to form U_3O_8, which has a lower density of 8.35

g/cm^3 (Reference 2.2.88 [DIRS 127163], p.B-151). This U_3O_8 density is also used in PNNL-11929 (Reference 2.2.34 [DIRS 101672], Table 2.1).

Fuel fines immediately released from accident events at the repository would not likely contain many voids commonly found in the fuel because of their small size. Hence, the theoretical density of UO_2 is justifiably applied in the calculations of this analysis. Fuel fines after complete oxidation become U_3O_8, which has smaller particles and a relatively lower density when U_3O_8 powder is released into the environment. The density values are from Weast (Reference 2.2.88 [DIRS 127163]), which is generally accepted by the scientific and engineering community and is technically defensible.

Crud is composed of hematite, and its density is 5.2 g/cm^3. This value is taken from *CRC Handbook of Chemistry and Physics* (Reference 2.2.88 [DIRS 127163], p.B-99), which is generally accepted by the scientific and engineering community and is technically defensible. Hematite is commonly found on BWR fuel rods, and is approximately the density of spinel (e.g., of the form $Ni_xFe_{3-x}O_4$) that is commonly found on PWR fuel rods.

With the values of the dynamic shape factor (κ) for UO_2 (1.3), and the particulate density (10.96 g/cm^3) of the aerosol for commercial SNF (UO_2), the cut-off diameter ($d_{c/o}$) for respirable particles from commercial SNF is calculated to be about 3.5 µm using Equation 21 and an AED of 10 µm. Similarly, for the density of 8.35 g/cm^3 of the oxidized fuel (U_3O_8), the cut-off diameter ($d_{c/o}$) for respirable particles from the oxidized fuel powder is calculated to be about 4.0 µm. For the density of 2.7 g/cm^3 for HLW vitrified glass (Reference 2.2.23 [DIRS 102812], Table 3.3.1), which is discussed in Section 6.7, the cut-off diameter ($d_{c/o}$) for respirable particles from HLW is calculated to be about 7.0 µm. Finally, for the crud dynamic shape factor of 1.3 and the crud particle density of 5.2 g/cm^3, the cut-off diameter ($d_{c/o}$) for respirable particles from crud is calculated to be about 5.0 µm.

ATTACHMENT D

PRELIMINARY TEST DATA FROM THE PNNL FUEL IN AIR TESTS

This attachment contains some preliminary test data from the PNNL fuel in air tests through an email. Two data sets used in this document are: *2007-05May-18 109-A500.xls* received on 5/21/07, and *105-LOW Powder Rev 0.xls* received on 6/13/07.

Worksheet *109-A500-Data* from file *2007-05May-18 109-A500.xls* contains particle size distribution data measured by an optical particle counter through airborne release of ATM-109 fuel oxidation powder (about 60 GWd/MTU). Worksheet *Cumulative Data* from file *105-LOW Powder Rev 0.xls* contains particle size distribution measured by an optical particle counter through airborne release of ATM-105 fuel oxidation powder (about 30 GWd/MTU). These two worksheets are imported into a new Excel file, *Test Results Comp.xls*. Raw data were processed to calculate volumetric particle size distribution for each particle size bin. Two particle size distributions are compared as shown in worksheet *powder chart*. Two original files and a calculation file are attached to this document in Attachment E.

The email sent on 5/21/07:

From: Daniel, Richard C [mailto:richard.daniel@pnl.gov]
Sent: Monday, May 21, 2007 08:28
To: Schulz, Jorge
Cc: Hanson, Brady D
Subject: Fuel-In-Air Test Data

Dr. Schulz,

As requested, I am attaching the raw data files for our measurements last week. Please note that I have not had a chance to analyze or cleanup the presentation of data in these files. Let me know if you have any questions, and I will do my best to answer them.

<<2007-05May-16-539B3 And 539D3.xls>> <<2007-05May-17-539F5 And ATM106.xls>> <<2007-05May-18 109-A500.xls>>

It was a pleasure to meet you, and I hope you had an enjoyable and informative visit to the RPL.

Sincerely,

Richard C Daniel

Radiochemical Engineering Team

Pacific Northwest National Laboratory

Phone: (509) 372-1389

Email: richard.daniel@pnl.gov

The email sent on 6/13/07:

From: Hanson, Brady D [mailto:brady.hanson@pnl.gov]
Sent: Wednesday, June 13, 2007 13:30
To: Schulz, Jorge
Subject: Sample 3

FYI-

_____

From: Daniel, Richard C

Sent: Wednesday, June 13, 2007 12:15 PM

To: Hanson, Brady D

Subject: RE: Any ideas- we seem to be off by 3 orders of magnitude

Brady,

Here are the next set of results. Let me know if they show the same 1/1000th factor seen in the HIGH results:

<<105-LOW Powder Rev 0.xls>>

Thanks,

Richard C Daniel

Radiochemical Engineering Team

Pacific Northwest National Laboratory

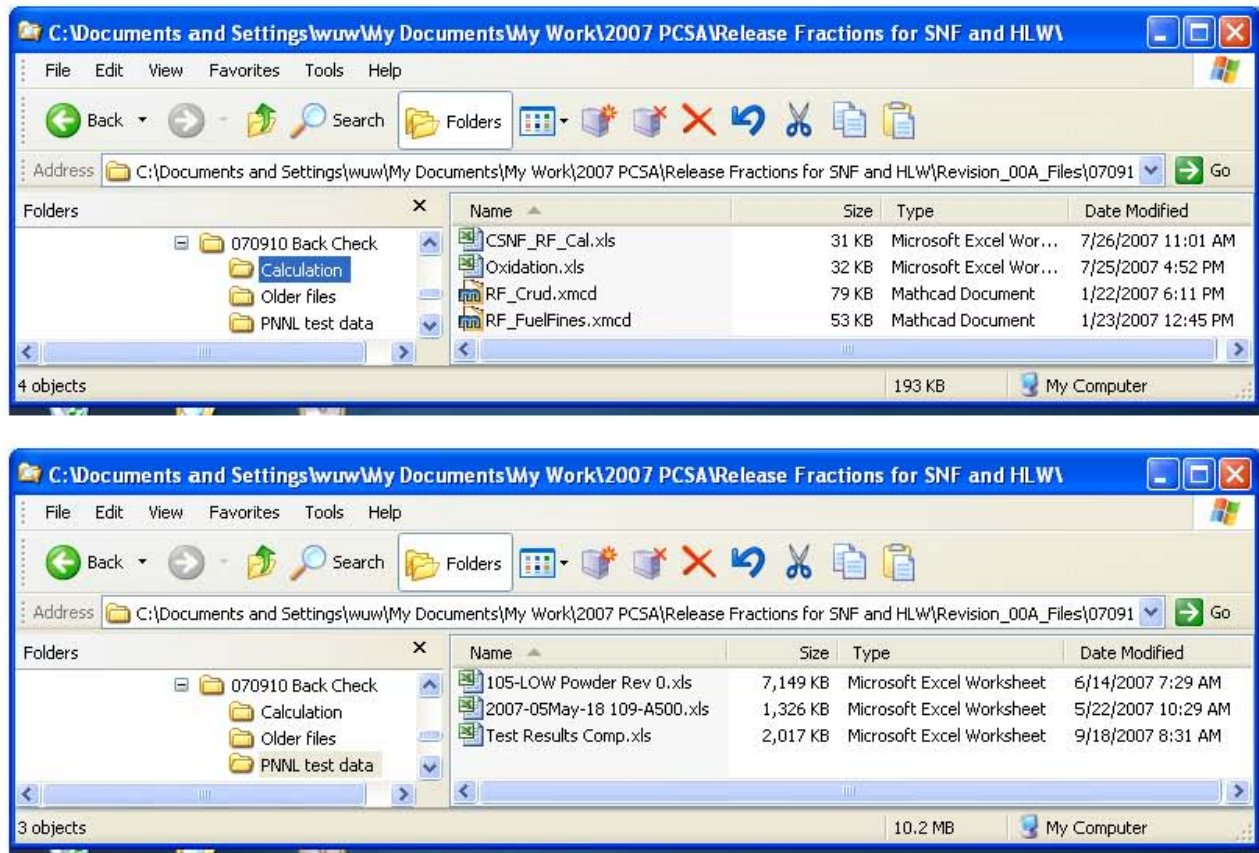Phone: (509) 372-1389

Email: richard.daniel@pnl.gov

Figure 23. Electronic Files For Calculations and Results

INTENTIONALLY LEFT BLANK